



UNIVERSITY OF
BIRMINGHAM

**Transcriptomic and metabolomic
approaches to investigate molecular
responses of human cell lines
exposed to flame retardants**

by

Jinkang Zhang

A thesis submitted to the University of Birmingham for the
degree of DOCTOR OF PHILOSOPHY

School of Biosciences
The University of Birmingham
July 2015

UNIVERSITY OF
BIRMINGHAM

University of Birmingham Research Archive

e-theses repository

This unpublished thesis/dissertation is copyright of the author and/or third parties. The intellectual property rights of the author or third parties in respect of this work are as defined by The Copyright Designs and Patents Act 1988 or as modified by any successor legislation.

Any use made of information contained in this thesis/dissertation must be in accordance with that legislation and must be properly acknowledged. Further distribution or reproduction in any format is prohibited without the permission of the copyright holder.

ABSTRACT

With intensive and global usage, flame retardants (FRs) have played critical roles in the prevention of fires for decades. However, there are increasing concerns about the potential adverse effects of these chemicals due to the well documented environmental and human exposures to FRs. To date, relatively little is known about the molecular mechanisms of the potential toxic effects of human exposure to FRs. Toxicogenomic approaches utilizing transcriptomics, proteomics and metabolomics technologies have been demonstrated to provide unbiased insights into perturbations of molecular signatures, gene expression patterns, biological pathways and the networks of interactions between chemicals and organisms. In this study, microarray-based transcriptomics and direct injection mass spectrometry based metabolomics were employed to investigate the molecular responses of human lung cancer cells (A549) and human hepatoma cells (HepG2/C3A) exposed to a range of sub-lethal concentrations of hexabromocyclododecane (HBCD), tris (1, 3-dichloro-2-propyl) phosphate (TDCIPP) and a mixture of FRs at equivalent concentrations to those found in typical household dust. These represent of commonly used brominated FRs and phosphorus FRs. Combined with the quantification of HBCD levels in cells after exposure, the results suggest that following 24-hour HBCD exposure, no detectable acute toxicity was detected in the cell lines studied here at concentrations estimated to be achievable following exposure in humans. TDCIPP, however, induced defensive responses in gene expression (e.g. xenobiotic metabolism and ABC transporters) in HepG2/C3A cells following exposure to a sub-cytotoxic concentration for 24 hours. Functional pathways (e.g. ABC transporters) were disrupted after 72 hours in HepG2/C3A cells exposed to 100 μ M TDCIPP, which corresponded to the transcriptional and metabolic changes at 24 hours. These results indicate that defensive changes to TDCIPP exposure precede the cytotoxic effects in HepG2/C3A cells. An exploratory investigation of the effects of mixtures of FRs, to mimic real-life human exposures, revealed no adverse effect on cell viability in HepG2/C3A cells treated with a surrogate of dust (a solvent extract of a dust standard reference material) and with mixtures of FRs (at equivalent concentrations to those found in dust samples). However, subsequent transcriptomic and non-targeted metabolomic analyses suggested that potential toxicity from dust exposure lies in components (e.g. polycyclic aromatic hydrocarbons) other than the FRs contained within. Overall, this work using the non-targeted capabilities of multi-omics approaches has revealed that at the concentrations investigated, and which are relevant to human exposures, significant molecular perturbations are not induced by exposure to the FRs under study. The molecular responses identified in this work are beneficial for both understanding the potential mechanisms of effects of human exposure to FRs and for future risk assessment of these chemicals.

ACKNOWLEDGEMENTS

I would like to thank my supervisors, Professor Mark Viant and Professor Kevin Chipman for their constant support and enthusiastic help throughout my PhD project. I also would like to acknowledge the Marie Curie Initial Training Network program_INFLAME project for funding my PhD and its coordinator Professor Stuart Harrad for his encouragement and support. Thanks also go to all the other INFLAMERs for those great network meetings and for the friendships...

I am grateful to Dr Tim Williams for his kind help on microarray data analysis and proofreading chapters of my thesis. Many thanks go to Dr. Mohamed Abou-Elwafa Abdallah for his expertise with analysing FRs in cell samples and preparing the solvent extract of dust samples and mixture of FRs used in this thesis. I extend my thanks to Dr. Jennifer Kirwan and Dr. Ulf Sommer for their instruction on the FT-ICR. Also, I would like to thank Professor Ronny Blust and Maximilian Behr (University of Antwerp) for providing HepG2/C3A cells and Lorraine Wallace (the Functional Genomics facility, University of Birmingham) for her assistance with microarray analysis. In addition, thanks go to all my friends from the 4th floor at the School of Biosciences for their kind help during my PhD.

Huge thanks to my Chinese friends at Birmingham who speak Chinese to me and share Chinese food with me.

Finally, 深深感谢父母的养育之恩!

TABLE OF CONTENTS

ABSTRACT	II
ACKNOWLEDGEMENTS	III
LIST OF FIGURES AND TABLES	VIII
ABBREVIATIONS	XI
CHAPTER 1 Introduction	1
1.1 Flame retardants	2
1.1.1 Brominated flame retardants	4
1.1.2 Organophosphorus flame retardants	6
1.2 Human exposure to BFRs and OPFRs	8
1.2.1 Human exposure to PBDEs.....	9
1.2.2 Human exposure to HBCD	10
1.2.3 Human exposure to OPFRs.....	11
1.3 Toxicity of HBCD and OPFRs	12
1.3.1 Toxicity of HBCD.....	12
1.3.2 Toxicity of TDCIPP.....	15
1.3.3 Toxicity of TCIPP and TCEP	17
1.4 <i>In vitro</i> models - A549 and HepG2/C3A cells	18
1.5 Toxicogenomics - use of omics techniques in toxicology	20
1.5.1 Transcriptomics	21
1.5.1.1 DNA microarray	22
1.5.1.2 RNA-seq.....	24
1.5.2 Metabolomics	26
1.5.2.1 NMR and MS based metabolomics	27
1.5.2.2 DIMS based-metabolomics experiment.....	30
1.6 Research aims and objectives	36
CHAPTER 2 Materials and methods	37
2.1 Chemicals and reagents	38
2.2 Cell culture	38
2.3 Cytotoxicity assays	39
2.3.1 MTT assay.....	39
2.3.2 CCK-8 assay	40
2.3.3 AK assay	40
2.3.4 Cytotoxicity of HBCD to proliferating and confluent cells	41

2.4 Transcriptomics analysis	42
2.4.1 RNA isolation	42
2.4.2 Microarray analysis.....	43
2.4.3 Quantitative real time-PCR analysis	45
2.5 Metabolomics analysis	47
2.5.1 Extraction of metabolites	47
2.5.1.1 Extraction of metabolites (cells harvested from T75 culture flask)..	47
2.5.1.2 Extraction of metabolites (cells harvested from 6 well plate).....	48
2.5.2 Direct infusion mass spectrometry analysis.....	49
2.5.3 Putative annotation and Pathway analysis	51
2.6 Quantification of FRs in HepG2/C3A cells and in cell media	51
2.6.1 Quantification of HBCD levels in HepG2/C3A cells and cell media after exposure.....	51
2.6.2 Quantification of TDCIPP, TCIPP, TCEP and HBCD levels in HepG2/C3A cells and cell media	52
CHAPTER 3 Transcriptomic and metabolomic approaches to investigate the molecular responses of human cell lines exposed to the flame retardant hexabromocyclododecane (HBCD)*	54
3.1 Introduction	55
3.2 Materials and Methods	57
3.2.1 Chemicals and reagents	57
3.2.2 Cell culture.....	57
3.2.3 Cytotoxicity assays	57
3.2.3.1 MTT assay	57
3.2.3.2 CCK-8 assay	58
3.2.4 HBCD exposure experiments and sample preparation for metabolomics and transcriptomics	58
3.2.4.1 A549 cells.....	58
3.2.4.2 HepG2/C3A cells	59
3.2.5 Direct infusion mass spectrometry (DIMS) analysis	59
3.2.6 Transcriptomic analyses	60
3.2.7 Quantification of HBCD in A549 and HepG2/C3A cells and cell media	60
3.3 Results.....	61
3.3.1 Cytotoxicity of HBCD to A549 cells and HepG2/C3A cells.....	61
3.3.2 Molecular responses of A549 cells exposed to HBCD.....	63
3.3.2.1 Gene expression profiles of A549 cells exposed to HBCD.....	63
3.3.2.2 Metabolic responses of A549 cells exposed to HBCD	67
3.3.3 Molecular responses of HepG2/C3A cells exposure to HBCD.....	67
3.3.3.1 Gene expression profiles of HepG2/C3A cells exposed to HBCD ..	67

3.3.3.2	Metabolomics analysis of HepG2/C3A cells exposed to HBCD	72
3.3.4	Uptake of HBCD into A549 and HepG2/C3A cells	77
3.4	Discussion.....	79
3.5	Conclusions	87
CHAPTER 4	Transcriptomic and metabolomic responses of human cell lines exposed to tris (1, 3-dichloro-2-propyl) phosphate (TDCIPP)*	89
4.1	Introduction.....	90
4.2	Materials and Methods	92
4.2.1	Chemicals and reagents	92
4.2.2	Cell culture.....	92
4.2.3	Cytotoxicity assay	93
4.2.4	Design of exposure experiment	93
4.2.5	Transcriptomics analysis	94
4.2.6	Metabolomics analysis.....	95
4.3	Results.....	95
4.3.1	Cytotoxicity of TDCIPP to HepG2/C3A cells and A549 cells.....	95
4.3.2	Omics effects of TDCIPP on HepG2/C3A and A549 cells.....	97
4.3.2.1	Transcriptomic responses of HepG2/C3A and A549 cells exposed to TDCIPP for 24 hours	97
4.3.2.2	Metabolomic responses of HepG2/C3A and A549 cells exposed to TDCIPP for 24 hours	102
4.3.2.3	Metabolomic responses of HepG2/C3A exposed to TDCIPP for 72 hours	104
4.4	Discussion.....	106
4.5	Conclusions	112
CHAPTER 5	Toxicogenomic responses of HepG2/C3A cells exposed to environmental levels of flame retardants and indoor dust extracts*	113
5.1	Introduction.....	114
5.2	Materials and Methods	117
5.2.1	Chemicals and reagents	117
5.2.2	Cell culture.....	117
5.2.3	Design of Exposure experiment.....	117
5.2.4	Cytotoxicity assays	119
5.2.5	Transcriptomics analysis	120
5.2.6	Metabolomics analysis.....	120
5.2.6.1	Extraction of Metabolites	120

5.2.6.2	DIMS analysis and data processing	121
5.2.6.3	MS peaks annotation and pathway analysis	121
5.2.7	Quantification of FRs in HepG2/C3A cells and cell media	122
5.3	Results.....	122
5.3.1	Cytotoxicity of dust extracts and mixture of FRs to HepG2/C3A cells	122
5.3.2	Transcriptomic analysis	123
5.3.3	Metabolomic analysis	130
5.3.4	Quantification of FRs in HepG2/C3A cells after exposure	134
5.4	Discussion.....	136
5.5	Conclusions	143
CHAPTER 6	Conclusions and Future work.....	144
6.1	Molecular responses of A549 and HepG2/C3A cells exposed to HBCD	145
6.2	Defensive and adverse energy-related molecular responses precede TDCIPP cytotoxicity.....	147
6.3	Mixture of FRs at environmental level are less toxic than indoor dust extract.....	149
6.4	Future work	150
References.....		153
Appendix.....		177
1.	List of publications	177
2.	List of conference presentations	177
3.	List of additional files saved on the enclosed CD	178

LIST OF FIGURES AND TABLES

CHAPTER 1 Introduction	1
Table 1.1 Physicochemical properties of important brominated flame retardants	5
<i>Figure 1.1 Basic chemical structure of organophosphate.</i>	6
Table 1.2 Physicochemical properties of chlorinated phosphorus flame retardants	8
<i>Figure 1.2 Major routes of human exposure to FRs.</i>	9
<i>Figure 1.3 The overview of analysis workflows of microarray and RNA-seq data</i>	22
<i>Figure 1.4 Workflow of a cDNA microarray experiment</i>	24
<i>Figure 1.5 A typical RNA-Seq experiment.</i>	25
Table 1.3 Comparison of microarray and RNA-seq.....	26
Table 1.4 Comparison of analysis by Nuclear Magnetic Resonance (NMR) versus Mass Spectrometry (MS) for metabolomics applications	28
<i>Figure 1.6 The trade-off between analytical platforms and the objectives of metabolomics</i>	30
<i>Figure 1.7 An overview of a pipeline of metabolomics experiment</i>	31
<i>Figure 1.8 Data processing workflow for direct infusion FT-ICR mass spectrometry-based metabolomics dataset</i>	33
CHAPTER 2 Materials and methods	37
Table 2.1 Genes, primers, and T _m values used in the RT-PCR analysis	47
CHAPTER 3 Transcriptomic and metabolomic approaches to investigate the molecular responses of human cell lines exposed to the flame retardant hexabromocyclododecane (HBCD)*	54
<i>Figure 3.1 Cytotoxic effects of HBCD to A549 cells and HepG2/C3A cells.</i>	62
<i>Figure 3.2 PCA scores plots of microarray dataset (A) and DIMS dataset (B) in A549 cells exposed to HBCD for 24 hours.</i>	64
Table 3.1 Summary of the principal component (PC) analyses of both the microarray and DIMS datasets of A549 cells and HepG2/C3A cells following exposure to HBCD.....	65
<i>Figure 3.3 qPCR analysis of mRNA expression of six selected genes in A549 cells (A) and in HepG2/C3A cells (B) following HBCD or DMBA treatments.</i>	66
<i>Figure 3.4 PCA scores plots of microarray dataset (A) and DIMS dataset (B) in HepG2/C3A cells exposed to 4 μM HBCD and 10 μM DMBA for 24</i>	

hours.	68
Table 3.2 DAVID analysis of genes modulated in HepG2/C3A cells exposed to DMBA.	69
Table 3.3 Gene Set Enrichment Analysis of up-regulated gene sets in HepG2/C3A cells exposed to DMBA.	71
Table 3.4 Significant MS peaks in DIMS dataset from HepG2/C3A cells exposed to HBCD for 72hours.	73
Figure 3.5 Recovery of HBCD from cell pellets in A549 cells and HepG2/C3A cells exposed to HBCD for 24 hours.....	78
Table 3.5 Concentration of ΣHBCDs in cell pellets and cell media of A549 and HepG2/C3A cells after 24-hour exposure	78
Figure 3.6 Cytotoxic effects of proliferating and confluent HepG2/C3A cells exposed to 60 μM HBCD and 10 μM DMBA for 24 hours.	81
Table 3.6 Gene expression of CYPs in A549 cells exposed to HBCD for 24 hrs from microarray dataset.....	83
Table 3.7 Gene expression of CYPs in HepG2/C3A cells exposed to HBCD and DMBA for 24 hours from microarray dataset.	85

CHAPTER 4 Transcriptomic and metabolomic responses of human cell lines exposed to tris (1, 3-dichloro-2-propyl) phosphate (TDCIPP)* 89

Table 4.1 Experimental design of TDCIPP exposure experiment.....	94
Figure 4.1 Cytotoxic effects of TDCIPP to HepG2/C3A cells and A549 cells. .	96
Figure 4.2 PCA scores plot of all genes of HepG2/C3A and A549 cells exposed to TDCIPP for 24 hours (n=4).	97
Table 4.2 Normalized Enrichment Scores of significant pathways in HepG2/C3A cells and A549 cells exposed to TDCIPP for 24 hours.....	99
Table 4.3 Fold changes of selected genes in HepG2/C3A and A549 cells exposed to 10 μM TDCIPP for 24 hours.	101
Figure 4.3 PCA scores plot of the polar metabolome of HepG2/C3A cells (A) and A549 cells (B) exposed to TDCIPP (n=8).	102
Table 4.4 Summary of principal component (PC) analyses of microarray and DIMS datasets of A549 cells and HepG2/C3A cells exposed to TDCIPP.	103
Figure 4.4 PCA scores plot of the polar metabolome of HepG2/C3A cells exposed to TDCIPP for 24 hours and 72 hours (n=8).....	105
Figure 4.5 PCA scores plot of DIMS data of polar extracts of HepG2/C3A cells exposed to TDCIPP in FBS containing media or FBS-free media (n=8).	107

CHAPTER 5 Toxicogenomic responses of HepG2/C3A cells exposed to environmental levels of flame retardants and indoor dust extracts*

Table 5.1 Experimental design of mixture of FRs and dust extracts exposure study.	119
<i>Figure 5.1 Cytotoxic effects of HepG2/C3A cells exposed to dust extract, mixture of FRs, DMBA and HBCD.</i>	123
<i>Figure 5.2 PCA scores plots of the gene expression of HepG2/C3A cells (A) and (B, which excludes DMBA group) following 72-hour treatments (n=4).</i>	124
Table 5.2 Summary of principal component (PC) analyses of both microarray and MS datasets of HepG2/C3A cells after 72 hours treatment	125
<i>Figure 5.3 Univariate statistics analysis of significantly changed transcripts in HepG2/C3A cells following 72-hour treatments (n=4).</i>	126
Table 5.3 GSEA of gene expression of HepG2/C3A cells from different treatment groups for 72 hours.	128
<i>Figure 5.4 PCA scores plots of the DIMS datasets of polar (A) and non polar (B) extracts of HepG2/C3A cells following 72-hour treatments (n=5).</i>	131
<i>Figure 5.5 Number of significantly changed DIMS peaks between various treatment groups in the polar and non-polar DIMS datasets of HepG2/C3A cells following 72-hour treatments (n=5).</i>	132
Table 5.4 Pathway over-representation analysis of putative annotation of significant MS peaks from polar metabolomics dataset in the DMBA group	133
Table 5.5 Concentration of FRs in cell pellets and cell media in HepG2/C3A cells after 72 hours exposure.....	135
<i>Figure 5.6 Proposed metabolic profile of biotransformation of HBCDs by human HepG2/C3A cells.</i>	141
<i>Figure 5.7 Representation of biotransformation of TDCIPP by human hepatocytes.</i>	142
CHAPTER 6 Conclusions and Future work.....	144
References.....	153
Appendix	177

ABBREVIATIONS

A ₄₆₀	Absorbance at 460 nm
A549 cells	Adenocarcinomic human alveolar basal epithelial cell line
ABS	Acrylonitrile-Butadiene-Styrene
AK	Adenylate kinase
ANOVA	Analysis of variance
AR	Androgen receptor
ATH	Aluminium hydroxide
B[a]P	benzo[a]pyrene
BDCIPP	Bis(1,3-dichloro-2-propyl) phosphate
BFR	Brominated Flame Retardant
CALUX	Chemically activated luciferase gene expression
CCK-8	Counting Kit-8
cDNA	complementary DNA
CE	Capillary electrophoresis
CHO-K1 cells	Chinese hamster ovary cell line
Cy3	cyanine dye 3
CYP	Cytochrome P450
DAVID	Database for Annotation, Visualisation and Integrated Discovery
DCM	Dichloromethane
DEHP	Di(2-ethylhexyl) phthalate
DIMS	Direct injection (or direct infusion) mass spectrometry
DMBA	7,12-dimethylbenz[a]anthracene
DMHP	Dimethyl phosphonate
DMSO	Dimethyl sulfoxide
DPHP	Diphenyl phosphate
E2	17 β -estradiol
EC ₅₀	Half maximal effective concentration
EI	Electron Ionisation
EPS	Expanded polystyrene
ER α	Estrogen receptor α
ESI	Electrospray Ionisation
FAC	Functional Annotation Clustering
FBS	Fetal bovine serum
FDR	False discovery rate ()
FR	Flame Retardant
FT-ICR	Fourier transform ion cyclotron resonance
GC-MS	Gas Chromatography Mass Spectrometry
Glog	Generalised logarithm
GR	Glucocorticoid receptor

GSEA	Gene set enrichment analysis
GSH	Glutathione
HBCD	Hexabromocyclododecane
HepG2/C3A cells	Human hepatocellular carcinoma cell line
HIPS	High impact polystyrene
HMDB	Human Metabolome Database
HPLC	High Performance Liquid Chromatography
KEGG	Kyoto Encyclopedia of Genes and Genomes
KNN	k-Nearest Neighbors
KOW	Octanol:water partition coefficient
LC-MS/MS	Liquid Chromatography tandem Mass Spectrometry
MDH	Magnesium hydroxide
MS	Mass spectrometry
MTT	3-(4,5-dimethylthiazol-2-yl)-2,5-diphenyltetrazolium bromide
NMR	Nuclear magnetic resonance
NOAEL	No Observed Adverse Effect Level
OPFR	Organophosphorus flame retardants
PAH	Polycyclic aromatic hydrocarbon
PBDE	Polybrominated Diphenyl Ether
PBS	Phosphate buffered saline
PBT	Persistent Bioaccumulative Toxic
PC	Principal component
PCA	Principal component analysis
PLS-DA	Partial least squares discriminant analysis
POP	Persistent Organic Pollutant
PQN	Probabilistic quotient normalization
PVC	Polyvinyl Chloride
PXR	Pregnane X receptor
QC	Quality Control
QQQ	Triple quadrupole
QTOF	Quadrupole-TOF
RLUs	Relative Light Units
(c/m)RNA	(complementary/messenger) Ribonucleic acid
ROS	Reactive oxygen species
RSD	Relative Standard Deviation
RT- PCR	Reverse transcription polymerase chain reaction
SAM	Significance Analysis of Microarrays
SD	Standard deviation
SE	Standard error
SIM	Selected ion monitoring
SPE	Solid Phase Extraction

SPS	Single peak search
SRM	Standard Reference Material
T4	Thyroxine
TBBPA	Tetrabromobisphenol A
TCEP	Tris(2- chloroethyl)phosphate
TCP	Tricresyl phosphate
TCPP	Tris(chloropropyl)phosphate
TCIPP	Tris(2-chloroisopropyl) phosphate
TDCIPP	Tris(1,3-dichloro-2-propyl)phosphate
TIC	Total ion current
TM	Transformation mapping
TOF	Time-of-flight
TPP	Triphenyl phosphate
TR	Thyroid hormone receptor
V6	Tetrekis(2-chlorethyl) dichloroisopentyldiphosphate
VP	Vapour Pressure
XPS	Extruded polystyrene

CHAPTER 1 Introduction

Fire is one of the most serious risks to life, property and the environment. It has been estimated that fires kill 10 to 20 people per million of the population every year in developed countries (ISO/TC92, 2014). In Europe alone, fire fatalities reach several thousand each year. In 2013-14, there were 322 fire-related deaths in Great Britain, of which 80% were dwelling fires (UK Department for Communities and Local Government, 2015). The direct and indirect costs of fire are estimated at around 1% of global GDP per year (The Geneva Association, 2014). To protect people's lives and properties from fires, fire safety standards and regulations have been introduced in many countries. In the UK, the Furniture and Furnishings (Fire Safety) Regulations 1988 (amended 1989, 1993 and 2010) are designed to ensure that upholstery materials used for furniture supplied in the UK meet specified fire resistant ignitability standards (<http://www.firesafe.org.uk/furniture-and-furnishings-fire-safety-regulations-19881989-and-1993/>). Similar standards (e.g. Furniture - Assessment of the ignitability of upholstered furniture) were also introduced by the European Committee for Standardization (<http://www.bsef.com/fire-standards-and-regulations/>). To comply with these standards and regulations, application of flame retardants (FRs) is an important means to reduce flammability and increase the fire resistance of a variety of materials and products.

1.1 Flame retardants

Flame retardants (FRs) are chemicals added into various consumer products including electronics, textiles, furniture and building materials to reduce their flammability and inhibit the spread of combustion after ignition. Four main classes of flame retardants are produced and used, comprising together more than 175

chemicals (Alaee et al., 2003;van Esch, 1997). These include: halogenated organic, organophosphorus, inorganic and nitrogen based flame retardants. They can be so-called additive compounds, meaning physically mixed within a base material, or reactive compounds, meaning covalently bonded to a material.

Among these chemicals, halogenated organic flame retardants include chlorinated FRs (e.g. chlorinated paraffins) and brominated FRs (e.g. hexabromocyclododecane (HBCD), tetrabromobisphenol A (TBBPA) and polybrominated diphenyl ethers (PBDEs)). The class of organophosphorus FRs can be divided into three main subclasses: phosphate ester (e.g. triphenyl phosphate (TPP) and tricresyl phosphate (TCP)); phosphonates (e.g. dimethyl phosphonate (DMHP)); and phosphinates (e.g. aluminum diethyl phosphinate) (van der Veen and de Boer, 2012). Some flame retardants contain both phosphorus and halogen, such as tris(1,3-dichloro-2-propyl)phosphate (TDCIPP), tris(2-chloroethyl)phosphate (TCEP), Tris(2-chloroisopropyl) phosphate (TCIPP) and tetrakis(2-chloroethyl) dichloroisopentyldiphosphate (V6) and can also be recognized as OPFRs (van der Veen and de Boer, 2012). Aluminium hydroxide (ATH) and magnesium hydroxide (MDH) are the two most notable members of the class of inorganic FRs. In addition, melamine and its derivatives belong to the group of nitrogen based flame retardants (PINFA, 2015).

Flame retardants can slow down or suppress the combustion process through chemical and/or physical actions in the gas or condensed phases, during a certain stage of this combustion process (i.e. during heating, decomposition, ignition or flame spread) (BSEF, 2012). The most effective chemical action of flame retardants to interfere with the combustion processes is to eliminate highly reactive radicals (i.e.

H• and OH• radicals) by hydrogen chloride or hydrogen bromide. Hydrogen chloride or hydrogen bromide are generated from halogenated flame retardants or metal halogen compounds from antimony trioxide in the gas phase. Flame retardants exert physical effects by cooling (endothermic degradation of FRs) or diluting combustible gases (i.e. formation of carbon dioxide and water), or by generating a char layer (shielding the material against oxygen and heat) with phosphorous and nitrogen compounds (www.flameretardants-online.com, 2015).

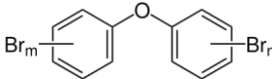
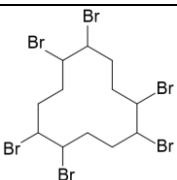
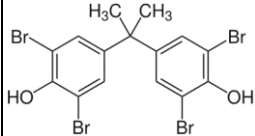
It was estimated that the consumption of flame retardants in Europe was 465,000 tonnes in 2006, of which brominated flame retardants have the highest market share by value (EFRA, 2007).

1.1.1 Brominated flame retardants

There are currently more than 75 different commercial BFRs available on the market (EFRA, 2007). Depending on the nature of the material, BFRs can be additive (such as PBDEs and HBCD) or reactive (such as TBBPA) (Alaee et al., 2003). BFRs are mainly applied to electronics and electrical devices (i.e. televisions and computer monitors) accounting for more than 50% of their usage, while other applications include insulation materials, carpets, furniture, and thermoplastics (e.g. high impact polystyrene (HIPS) and acrylonitrile-butadiene-styrene (ABS) resins) (EFRA, 2007; Rauert et al., 2014). Physicochemical properties and chemical structures of the most important BFRs are summarized in Table 1.1. These properties determine their environmental fate, persistence and bioaccumulation.

Table 1.1 Physicochemical properties of important brominated flame retardants

(reviewed in Rauert, 2014).

Compound	penta-bromodiphenyl ether	Octa-bromodiphenyl ether	Deca-bromodiphenyl ether	Hexabromocyclododecane	Tetrabrominated bisphenol-A
Abbreviation	PentaBDE	OctaBDE	DecaBDE	HBCD	TBBPA
CAS number	32534-81-9	32536-52-0	1163-19-5	25637-99-4	79-94-7
Chemical structure					
Molecular Formula	C ₁₂ H _{10-x} Br _x O	C ₁₂ H _{10-x} Br _x O	C ₁₂ Br ₁₀ O	C ₁₂ H ₁₈ Br ₆	C ₁₅ H ₁₂ Br ₄ O ₂
Molecular Weight (g·mol ⁻¹)	example: 564.7 (BDE-99)	example: 801.4 (BDE-203)	959.2	641.7	543.9
Melting point	-7 to -3°C	85 to 89 °C	290 to 306 °C	180-185 °C	178 °C
Water solubility (µg·L ⁻¹ at 25 °C)	not soluble	not soluble	20-30	8.6	insoluble
Octanol-water coefficient (Log K _{ow})	6.57 to 6.97	6.29	~10	5.63 to 5.81	4.5
Vapour pressure (Pa at 25°C)	2.92 x 10 ⁻⁵ to 7.32 x 10 ⁻⁵	1.20 x 10 ⁻⁸ to 2.26 x 10 ⁻⁷	4.26 x 10 ⁻⁶ to 4.62 x 10 ⁻⁶	7.47 x 10 ⁻¹⁰	8.47 x 10 ⁻⁹
Main isomers/congeners in commercial product(s)	BDE-47, BDE-99, BDE-100, BDE-153	BDE-183, BDE-196, BDE-197, BDE-203	BDE-209	α-HBCD, β-HBCD, γ-HBCD	n.a.

Since some BFRs (i.e. PBDE and HBCD) have been shown to be persistent, bioaccumulative, (potentially) toxic to the environment and are capable of long-range atmospheric transport (Marvin et al., 2011), their production and usage has been restricted. For example, pentaBDE, the first commercialized BFR, was banned in the EU from 2004 and phased out in the USA from 2005 owing to concerns regarding its persistence and adverse effects (Dodson et al., 2012). HBCD, another widely used BFR, has been listed under the UNEP Stockholm Convention on persistent organic pollutants (POPs) in 2013, but with specific time-limited exemptions for production and use in extruded polystyrene (XPS) and expanded polystyrene (EPS) in buildings

(UN, 2013). The main applications of HBCD are addition to XPS and EPS foams used for thermal insulation in the building industry. Other uses of HBCD include upholstery textiles, furniture and electrical and electronic products (Covaci et al., 2006; Marvin et al., 2011). One of the primary applications of TBBPA is in the resin of printed circuit boards where it is used as reactive BFR which is less readily leached out from the products. As such TBBPA was regarded as no risk to human health in an EU risk assessment in 2005 (EU, 2006).

1.1.2 Organophosphorus flame retardants

In recent years, organophosphorus flame retardants (OPFRs) have become increasingly popular in the market and are often proposed as suitable alternatives to BFRs (Veen and Boer, 2012). OPFRs comprised 20% (91,000 tonnes) of the total consumption of flame retardants in 2006 in the EU (EFRA, 2007). The basic chemical structure of organophosphate (one subclass of OPFRs) is depicted in Figure 1.1 and the physicochemical properties of three chlorinated phosphorus flame retardants (which were investigated in this thesis) are summarized in Table 1.2.

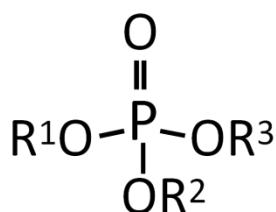
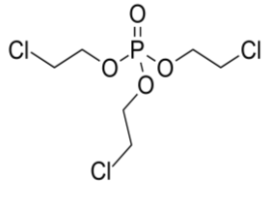
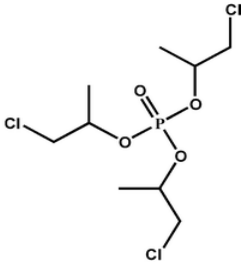
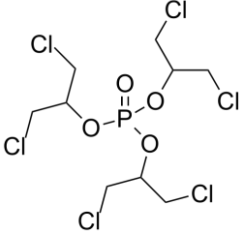


Figure 1.1 Basic chemical structure of organophosphate. Organophosphates are derivatives of phosphoric acid. The various side chains (R1, R2 and R3) can be for example alkyl, aryl or haloalkyl either alone or in combination.

OPFRs have a broad range of applications including addition to polyvinyl chloride (PVC) and polyurethane foam, resulting in satisfactory fire safety performance. For

example, TDCIPP is a high volume production OPFR which is added to flexible polyurethane foam in the automotive upholstery, foams for household furniture and other commercial products, i.e. beddings (van der Veen and de Boer, 2012). In terms of production volumes of OPFRs, TPHP, TDCIPP and TCIPP are the three most used PFRs (Brommer, 2014).

Table 1.2 Physicochemical properties of chlorinated phosphorus flame retardants_ (reviewed in Brommer, 2014).

Compound	Tris(2-chloroethyl) phosphate	Tris(2-chloroisopropyl) phosphate	Tris(1,3-dichloroisopropyl) phosphate
Abbreviation	TCEP	TCIPP	TDCIPP
CAS number	115-96-8	13674-84-5	13674-87-8
Chemical structure			
Molecular Formula	C ₆ H ₁₂ Cl ₃ O ₄ P	C ₉ H ₁₈ Cl ₃ O ₄ P	C ₉ H ₁₅ Cl ₆ O ₄ P
Molecular Weight (g·mol ⁻¹)	285.49	327.57	430.91
Melting point	-35 °C	-40 °C	27 °C
Boiling point	330 °C	>270 °C	236-237 °C at 5 mm Hg
Water solubility (mg·L ⁻¹)	7000	1200	7
Octanol-water coefficient (Log K _{ow})	1.44	2.59	3.65
Vapour pressure (mm Hg at 25°C)	6.13 x 10 ⁻²	2.02 x 10 ⁻⁵	7.36 x 10 ⁻⁸

1.2 Human exposure to BFRs and OPFRs

Due to the widespread use of FRs in various consumer products all over the world, especially the extensive applications of additive FRs which are easily released from

products into the environment, FRs have been reported to occur ubiquitously in the environment, in wildlife and in humans (Alaee et al., 2003; Law et al., 2014; van der Veen and de Boer, 2012). The major routes of non-occupational human exposure to FRs (Figure 1.2) have been summarized as via ingestion of indoor dust, diet, inhalation of air, and dermal contact with dust/products containing FRs (Abdallah et al., 2015a).

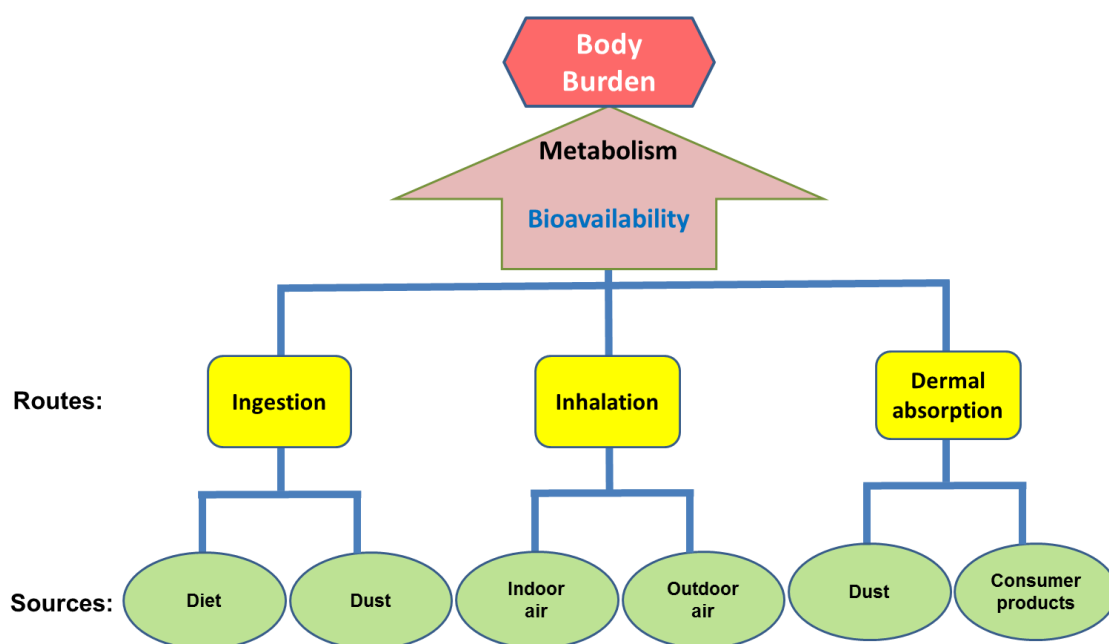


Figure 1.2 Major routes of human exposure to FRs (Adapted from Abdallah et al., 2015a).

1.2.1 Human exposure to PBDEs

Although dietary intake has been considered as one of the most significant exposure pathway for PBDEs in adults (Domingo, 2012), indoor dust ingestion and diet seem to be the predominant exposure routes both at work and at home in the UK and USA, with high consumption of PBDEs (Besis and Samara, 2012; Harrad et al., 2008, 2006, 2004). Many studies have found that concentrations of PBDEs in air and dust were

higher in indoor environment than in outdoors (Besis and Samara, 2012). PBDE concentrations in house dust have also been reported to be significantly correlated with levels in adults' serum (Johnson et al., 2010) and in umbilical cord plasma (Frederiksen et al., 2010). Moreover, positively significant associations have been found between PBDE concentrations in first-time mothers' breast milk and domestic dust ($r = 0.76$, $p = 0.003$), as well as with the dietary consumption of dairy products and meat, which indicates that both house dust and diet are important sources for human exposure to PBDEs (Wu et al., 2007). It was reported that toddlers had a higher PBDE intake (49 ng/kg bw/day) than adults (7.7 ng/kg bw/day) because of a higher dust ingestion rate and lower body weight in toddlers (Lorber, 2008).

1.2.2 Human exposure to HBCD

Like PBDEs, human exposure to HBCDs can occur via multiple sources including diet, dust, air, and consumer products (Marvin et al., 2011). Although diet is a main exposure route in Europe and USA (Covaci et al., 2006; Schechter et al., 2012), indoor dust and air can be important contributors for exposure in both toddlers and adults (Abdallah et al., 2008a, 2008b; Marvin et al., 2011). Exposure to HBCDs via dust ingestion was estimated to contribute 24% of total exposure in adults and 63% in children in a comparison study of exposure to HBCD through indoor dust, diet and inhalation (Abdallah et al., 2008a). Human exposure to HBCD has been confirmed by its presence in breast milk, adipose tissue and blood (Marvin et al., 2011; Rawn et al., 2014a). The levels of HBCD detected in human milk samples in Spain were up to 188 ng/g lipid weight, with a median value of 27 ng/g (Eljarrat et al., 2009). The intake of HBCDs in breast-fed infants (0-6 months) was estimated up to 90 ng/kg bw/day based on a Canadian exposure estimate model which included uptake of HBCDs

from breast milk, dust and other environmental media (Environment Canada, 2011). A recent study (Rawn et al., 2014a) reported concentrations of HBCD in fetal liver (median 29 ng/g lipid) and placental tissues (median 49 ng/g lipid) collected between 1998 and 2010 in Canada. Weiss et al. (2004) detected HBCD in both maternal and cord blood (average values of 1.1 ng/g and 1.7 ng/g lipid weight, respectively) in the Netherlands. That have also been report of concentration of HBCD in human serum was up to 856 ng/g lipid (Thomsen et al., 2007).

1.2.3 Human exposure to OPFRs

Although several studies reported levels of different types of OPFRs in the environment including indoor dust, air, surface water, drinking water, sediments and biota (reviewed in van der Veen and de Boer, 2012), there is still a paucity of knowledge about human exposure to OPFRs (Abdallah and Covaci, 2014). For example, Carignan et al. (2013) found that the TDCIPP level in office dust samples from Boston, USA was up to 72 µg/g. The average concentration of TDCIPP in car dust in Germany was 130 µg/g (Brommer et al., 2012). These studies reported a high prevalence of TDCIPP in dust samples suggesting that dust could contribute as a source of human exposure to TDCIPP within indoor or enclosed environments (Abdallah and Covaci, 2014; Stapleton and Klosterhaus, 2009), especially for toddlers who may have more dust exposure due to frequent hand-mouth behaviour (Butt et al., 2014). Moreover, significant correlations have been found between the concentrations of diphenyl phosphate (DPHP) (1.1 ng/mL) and bis(1,3-dichloro-2-propyl) phosphate (BDCIPP) (0.23 ng/mL) in childrens' urine and their precursor compounds (TPHP and TDCIPP, respectively) in indoor dust and air; while no significant associations between OPFRs metabolite concentrations in urine

and diet data were observed (Hoffman et al., 2015). Cumulative results suggest that indoor dust and air are important sources of TDCIPP (Cequier et al., 2015). Total intakes of TPHP and TDCIPP in children from indoor dust and air were 6.26 and 4.52 ng/kg bw/day, respectively (Cequier et al., 2015, 2014). A few studies have also reported the levels of TDCIPP or its metabolites in humans. For example, the concentration of TDCIPP was reported up to 252 ng/g lipid in human adipose tissue samples (LeBel and Williams, 1986) and up to 162ng/g lipids in human breast milk (Kim et al., 2014). In addition, the concentration of BDCIPP (which is the primary metabolite of TDCIPP) in human urine was up to 25 ng/mL (Meeker et al., 2013)

1.3 Toxicity of HBCD and OPFRs

Human exposure to FRs is bound to occur due to their widespread usage and their physicochemical properties. While FRs reduce risk to human health by effective fire retardation, they might also increase risk to human health unless they exert low levels of toxicity.

1.3.1 Toxicity of HBCD

To respond to the environmental and human health concerns regarding exposure to HBCD, toxicity studies have investigated and reported potentially adverse effects of HBCD in animal models and human cell lines, including acute toxicity, endocrine and reproductive toxicity, neurotoxicity, and hepatotoxicity (reviewed in Marvin et al., 2011; Wikoff and Birnbaum, 2011).

Generally, the acute toxicity of HBCD is very low, following oral, inhalation, or dermal exposures in rodents (reviewed in Wikoff and Birnbaum, 2011). For example, there was no increase in mortality could be observed after oral exposure, and the LD₅₀ of

HBCD was estimated as to >6400 mg/kg bw in mice and >10000 mg/kg bw in rats (KEMI, 2002).

Endocrine disruption (especially disruption of thyroid function) has been found as a consistent response to exposure to HBCD (Marvin et al., 2011) according to a number of *in vivo* and *in vitro* studies, including using rats (van der Ven et al., 2009, 2006), fish (Palace et al., 2010, 2008) and chicken (Crump et al., 2008). Significant increase of thyroid weight and decrease of circulating serum thyroxine (T4) levels were observed in female rats in 28-day repeated dietary exposure, with effect-specific no observed adverse effect levels (NOAELs) of 1.6 and 55.5 mg/kg bw/day, respectively (van der Ven et al., 2006). *In vitro* studies suggested that HBCD can bind to thyroid receptors (Schriks et al., 2007; Yamada-Okabe et al., 2005) affecting triiodothyronine (T3) mediated cellular events (Schriks, et al., 2007; Schriks, et al., 2006). Even at low-dose (10^{-4} μ M), HBCD can suppress thyroid hormone receptor (TR) -mediated gene expression in cerebellar Purkinje cells (Kingsley Ibhazehiebo et al., 2011).

In reproductive toxicity studies with rats, adverse effects were observed. These included decrease of testis weight, the induction of aromatase enzyme activity in ovaries and a decrease in the number of primordial follicles in ovaries, with a NOAEL of 10 mg/kg-day (Ema et al. 2008; van der Ven et al. 2009). HBCD has also been shown to be antagonistic to the progesterone receptor, androgen receptor, estrogen receptor and aryl hydrocarbon receptor in the chemically activated luciferase gene expression (CALUX) assay (Hamers et al., 2006).

Significant changes in spontaneous behaviour, learning and memory were found after neonatal exposure of mice to HBCD (Eriksson et al., 2006), implying some degree of neurotoxicity. HBCD has also been shown to inhibit the uptake of dopamine in rat

brain synaptosomes *in vitro* (Mariussen and Fonnum, 2003) and to suppress the release of neurotransmitter (catecholamine) (Dingemans et al., 2009). Low micromolar concentrations of HBCD have been shown to give rise to neurotoxic effects in *in vitro* cultured neuronal cells (e.g. PC12 cells (Dingemans et al., 2009) and SH-SY5Y cells (Al-Mousa and Michelangeli, 2012)) by interfering with calcium (Ca^{2+}) homeostasis and intracellular signalling pathways. One study focused on behaviour in humans; neurobehavioral function and serum levels of HBCD in a group of adolescents in Belgium were assessed. HBCD did not show consistent associations with performance in the neurobehavioral tests (Kiciński et al., 2012), which did not show agreement with previous results in model animals.

Hepatotoxicity of HBCD has been reported in a wide range of studies, which showed that liver is one of the main target organs (Hakk et al., 2012; Marvin et al., 2011). Long term exposure to HBCD at a relatively high dose (30 mg/kg/day, 28 days) increased liver weight in female rats (van der Ven et al., 2006) and induced hepatic cytochrome P450 (CYP) enzyme activities (CYP2B1 and CYP3A1) in rats (Cantón et al., 2008; Germer et al., 2006). Other hepatic transcription (i.e. fatty acid desaturase 1, hydroxymethylglutaryl-CoA synthase, glutathione-S-transferase) in rats liver were also altered after exposure, which are relevant to lipid metabolism, cholesterol biosynthesis, and glutathione metabolism and conjugation pathways (Cantón et al., 2008). Yanagisawa et al. (2014) also reported that HBCD can increase gene expression of peroxisome proliferator-activated receptor- γ in liver and decrease transcripts of glucose transporter 4 in adipose tissue in high fat diet-fed mice, which indicate that HBCD can contribute to disruption of lipid and glucose homeostasis. In juvenile rainbow trout (*Oncorhynchus mykiss*) (Ronisz et al., 2004) and Chinese rare

minnow (*Gobiocypris rarus*) (Zhang et al., 2008), HBCD inhibited CYPs enzyme activities in the liver after a 28-day exposure.

In several *in vitro* studies, induction of cell apoptosis followed exposure to high concentrations of HBCD. This was seen in HepG2 cells (hepatocellular carcinoma cells) (An et al., 2014; Hu et al., 2009) and human L02 hepatocytes (An et al., 2013). Induction of apoptosis was suggested to result from increased production of reactive oxygen species (ROS). A slight increase in ROS was also observed after low concentration (10^{-7} - 10^{-1} μ M) exposures in human L02 hepatocytes, while no acute toxic effect was reported (An et al., 2013; Zou et al., 2013).

Collectively, there is limited information about molecular changes resulting from concentrations that are realistic for likely human exposures to HBCD. Therefore, further studies are needed in order to obtain a more comprehensive understanding of potential effects of HBCD exposure.

1.3.2 Toxicity of TDCIPP

Although less information is available on toxicity of OPFRs compared with BFRs, TDCIPP appears to be endocrine disruptive and neurotoxic in *in vitro* and *in vivo* studies. Meeker and Stapleton (2010) reported that altered thyroxine (T4) levels and decreased semen quality in men might be linked to exposure to TDCIPP. Other studies found that exposure to TDCIPP can change thyroid hormone concentrations in chicken (*Gallus gallus*) embryos (Farhat et al., 2013) and zebrafish (*Danio rerio*) (Wang et al., 2013) and alter sex hormone levels in human H295R cell lines and zebrafish (Liu et al., 2012). Dysregulation of gene expression related to thyroid hormone metabolism was found in zebrafish (Wang et al., 2013) and avian

hepatocytes (Crump et al., 2012). TDCIPP displays androgen receptor (AR), glucocorticoid receptor (GR) and pregnane X receptor (PXR) antagonistic activities in cell-based transactivation assays (Kojima et al., 2013).

Concentration-dependent neurotoxicity of TDCIPP was observed in rat PC12 cells. For example, oxidative stress increased following 50 μ M TDCIPP treatment (Dishaw et al., 2011), while dysregulation of gene and protein expression related to apoptosis, neurite growth and synapse formation, potentially disrupting neurodevelopment, were observed after exposure to TDCIPP (15 μ M) (Ta et al., 2014). Moreover, exposure to TDCIPP (3 μ M) can cause developmental toxicity in zebrafish larvae through altering gene expression relevant to regulating embryogenesis (Fu et al., 2013).

Limited studies of the hepatic toxicity of TDCIPP were focussed on chicken embryonic hepatocytes or liver; in which phase I and II xenobiotic-metabolizing enzymes were elevated after TDCIPP exposure (Crump et al., 2012; Farhat et al., 2014a).

TDCIPP has also been listed as a carcinogen in the Proposition 65 list by the California Environmental Protection Agency (OEHHA, 2013). In contrast, it was classified as a safe compound for its intended application in a risk assessment report (European Union, 2008). The evidence for TDCIPP's carcinogenicity *via* a genotoxic mechanism(s) has been building (OEHHA, 2011). For example, positive evidence for genotoxicity was found in *in vitro* tests including mutagenicity in multiple strains of *Salmonella* (Gold et al., 1978), chromosomal aberrations and sister chromatid exchanges in mouse (*Mus musculus*) lymphoma cells (Brusick et al., 1979) and unscheduled DNA synthesis in rat (*Rattus norvegicus*) hepatocytes (Sederlund et al., 1985), though negative results were also found in most *in vivo* genotoxicity studies

(OEHHA, 2011). As such, it has been suggested that the current available knowledge is yet sufficient to confirm that TDCIPP exposure can induce cancer in humans (ATSDR, 2012). However, in rats, exposure to TDCIPP can increase the rate of formation of tumours at multiple sites (i.e. liver, kidney and testes) (Freudenthal and Henrich, 2000).

1.3.3 Toxicity of TCIPP and TCEP

Compared to TDCIPP, there are fewer studies focusing on the toxicity of TCIPP and TCEP. In an risk assessment by EU, it was suggested that there was no adverse effects on male reproductive system in rats from a few available toxicity studies of TCIPP (European Chemicals Bureau, 2008a). However, TCEP exposure caused significant decrease of testicles weight in mice and adverse effects of sperm quality were reported in mice and rats (European Chemicals Bureau, 2008b). TCEP has also been listed as a carcinogen in the Proposition 65 list by the California Environmental Protection Agency (OEHHA, 2013). However, an ATSDR (The Agency for Toxic Substances and Disease Registry) report concluded that, like TDCIPP, limited information from available studies cannot confirm that TCEP exposure induce tumours in humans (ATSDR, 2012).

From *in vitro* studies, there are mixed or inconsistent effects reported on endocrine disruption .While no mutagenic potential or estrogenic effects of TCIPP and TCEP were detected in *Salmonella* (Föllmann and Wober, 2006); Liu et al. reported (2012) that both TCIPP and TCEP can increase the concentrations of 17 β -estradiol (E2) and testosterone (T) in H295R cells. In another study, TCEP showed notable antiestrogenic properties with lowest observed effect level (LOEL) at 1.0×10^{-5} M in a dual-luciferase reporter gene assay in Chinese hamster ovary cell line (CHO-K1 cells)

(Zhang et al., 2014). In addition, TCIPP displayed pregnane X receptor (PXR) agonistic activity, but no endocrine effects of TCEP were observed in reporter gene assays of human nuclear receptors (Kojima et al., 2013).

In short, although the toxic effects of some FRs have been reported, there remains a need to more fully understand the potential toxicities of FRs and their potentially toxic modes of action, especially considering the conflicting FR toxicity data reported in previous studies. Therefore, comprehensive investigations of the toxicity of FR's are necessary to determine any adverse effects and explain their underlying mechanisms, which eventually will be beneficial to understand the mode of actions of FRs and aid risk assessment of human exposures.

1.4 *In vitro* models - A549 and HepG2/C3A cells

The '3R' concept (replacement, reduction and refinement) has been widely accepted, due to the ethical, political and commercial pressure on the usage of animal models in toxicology studies (Kroeger, 2006). Compared to using animal models *in vivo*, *in vitro* analyses are a less costly and less time-consuming alternative option. These assays can be conducted in an identical genetic background using simple conditions and can overcome the drawbacks caused by the complexity of *in vivo* studies (Eisenbrand et al., 2002; Lilienblum et al., 2008).

Since human exposure to FRs can occur *via* inhalation, the lung represents one of the main target organs. Therefore, in the current investigation we selected an adenocarcinomic human alveolar basal epithelial cell line (A549 cells) as an *in vitro* model to test the potential molecular effects of FRs on the lung. A549 cells have been widely used as an *in vitro* model for a type II pulmonary epithelial cell drug

metabolism and as a transfection host (Ahamed et al., 2011; Billet et al., 2008; Courcot et al., 2012; Komori et al., 2008; Seo et al., 2007). As it is derived from pulmonary tissues, the A549 cell line has functional xenobiotic metabolism and allowing extrapolation of results to the lung *in vivo* (Hukkanen et al., 2000; Vulimiri et al., 2009).

The other *in vitro* model used in this study is a human hepatocellular carcinoma cell line (HepG2/C3A cells). This is a convenient alternative to primary human hepatocytes and has been shown to exhibit a degree of xenobiotic metabolic capacity (Gerets et al., 2012). HepG2 cells are regarded as a “gold standard” in toxicology (Kang et al., 2010). The use of human liver cell lines for monitoring toxicological relevant stress related endpoints is a logical choice since the liver is the primary detoxification organ (Nobels et al., 2012). Moreover, the xenobiotic metabolizing capacities of HepG2 cell lines are comparable to that of primary cultures of human hepatocytes (Sevastyanova et al., 2007). The HepG2/C3A cell line is clonal derivative of HepG2 cell line which is a suitable *in vitro* model system for the study of polarized human hepatocytes.

Both A549 cells and HepG2/C3A cells have been successfully employed in many toxicological studies to investigate transcriptional and/or metabolomic responses to various compounds (Bandeled et al., 2012; Castorena-Torres et al., 2008; Gualtieri et al., 2012; Li et al., 2007; Mitsopoulos and Suntres, 2010; Nobels et al., 2012; Ruiz-Aracama et al., 2011; Shintu et al., 2012). However, very few applications of these cell lines were focusing on FRs toxicity. Hence, in the present study, they were employed as *in vitro* models to investigate the potential toxic effects of FRs.

1.5 Toxicogenomics - use of omics techniques in toxicology

Toxicogenomics is a term to describe the investigation of the molecular responses to toxicants by analyzing genes, genetic polymorphisms, mRNA transcript expression, protein levels, or metabolite levels in cells, tissues or organisms (Foster et al., 2013). Combining toxicology with omics technologies (i.e. genomics, transcriptomics, proteomics, and metabolomics), toxicogenomics can provide unbiased insights into perturbations of molecular signatures, gene expression patterns, biological pathways and the networks of interactions between chemicals and organisms. Although conventional methods in toxicology can identify chemicals of potential concern, often they are unable to provide comprehensive mechanistic information on the underlying molecular responses that occur as a result of toxicant exposure (Chen et al., 2012; National Research Council (US), 2007)

Using advanced technologies, toxicogenomics does not only focus on global gene expression patterns after exposure to toxicants through microarray or RNA-seq based transcriptomics, but also can look at the overall changes occurring at the protein level (proteomics) and the physiological output (metabolites) of biochemical processes in a living systems (metabolomics)(Hamadeh et al., 2002). This can provide great opportunities to generate hypotheses regarding the mechanisms of action of toxicants in a high-throughput fashion.

There are, as yet, relatively few 'omics studies of the potential toxicity of FRs. For example, hypothyroidism reported in rats following a 28-day high dose exposure (30 and 100 mg HBCD/kg/day) of HBCD (Germer et al., 2006) was found to correlate well with gene expression changes in the cholesterol biosynthesis pathway in rats' liver, as revealed by transcriptomic analysis (Cantón et al., 2008). A proteomic study of

zebrafish (*Danio rerio*) liver cells found that protein metabolism decreased after 72-hour exposure to 5 μ M HBCD (Kling and Förlin, 2009). Few metabolomics studies of the effects of FRs have been reported using *in vitro* or *in vivo* systems.

Metabolomics has already been applied to a wide range of toxicological studies, including in mechanistic toxicology (Nicholson et al., 2002) and ecotoxicology (Bundy et al., 2009). For example, DIMS based metabolomics has been applied successfully to investigate toxic effects of environmental chemicals to fish (Southam et al., 2011) and water flea (*Daphnia magna*) (Taylor et al., 2008).

In the present study, transcriptomics and metabolomics were employed to investigate the molecular responses of human cell lines exposed to FRs so as to explore the potential mechanisms of the effects of FRs exposure in an overall view. The current primary technologies used in these two omics are summarized below.

1.5.1 Transcriptomics

Transcriptomics describes the global measurement of all species of transcripts, including mRNAs, non-coding RNAs and small RNAs in a biological system (Wang et al., 2009), which is essential to understand the molecular mechanisms of cellular responses to various treatments/conditions in cells or tissues at transcriptional level (Heijne et al., 2005). Transcriptomics has been widely employed in toxicogenomics studies and the application in accumulating research have suggested that transcriptional profiling of the exposure systems (*in vivo* and *in vitro*) is valuable for characterizing the mechanism of actions of toxicants and predicting toxicity of chemical compounds (Bandeled, et al., 2012; Castorena-Torres, et al., 2008; Gualtieri, et al., 2012; Katsiadaki et al., 2010; Li, et al., 2007; Mitsopoulos and Suntres, 2010; Santos et al., 2010; Van Aggelen et al., 2010; Williams et al.,

2009). Currently, DNA microarray and RNA sequencing (RNA-seq) are two commonly used technologies in the market for analyzing the global transcriptional patterns. The typical analysis workflows of these two platforms are shown in Figure 1.3 (Fang et al., 2012).

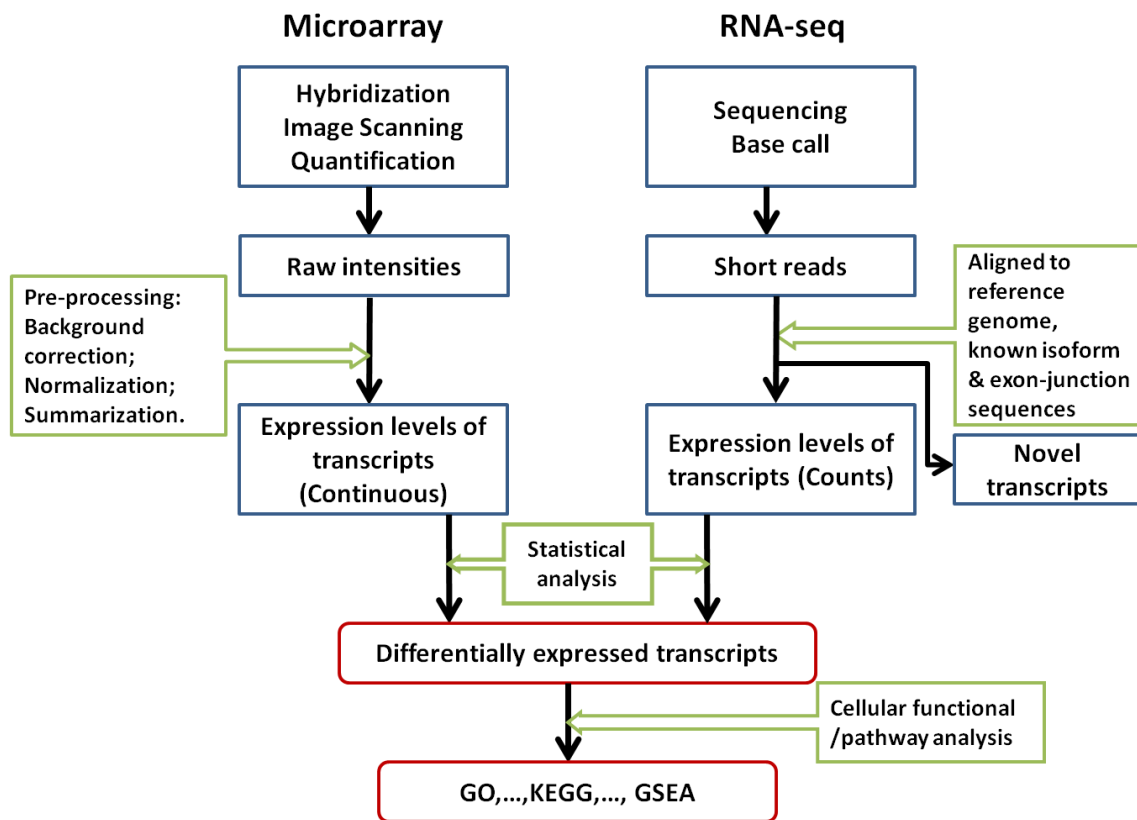


Figure 1.3 The overview of analysis workflows of microarray and RNA-seq data

(Adapted from Fang et al., 2012).

1.5.1.1 DNA microarray

A DNA microarray consist of a collection of oligonucleotide sequences immobilized in precise locations on a glass or a silicon chip in a high-density format which allows for the quantification of mRNAs from a biological sample under different conditions (Gabig and Węgrzyn, 2001). As mRNAs are the direct transcripts of genes, the changes of particular mRNAs indicate the specific gene pathways affected by toxicant

exposure (Schirmer et al., 2010). The basis of DNA microarray technology is nucleic acid hybridization with immobilized probes. Two primary microarray platforms are commonly used, cDNA microarrays, which utilize cloned probe molecules corresponding to characterized expressed sequences, and oligonucleotide microarrays, made of synthesized probes based on a priori knowledge on genome or transcriptome information (Gabig and Węgrzyn, 2001; Murphy, 2002).

A typical microarray experiment involves multiple steps which are shown in Figure 1.4. The first step is sample preparation starting by total RNA isolation from biological samples. The extracted mRNAs are converted into complementary DNA (cDNA) in a reverse-transcriptase enzyme reaction. The procedure of complementary RNA (cRNA) synthesis and amplification is also used for oligonucleotide microarray experiments. Next, the cDNA or cRNA samples are labeled, often with fluorescent cyanine dyes (i.e. Cy3 and Cy5). Labelled cDNA or cRNA samples are hybridized with the immobilised target probes. After washing steps, the slides/chips are scanned and image acquisition is followed by feature extraction, employing specialist software. The last step is data processing and analysis including pre-processing, background correction and normalization and statistical analysis.

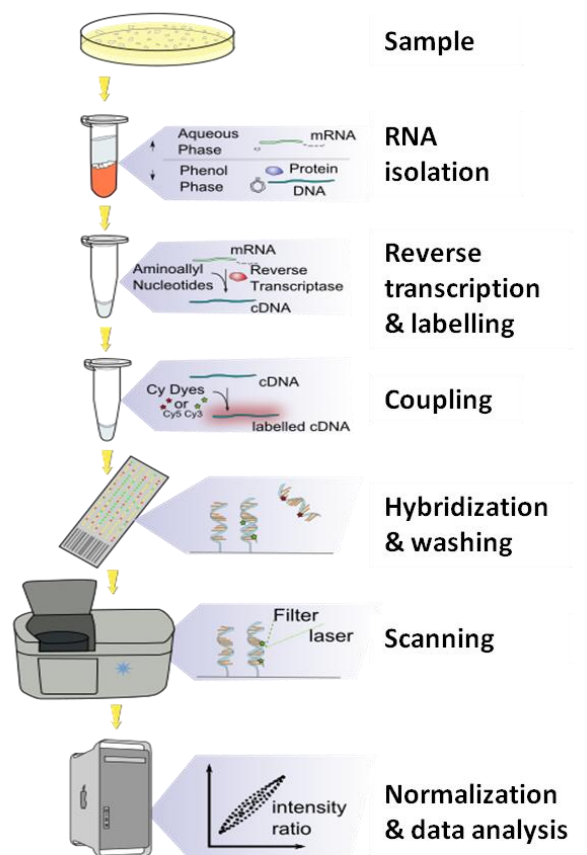


Figure 1.4 Workflow of a cDNA microarray experiment (Adapted from http://en.wikipedia.org/wiki/DNA_microarray_experiment)

1.5.1.2 RNA-seq

RNA-Seq is a recently developed approach for transcriptome profiling utilizing deep-sequencing technologies (Wang et al., 2009), which could provide the most extensive evaluation, with a wide dynamic range and higher sensitivity. The typical RNA-seq experiment involves four main steps (Figure 1.5). First, total RNA is isolated from samples of interest. Then, a library of cDNA fragments is created after RNA fragmentation or DNA fragmentation, in which each cDNA is attached with adaptors at one or both ends. The third step is high-throughput sequencing step, which produces

one read in a single-end sequencing reaction, or two reads separated by an unsequenced fragment in paired-end reactions. The fourth step is data analysis, including alignment to reference genome/transcriptome and downstream data analyses such as differential expression analysis and functional interpretation (Corney, 2013; Wang et al., 2009).

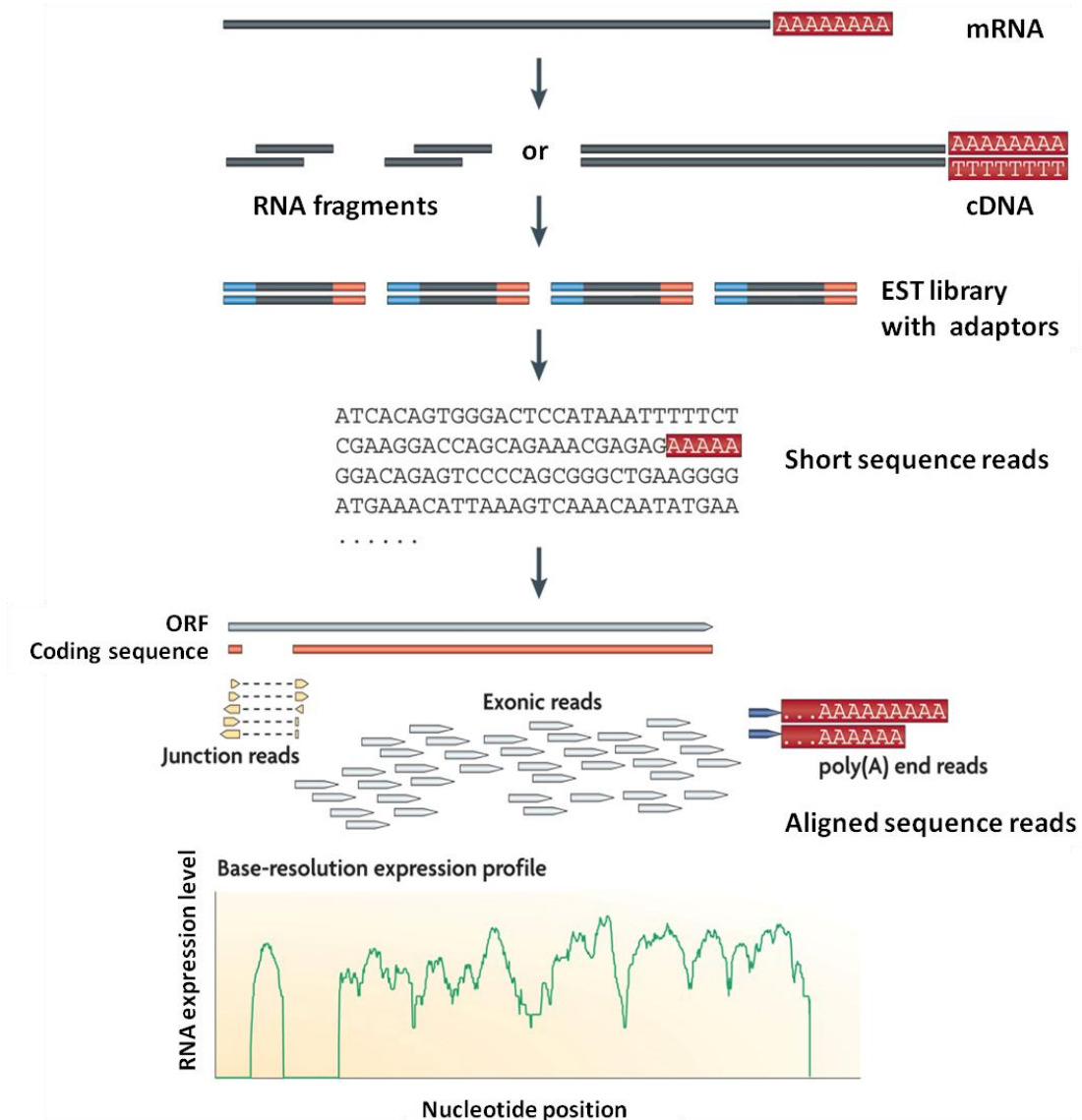


Figure 1.5 A typical RNA-Seq experiment (Adapted from Wang et al., 2009)

While RNA-seq technology offers some advantages (e.g. increased specificity and

sensitivity, wider dynamic range and detection of novel transcripts), it also suffers from some challenges such as bias introduced in library preparation and high complexity of data analysis(Chu and Corey, 2012; Wang et al., 2009). The comparison of these two technologies in different aspects (Wang et al., 2009) is shown in Table 1.3. The oligonucleotide microarray technology was employed for analyzing the gene expression of human cell lines in this thesis, because of the nature of scientific questions of this project was focusing on comparison of gene expression pattern after exposure to FRs. In addition, the local availability of a well-established microarray platform for human gene expression analysis has also been considered.

Table 1.3 Comparison of microarray and RNA-seq (Adapted from Wang et al., 2009)

	Microarray	RNA-Seq
Technology specifications		
Principle	Hybridization	High-throughput sequencing
Resolution	From several to 100 bp	Single base
Throughput	High	High
Reliance on genomic sequence	Yes	In some cases
Background noise	High	Low
Application		
Simultaneously map transcribed regions and gene expression	Yes	Yes
Dynamic range to quantify gene expression level	Up to a few-hundred fold	>8,000-fold
Ability to distinguish different isoforms	Limited	Yes
Ability to distinguish allelic expression	Limited	Yes
Practical issues		
Required amount of RNA	High	Low
Data size and storage	Small, cheap	large, expensive
Data analysis methods	Standardized	High complexity
Cost	Relatively cheap	Relatively high

1.5.2 Metabolomics

Metabolomics is the study of comprehensive collections of metabolites of diverse cellular processes in a biological system (Ramirez et al., 2013). Since these metabolites (e.g. small peptides, lipids, amino acids, nucleic acids etc.) directly reflect

the biochemical processes of the system under investigation, metabolomics analysis provides insights into both the dynamic activities of particular metabolites and the alteration of biochemical pathways caused by nutrition and environmental stresses or exogenous compound insults (Ramirez et al., 2013). Unlike the genome, transcriptome and proteome, the chemical diversity of metabolome components make their comprehensive analysis difficult by using any single analytical method (Kuehnbaum and Britz-McKibbin, 2013). Generally, two analytical platforms dominate in metabolomics; these are nuclear magnetic resonance (NMR) spectroscopy, and mass spectrometry (MS) (Bouhifd et al., 2013; Dunn et al., 2011).

1.5.2.1 NMR and MS based metabolomics

NMR has several unique advantages, such as reproducibility, quantitative analysis and automation (Bouhifd et al., 2013; Viant and Sommer, 2012). NMR is non-destructive or even non-invasive, which make it possible to detect molecules *in vivo* (Bouhifd et al., 2013; Griffin and Kauppinen, 2007). The application of NMR based metabolomics has also been used widely in toxicological studies including metabolic biomarkers discovery (reviewed in Coen et al., 2008). Proton NMR (^1H NMR) spectroscopy is suitable to the investigation of toxic events, for example, a biofluid fingerprint that reflects a toxicant-induced response can be rapidly achieved without bias (Coen et al., 2008). However, the main challenge NMR suffers from is relatively lower sensitivity compared with MS (Lei et al., 2011). Over the past decade, MS has become a powerful tool in metabolomics researches because of its high sensitivity, selectivity and dynamic ranges (Robertson, 2005; Viant and Sommer, 2012). Such advantages of MS allow MS-based metabolomics to be suitable for untargeted screening and discovering novel biomarkers or alterations in toxicity

pathways (Bouhifd et al., 2013). MS therefore met the requirements of the primary aim in this project (which is to explore the toxicity pathways perturbed by exposure to FRs). Therefore, a MS based-metabolomics approach was selected in this project. The two platforms for metabolomics application were compared by (Robertson, 2005) (Table 1.4).

Table 1.4 Comparison of analysis by Nuclear Magnetic Resonance (NMR) versus Mass Spectrometry (MS) for metabolomics applications (Robertson, 2005).

	NMR	MS
Logistics		
Capital cost		no advantage
Maintenance	advantage	
Per sample cost		no advantage
Footprint		no advantage
Required technical skill		advantage
Instrument “up-time”	advantage	
Analytical considerations		
Sensitivity		big advantage
Reproducibility (within lab)	advantage	
Reproducibility (across labs)	big advantage	
Quantitation	big advantage	
Average run speed		no advantage
Sample preparation requirements	advantage	
Sample analysis automation	advantage	
Metabonomics		
Resolvable metabolites		big advantage
Identification of unknowns		advantage
Potential for sample biasd	big advantage	
Data analysis automation		advantage

The diversity of ion sources (e.g. electrospray ionization (ESI) and electron ionization (EI)) and mass analyzer (e.g. ion trap, triple quadrupole (QQQ), time-of-flight (TOF) and quadrupole-TOF (QTOF), Fourier transform ion cyclotron resonance (FT-ICR) and Orbitrap detectors) of mass spectrometers offers multiple analysis approaches for metabolomics (Viant and Sommer, 2012). Generally, the main methods in MS

based metabolomics analysis are direct injection (or direct infusion) mass spectrometry analysis (DIMS) and hyphenated MS (coupled with gas chromatography (GC), liquid chromatography (LC) or capillary electrophoresis (CE)) (Bouhifd et al., 2013).

DIMS analysis of crude mixtures of metabolites provides a high throughput screening tool usually using high resolution mass spectrometers (i.e., Orbitrap, TOF and FT-ICR mass spectrometers)(Viant and Sommer, 2012). However, the limitations of DIMS analysis are ion suppression and MS peak identification. These limitations can be reduced by the chromatography coupled MS analyses (Lei et al., 2011). The benefits of chromatographic separation of metabolites prior to MS analyses are: (1) reducing ionization suppression in a complicated mixture, (2) improving separation of isobaric metabolites, (3) generating additional data (i.e. retention time) valuable for metabolite annotation, and (4) enhancing the accurate quantification of individual metabolites (Lei et al., 2011).The cost of these benefits in chromatography-coupled MS analysis is that they are time-consuming, thus resulting in lower throughput compared with DIMS analysis.

In short, currently, no single analytical tool can meet all requirements in metabolomics which needs to accurately identify and quantify thousands of small molecules of interest in a high throughput way (Bouhifd et al., 2013). Hence, the selection of the most suitable analytical tool is generally a compromise between advantages and disadvantages of the available tools (Bouhifd et al., 2013). As illustrated in Figure 1.6, DIMS provides high sensitivity and high-throughput data, but suffers from the limitations of metabolite annotation (Taylor, 2010).

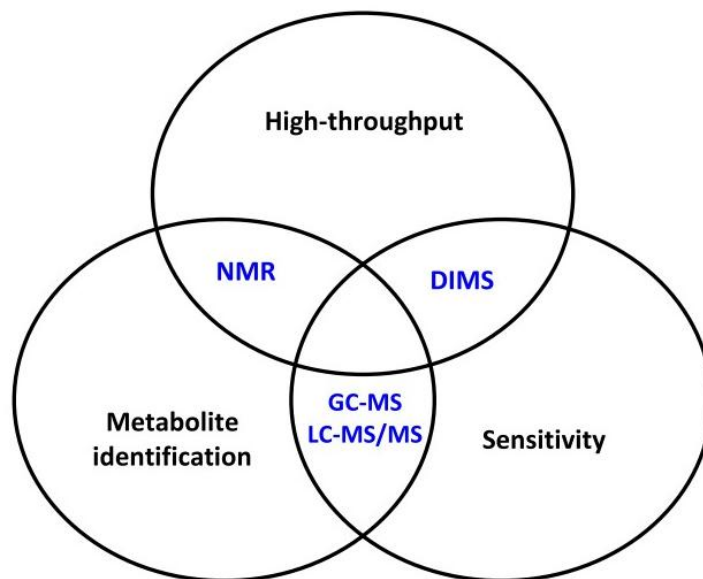


Figure 1.6 *The trade-off between analytical platforms and the objectives of metabolomics* Taken from (Taylor, 2010).

1.5.2.2 DIMS based-metabolomics experiment

The DIMS approach utilizing high resolution and high mass accuracy (<1 ppm) mass spectrometers is suitable for large-scale metabolic fingerprinting studies (Viant and Sommer, 2012). The work presented in this thesis used FT-ICR MS with ultrahigh resolution (>1,000,000 at 400 m/z), which matches the requirement of this project's primary aim to apply metabolomics to distinguishing the different molecular responses to FRs exposure and to identifying potential toxic effects and the underlying mechanisms of toxicity of FRs.

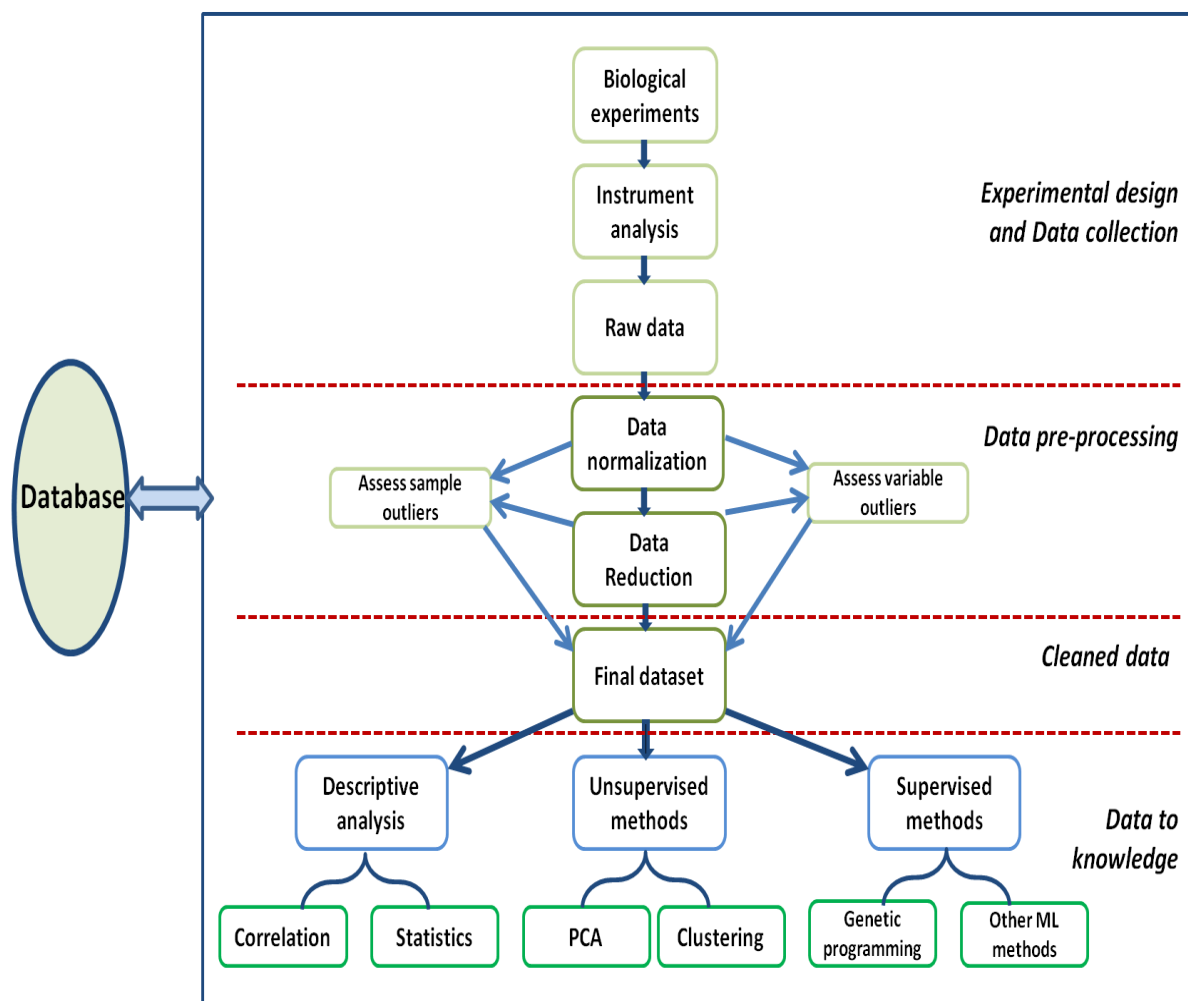


Figure 1.7 An overview of a pipeline of metabolomics experiment (Adapted from Brown et al., 2005).

Similar to the pipeline illustrated in Figure 1.7, the main steps of DIMS-based metabolomics experiments also consist of (1) experimental design and data collection, (2) data pre-processing, (3) cleaned data for statistical analysis and (4) data to knowledge (i.e. metabolites annotation and pathway analysis).

Southam et al. (2007) developed a “SIM-stitching” method for direct infusion FT-ICR mass spectrometry-based metabolomics. This method collects multiple overlapping selected ion monitoring (SIM) windows (using only 7 SIM windows each of m/z 100, overlapping by m/z 30, over the m/z range 70-590) in a short time analysis (2.25 mins

per sample)(Weber et al., 2011), which are then stitched together to generate a “SIM-stitched” spectrum with dynamic range (up to 16,000) and high mass accuracy (0.16 ppm).The detailed procedures of data processing (Figure 1.8) were also reported by (Kirwan et al., 2014), which includes a three-stage filters (TIC filter, replicate filter and sample filter), probabilistic quotient normalization (PQN) , missing value imputation using k-Nearest Neighbours (KNN) algorithm and generalised logarithm (Glog) transformation.

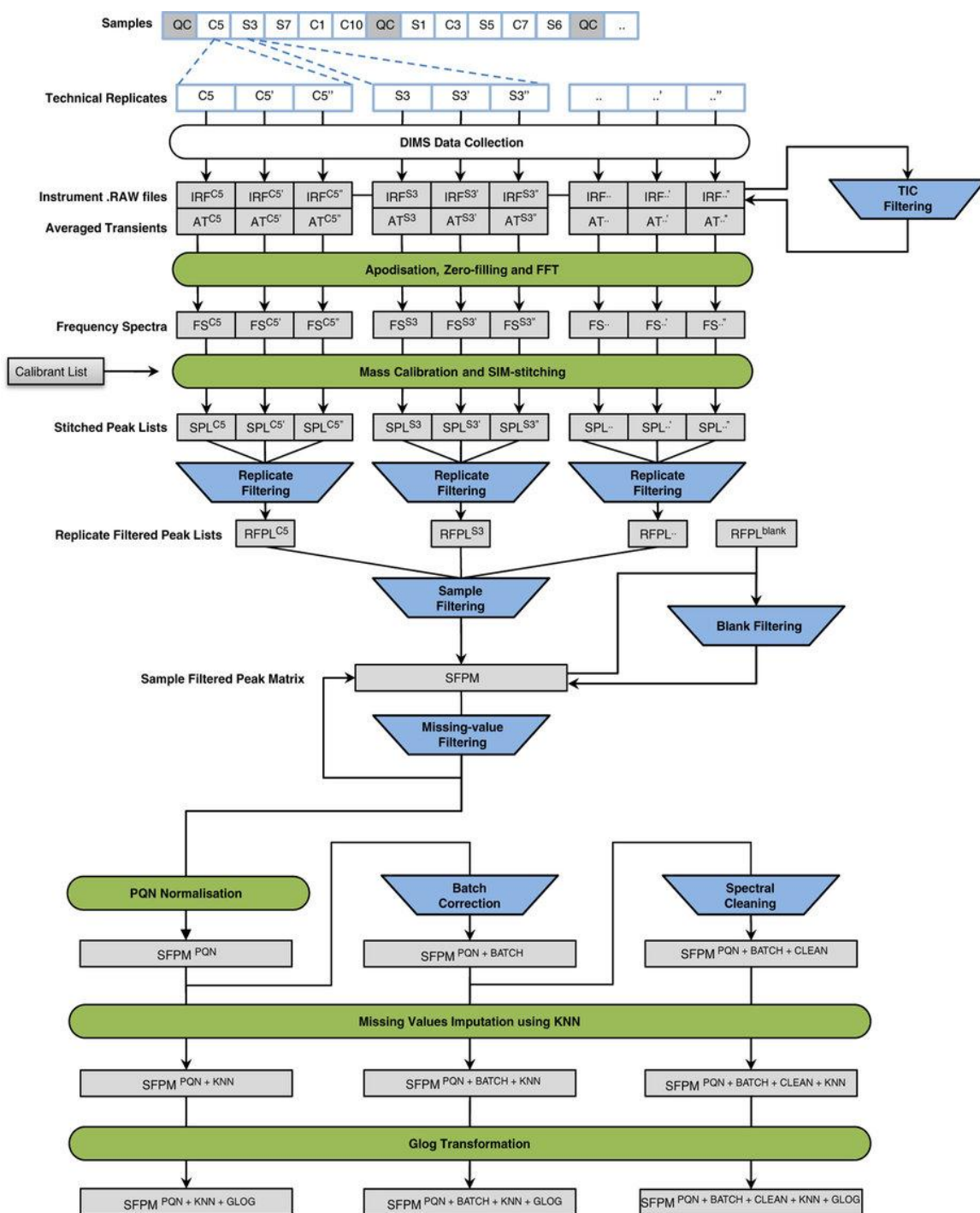


Figure 1.8 Data processing workflow for direct infusion FT-ICR mass spectrometry-based metabolomics dataset Taken from (Kirwan et al., 2014).

After data processing, a DIMS dataset can be subjected to statistical analysis. For univariate analysis, t-tests or ANOVA are often employed. Since the size of

metabolomics datasets is considerably large, the multiple comparisons of variables will produce a large number of false positives (Robertson et al., 2007). Thus, the false discovery rate (FDR) is introduced for calculating corrected significance level (Benjamini and Hochberg, 1995). The MS peak will be considered to be changing significantly if the FDR adjusted p-value is smaller than the criteria (adjusted $p < 0.05$). For multivariate analysis, unsupervised methods (e.g. principal component analysis (PCA)) or supervised methods (e.g. partial least squares discriminant analysis (PLS-DA)) can be applied. PCA has been widely used in analysis of various types of omic data, providing an overview of class separation, trends and outliers on the entire dataset (Bouhifd et al., 2013). PCA decomposes the data into scores and loadings, which indicate the relationship between samples and the correlations between the variables (MS peaks), respectively (Robertson, 2005). Principal components (PCs) represent degradation of variance in the data, where PC1 represent the greatest variance, followed by PC2 then PC3 and so on (Robertson 2005). The PC scores plots (i.e. PC1 versus PC2) are often displayed to show the similarities and differences between individual samples (Bouhifd et al., 2013; Robertson, 2005).

The putative annotation of MS peaks can be achieved by searching against metabolites database, such as Kyoto Encyclopaedia of Genes and Genomes (KEGG), Human Metabolome Database (HMDB) and LIPIDMAPS. For example, DIMS peaks collected by FT-ICR MS can be allocated with putative empirical formulae and metabolite names by using the metabolite annotation package MI-Pack (Weber and Viant, 2010), which is based on single peak search (SPS) and transformation mapping (TM) algorithms.

Pathway analysis allows us to decipher a list of putative metabolites which might be

linked to specific biochemical pathways or gene regulatory networks. However, such analysis can only be effective for known metabolic pathways (Bouhifd et al., 2013). Although pathway analysis of metabolomics data are still in their infancy, a few software packages have provided explorative tools to help generate hypothesis related to metabolic disruptions. For example, software available includes: IMPaLA (Kamburov et al., 2011), MPEA (Kankainen et al., 2011), MetaboAnalyst (Xia and Wishart, 2011; Xia et al., 2012) and MSEA (Persicke et al., 2012).

1.6 Research aims and objectives

With intensive and global usage, flame retardants have performed an important role in preventing fires for decades; however, there are increasing concerns about the potentially adverse effects of these chemicals as studies documenting human exposure to FRs have become ubiquitous (Birnbaum and Staskal, 2004; Costa et al., 2008; Sjodin et al., 2003).

Therefore, the overall aim of this project was to expand our knowledge about the molecular mechanisms of the potentially toxic effects of FRs following human exposure, using *in vitro* models. The specific objectives are:

1. To investigate the transcriptomic and metabolomic responses of A549 lung cancer cells and HepG2/C3A cells exposed to HBCD as a representative and commonly used brominated FR.
2. To analyze the toxicogenomic responses to TDCIPP as a representative and commonly used organophosphorus FRs, at a series of concentrations in HepG2/C3A cells and A549 cells.
3. To evaluate the potentially toxic effects of mixtures of FRs (HBCD, TDCIPP, TCIPP and TCEP) as well as indoor dust extracts at concentrations relevant to indoor environmental exposures to humans, using transcriptomic and metabolic approaches in HepG2/C3A cells.

These objectives are addressed in Chapters 3, 4 and 5 respectively.

CHAPTER 2 Materials and methods

Generic methods and materials used in this thesis are presented in this chapter. The details of different FRs exposure experiments used only within a single chapter are described in chapters 3, 4 and 5, respectively.

2.1 Chemicals and reagents

All chemicals, including 1,2,5,6,9,10-hexabromocyclododecane (HBCD) (CAS Number: 3194-55-6, purity >95%), tris (1, 3-dichloro-2-propyl) phosphate (TDCIPP) (CAS Number: 13674-87-8, purity >97%), tris(2-chloroisopropyl) phosphate (TCIPP) (CAS Number: 13674-84-5, purity >95%) and tris(2-chloroethyl) phosphate (TCEP) (CAS Number: 115-96-8, purity >95%) were obtained from Sigma-Aldrich company Ltd. (Dorset, UK) unless otherwise stated.

2.2 Cell culture

A549 cells (adenocarcinomic human alveolar basal epithelial cells) were from our group's storage and cultured in DMEM medium (Sigma-Aldrich, Dorset, UK) supplemented with 10% heat-inactivated fetal bovine serum (FBS) (PAA, Cölbe, Germany), 100 U penicillin/mL and 100 µg streptomycin/mL (PAA, Cölbe, Germany), 2 µM L-glutamine (PAA, Cölbe, Germany) and incubated in 37°C with humidified air containing 5% CO₂. HepG2/C3A cells were generously provided by Prof. R. Blust from the University of Antwerp, Belgium. HepG2/C3A cells were cultured in Williams' E medium (Sigma-Aldrich, Dorset, UK) supplemented with 5% heat-inactivated FBS (PAA, Cölbe, Germany), 100 U penicillin/mL and 100 µg streptomycin/mL (PAA, Cölbe, Germany), 4 µM L-glutamine (PAA, Cölbe, Germany) and 0.4 µM sodium pyruvate (Sigma-Aldrich, Dorset, UK) and incubated in 37°C with humidified air containing 5% CO₂. Cells were digested with 0.25% trypsin-EDTA and sub-cultured at

80% to 90% confluence. Exponentially growing cells were used for all assays.

2.3 Cytotoxicity assays

The cytotoxicity of FRs to A549 cells and HepG2/C3A cells were assessed using 3-(4,5-dimethylthiazol-2-yl)-2,5-diphenyltetrazolium bromide (MTT) assays, Cell Counting Kit-8 (CCK-8) assay or the adenylate kinase (AK) assay.

2.3.1 MTT assay

A549 cells or HepG2/C3A cells were seeded in 96-well plates and incubated at 37°C with a humidified atmosphere containing 5% CO₂ for 24 hours. Then, cells were treated with FRs at a range of concentrations for 24 or 72 hours. Solvent controls (no FRs treatment) and blank controls (only medium) were also included, each with 6 replicates. After 24 or 72 hours exposure, the culture media were removed and each well was washed with 100 µL phosphate buffered saline (PBS). 90 µL fresh media and 10 µL MTT solution (5mg/mL) were added to each well and mixed. The 96 well plates were then incubated at 37°C for an additional 3 hours. Culture supernatant was removed, 100 µL pure DMSO was added into each well and culture plates were gently rocked at low speed for 10 minutes to fully dissolve the blue crystals.

Absorbance was measured at 530 nm (A_{530}) using a plate reader (Tecan Spectrafluor Plus, Männedorf, Switzerland) against a DMSO blank. The percentage of cell viability was calculated at each concentration of flame retardant according to the following formula: cell viability (%) = $(A_{530} \text{ Treatment group} - A_{530} \text{ Blank}) / (A_{530} \text{ Solvent Control} - A_{530} \text{ Blank}) \times 100\%$. Dose-response curves were plotted and the half maximal effective concentration (EC₅₀) values were then calculated by applying equation (1) in OriginPro8 (OriginLab, USA):

$$y = A1 + \frac{A2 - A1}{1 + 10^{(\text{LOG}x0-x)p}}$$

where A1 is the bottom asymptote, A2 is the top asymptote, p is the slope of the gradient, y is the viability as a percentage of control, and x is the nominal concentration of the test compound.

2.3.2 CCK-8 assay

The CCK-8 assay was also employed to evaluate the potential cytotoxicity of FRs using a commercial kit which is more convenient to use. According to the manufacturers' instructions (Dojindo Laboratories, Kumamoto, Japan), HepG2/C3A cells or A549 cells were cultured in a 96-well plate overnight and the cells were treated in six replicates with several concentrations of FRs in culture medium for 24 hours or 72 hours. Then, 10 μ L of CCK-8 solution was added into each well to treat the cells for 1 hour and the absorbance at 460 nm (A_{460}) was measured using a plate reader (Tecan Spectrafluor Plus, Männedorf, Switzerland). Solvent control cells were considered as 100% viable. The viability of cells in the CCK-8 assays, in terms of EC_{50} values, was calculated using the same approach as for the MTT assay.

2.3.3 AK assay

The ToxiLight™ BioAssay kit (Lonza, Switzerland) was used, measuring the release of adenylate kinase from the damaged cells which can reflect the integrity of cell membrane. Following the manufacturers' instructions, after 24 or 72 hours treatments, 20 μ L of cell supernatants were transferred to a luminescence compatible 96 well plate, with 100 μ L AK detection reagent for 10 mins. The 100% lysates of cells without treatment were used as total adenylate kinase control. 1-second integrated luminescence was measured using a Tecan M200 Pro Infinite plate reader

(Männedorf, Switzerland). Ratio of AK release relative to total cell lysis was calculated using the direct luminometer light output (Relative Light Unit (RLUs)). The percentage of cytotoxicity was calculated at each treatment according to the following formula:
Cytotoxicity (%) = Ratio of AK release at treatment group / Ratio of AK release at Solvent Control group × 100%.

2.3.4 Cytotoxicity of HBCD to proliferating and confluent cells

To compare the cytotoxicity of HBCD (60 µM) to proliferating cells and confluent cells, additional protein content assay (indicating the number of cells) while the CCK-8 assay (reflecting the mitochondrial dehydrogenase activity) and AK assay (assessing the loss of cell integrity) were also employed. Specifically, HepG2/C3A cells were cultured in 96-well plates at different cell densities (1× 10⁴ cells; 2× 10⁴ cells; 4× 10⁴ cells and 6× 10⁴ cells per well) which represent a gradient from proliferating cells to confluent cells. After an overnight acclimatisation, cells were treated with 60 µM HBCD or 10 µM DMBA (7,12-dimethylbenz[a]anthracene; positive control) in six replicates. Solvent control cells were treated with 0.5% DMSO (v/v). After a 24-hour exposure, the CCK-8 assays and AK assays were performed as above described on the proliferating (cultured at relatively low density) and confluent cells (cultured at relatively high density).

For the total protein content assay, the BioRad DC Protein Assay (BioRad, USA) was employed. After treatment, cells were washed by PBS three times and lysed by RIPA buffer for 15 mins. The total protein content of cell lysates was determined the following manufacturer's instructions, in which absorbance at 645 nm (A_{645}) to indicate the protein concentration was measured using a plate reader (Tecan Spectrafluor Plus, Männedorf, Switzerland).

Test results for each assay were expressed as a percentage of the untreated control \pm standard error (SE) or standard deviation (SD). Control groups were set as 100%. Differences between treated samples and the controls were evaluated using the statistical analysis package Minitab16. Statistically significant differences were set at $p < 0.05$. At least three independent experiments with six replicates for each group were conducted for each toxicity endpoint.

2.4 Transcriptomics analysis

2.4.1 RNA isolation

Total RNA of cells harvested as described above were extracted using Qiagen's mini RNeasy Kit and QIAshredder (Qiagen, Crawley, UK) with subtle modification of manufacturer's instructions. Briefly, harvested cell pellets were centrifuged at 1,500 g (4,000rpm), 5 mins and the supernatant (methanol solution) were removed with Pasteur pipette as much as possible. Buffer RLT (350 μ L per tube) were added to cell pellets in Eppendorf tube. The whole lysate was transferred directly into QIAshredder spin column and centrifuge at full speed for 2 mins. One volume (i.e. 350 μ L) 70 % ethanol was added to lysate and was mixed well by pipetting. Then, totally 700 μ L of sample including any precipitate, was transferred into RNeasy spin column. After centrifuge at 8,000 g (10,000 rpm) for 15 seconds, flow through was discarded. The DNase digestion step was added to yield the high quality of RNA samples as following steps: 350 μ L Buffer RW1 was added to spin column and after centrifuged at 8000 g (10,000 rpm) for 15 seconds to wash membrane, flow through was discarded. Then, 80 μ L DNase I incubation mix (10 μ L DNase I stock solution to 70 μ L Buffer RDD) was directly added to spin column membrane and incubate at room temperature for 15 mins. After incubation, 350 μ L Buffer RW1 was added to spin

column and centrifuged at 8,000 g (10,000 rpm) for 15 seconds. Then 500 μ L Buffer RPE was added to spin column to wash membrane twice with centrifuge at 8,000 g (10,000 rpm) for 15 seconds or 2 mins respectively. Then a new eppendorf tube was placed into the spin column, and 30-50 μ L RNase-free water was *directly* added to spin column membrane (incubate the RNeasy spin column on the bench for 10 mins with RNase-free water before centrifuging) to elute RNA with centrifuge at 8,000 g (10,000 rpm) for 1 minute. RNA was quantified with a NanoDrop 1000 spectrophotometer (Thermo Scientific, Waltham, MA), and the integrity of RNA was evaluated with a Agilent 2100 Bioanalyzer (Agilent Technologies, Santa Clara, CA). Only good quality RNA with RNA integrity numbers (RINs) greater than 7.5 were used for subsequent gene expression analyses or microarray experiments.

2.4.2 Microarray analysis

In the sub-project of HBCD study, six replicates of RNA samples from A549 cells (randomly selected from the total of eight replicates, to reduce costs) were used for each of the HBCD treated groups (2 nM (*Very low*), 20 nM (*Low*), 200 nM (*Medium*) and 2 μ M (*High*)) while the solvent (DMSO) control group comprised of eight replicates. For RNA samples from HepG2/C3A cells, a total of 16 samples were subjected to microarray analyses, comprising six samples from the HBCD (4 μ M) treated group, six from the solvent (DMSO) control group, and the remaining four from the DMBA (10 μ M) positive control group.

In the second sub-project of TDCIPP study, only HepG2/C3A cells and A549 cells exposed to 10 μ M (*Medium concentration*) and 100 μ M (*High concentration*) in the FBS-containing media for 24 hours were analysed (n=4). The solvent control groups in each treatment condition were treated with 0.5% DMSO (v/v) with the same

number of replicates for omics analyses.

In the third sub-project of mixture of FRs study, HepG2/C3A cells were exposed to SRM2585 dust extract (equivalent to ca. 0.6mg dust per million cells), Mix 1, Mix 2, DMBA (2 μ M), HBCD (4 μ M) or 0.1% (v/v) DMSO as control for 72 hours with four replicates in each group.

The procedures for microarray analysis were performed following the manufacturer's protocols (Agilent Technologies, Santa Clara, CA). Briefly, following synthesis of cRNA from 50 ng of total RNA per sample, the probe RNA was amplified and labelled with Cy3-CTP (Agilent One-Color RNA Spike-In Kit and QuickAmp Labelling kit, Agilent Technologies). The Cy3-labeled cRNA was then fragmented and hybridized to Agilent Human gene expression 8x60k microarray (Design ID: 028004 and 039494), at 65 °C for 17 hours. The hybridised microarrays were scanned with an Agilent G2565BA microarray scanner (Agilent Technologies, Santa Clara, CA) at OD₅₃₅ for Cy3. Scanned images were processed according to manufacturer's instructions (Agilent Technologies, Santa Clara, CA) and the microarray results were extracted using Agilent Feature Extraction software (Agilent Technologies, Santa Clara, CA).

Microarray data processing and analyses were performed within GeneSpring version GX7.3.1 and GX11 (Agilent Technologies, Santa Clara, CA) and MultiExperimental Viewer v4.9 (Saeed et al., 2003). In the sub-project of HBCD study, microarray data were first Quantile normalized using GeneSpring version GX11, batch effects were corrected using ComBat (Johnson et al., 2007). In other sub-projects, Microarray data were first median normalized using GeneSpring version GX7.3. To visualise the similarities and differences in the gene expression profiles and to identify any significant trends, PCA was conducted using PLS_Toolbox Eigenvector Research,

Wenatchee, WA) in MatLab. ANOVA (or t-test) with a Tukey-Kramer's post-hoc test was conducted on the scores for the top three or four PCs from each model (FDR <10%).

The log₂ transformed normalised microarray dataset was subjected to Significance Analysis of Microarrays (SAM) (Tusher et al., 2001), embedded in MultiExperimental Viewer v4.9, to identify significant differential gene expression between groups. The delta parameter was adjusted to achieve a FDR <5% and this delta value were applied to determine significantly changed genes.

Any significantly altered genes were then analysed using the Functional Annotation Clustering (FAC) tool contained in the Database for Annotation, Visualisation and Integrated Discovery (DAVID) (Huang et al., 2009) to determine the most relevant pathways and processes based on the Gene Ontology annotation function, with FDR <5% selected for the significant functions. Gene set enrichment analysis (GSEA) (Subramanian et al., 2005) was also applied to the above normalised microarray dataset to determine differentially expressed gene sets in FRs treated groups comparing to control.

Microarray datasets are available in the ArrayExpress database (www.ebi.ac.uk/arrayexpress): E-MTAB-2173 (HBCD_1), E-MTAB-2174 (HBCD_2), E-MTAB-3323 (TDCIPP) and E-MTAB-3324 (mixture of FRs).

2.4.3 Quantitative real time-PCR analysis

Reverse transcription real time-PCR were performed to quantify the mRNA levels of a selected set of genes in A549 or HepG2/C3A cells from different treatment group across this project. Firstly, 1 µg of DNase-treated total RNA was reverse transcribed to cDNA according to the manufacturer's protocol with a Tetro cDNA synthesis Kit

(Bioline, UK). Real-time PCR reactions were carried out in a 96-well reaction plate format on a Maxpro 3005 Detector (Agilent) using the SensiFAST SYBR Hi-ROX kit (Bioline, UK). The primers of selected genes (Table 2.1) were designed and bought from Sigma-Aldrich, UK. PCR reactions were performed in a total volume of 20 μ L containing 500 nM of each primer and 1 μ L of cDNA template. Thermal cycling was initiated with an initial incubation at 95 °C for 2 min. After that, 40 cycles of PCR were performed, with each PCR cycle consisting of a heating step at 95 °C for 15 s and an annealing/extension step at 60 °C for 30 s. As an endogenous control, the expression of the ACTB gene was measured in parallel. Negative controls were included in the same plate. A melting curve analysis was performed to ensure that single product was generated. Each biological sample was analysed in quadruplicate, and each dose group contained four biological replicates. Relative gene expression was analyzed using the $2^{-\Delta\Delta C_t}$ quantification method (Livak and Schmittgen, 2001) and tested for significance using one-way ANOVA and Tukey's test ($p < 0.05$) in Minitab16 (Minitab Inc., State College, Pennsylvania, USA).

Table 2.1 Genes, primers, and T_m values used in the RT-PCR analysis

Gene symbol	GenBank accession #	Sequence : (5' to 3')	T _m	PCR product size (bp)
ACTB	NM_001101	Forward: GACGACATGGAGAAAATCTG Reverse: ATGATCTGGGTCATCTTCTC	59.7 58	131
CDK2	NM_001798	Forward: TGTTATCGCAAATGCTGC Reverse: TCAAGAAGGCTATCAGAGTC	61 56.1	125
CYP1A1	NM_000499	Forward: CATTAAACATCGTCTTGACC Reverse: TCTTGATCTTTCTCTGTACC	59.4 57.4	114
CYP3A4	NM_017460	Forward: AGTCTTTCCATTCTCATCC Reverse: TGCTTTTGTGTATCTTCGAG	59.5 58.1	129
EEF1A1	NM_001402	Forward: TGGTATTGGTACTGTTCTCTG Reverse: CTTCACTCAAAGCTTCATGG	57.5 60	134
GJB1	NM_001097642	Forward: CAGGGAGGTGTGAATGAG Reverse: AAGATGAAGATGACCGAGAG	59.2 58.4	115
GSR	NM_000637	Forward: GACCTATTCAACGAGCTTTAC Reverse: CAACCACCTTTCTCCTTG	57.1 61.1	104
ABCC2	NM_000392	Forward: AAATTGCTGATCTCCTTTC Reverse: GATAGCTGTCCGTACTTTAC	60.8 54.7	159
ATP5J2	NM_004889	Forward: GTTTCAAAGAGTTACTACCG Reverse: AAGGAGTAGCTAAAGAGCAC	57 54.6	111
NQO1	NM_000903	Forward: GCAGACCTGTGATATTCCAGTT Reverse: ATGGCAGCGTAAGTGAAGC	57.5 56.7	113
NDUFB3	NM_002491	Forward: AGCATCACTAAAAACATGGC Reverse: GTATCTCCAAGCTTCATTGC	59.2 58.9	174
MT1L	AJ011772	Forward: AACCTCCTGCAAGAAGAG Reverse: CAGGTTGCTCTGTTACATC	57 57.3	151

2.5 Metabolomics analysis

2.5.1 Extraction of metabolites

2.5.1.1 Extraction of metabolites (cells harvested from T75 culture flask)

After 24 hours exposure, A549 cells were rapidly washed with 10 mL PBS at room temperature twice. Then, 10 mL 60% methanol/40% water (pre-cooled on dry ice) was added into flask to quench cells. The residual was removed and the quenched flask was kept on the dry ice until harvest. After washing and quenching, 4.0 mL 100% methanol (pre-cooled on dry ice) was added into the flask. Cells were carefully scraped into methanol solution on dry ice and then transferred into a 5 mL cryovial (pre-cooled on dry ice), mixed well by pipetting several times and split in three parts (one for transcriptomic analyses, the second one for DIMS analysis and the third one

for NMR analysis (NMR data were not included in this study)). Specifically, 0.4 mL cell-methanol solution from a 5 mL cryovial was transferred into a 2 mL Eppendorf tube and centrifuged for 5 mins at 4000 rpm, -9°C and the supernatants were removed by Pasteur pipette. The cell pellets were then frozen at -80°C until extraction of RNA for transcriptomic analysis. The rest of cell-methanol solution (3.6 mL) went to freeze/thaw cycle (Liquid N₂/Dry ice) three times before distributing into three 2 mL Eppendorfs (labelled A and B (1.6 mL per tube) for NMR analysis and labelled C (0.4 mL per tube) for MS analysis separately).

For extraction of metabolites, cell pellets in 400µL methanol/water solution were extracted by adjusting the solvent ratios to methanol/chloroform/water of 1:1:0.9 (v/v/v). After vortexing and centrifuging the mixture had been separated into two phases (upper polar phase and lower non-polar phase). 300 µL aliquots of the polar phase were transferred into clean 1.5 mL Eppendorf tubes and then dried using a speed vac concentrator (Thermo Savant, Holbrook, NY) for 4 hr with a fixed temp of 35 °C. All dried samples were then frozen at -80 °C until analysis. The non-polar aliquots were not used in this study.

2.5.1.2 Extraction of metabolites (cells harvested from 6 well plate)

After 24 hours or 72 hours exposure, cells cultured in the 6 well plates were quickly washed with 2 mL PBS twice before the 6-well plates were quenched on liquid nitrogen for 60 seconds. Then, 600 µL 80% methanol (pre-cooled on dry ice) was added into each well and the cells were scraped from the bottom of the wells while resting the plate on dry ice. Each cell pellet in the aqueous methanol solution (combining with additional 400 µL 80% methanol to wash the well) was transferred into a glass vial. The glass vial was pre-filled into 600 µL pre-cooled chloroform and

340 μL H_2O . Then the well was washed with 400 μL 80% methanol (pre-cooled on dry ice) and all contents were transferred into the above-mentioned glass vial for the following metabolites extraction. After adjusting the ratio of methanol:chloroform:water (v/v/v) to 1:1:0.9, glass vials were vortexed for 30 s three times, at 30 s intervals. The glass vials were then cooled on dry ice for 10 mins before 10 mins centrifugation at 1800 rcf at -9°C . After vortexing and centrifuging, the mixture separated into two phases (upper polar phase and lower non-polar phase). Next, 300 μL aliquots of the polar phase were transferred into clean 1.5mL Eppendorf tubes and then dried in a speed vac concentrator (Thermo Savant, Holbrook, NY) for 4 hours. 300 μL aliquots of the non-polar phase were transferred into clean 1.8mL glass vial and then were dried under a stream of nitrogen to minimise oxidation. All dried samples were then stored at -80°C until analysis.

2.5.2 Direct infusion mass spectrometry analysis

The dried polar extracts of cells were re-suspended in 75 μL 80:20 (v/v) methanol:water (HPLC grade) with 0.25% formic acid (for positive ion mode) or 20 mM ammonium acetate (for negative ion mode), vortexed and centrifuged at 14000 rpm, 4°C for 10 mins. (For the dried non-polar extracts of cells, it was re-suspended in with 2:1 (v/v) MeOH:chloroform with 5 mM ammonium acetate.) Each sample was loaded into three wells of a 96-well plate (10 μL per well) and then analysed (in triplicate) using direct infusion Fourier transform ion cyclotron resonance mass spectrometry in negative ion mode or positive ion mode (for polar metabolomics) and negative ion mode (for lipidomics) (LTQ FT Ultra, Thermo Fisher Scientific, Germany, coupled to a Triversa nanoelectrospray ion source, Advion Biosciences, Ithaca, NY, USA). Mass spectra were recorded utilizing the selected ion monitoring (SIM) stitching approach from m/z 70 to 590 (for polar metabolomics) or from m/z 100 to

2000 (for lipidomics) (Southam et al., 2007) and then processed using custom-written Matlab scripts as previously reported (Kirwan et al., 2014; Payne et al., 2009; Southam et al., 2007). In brief, time domain ('transient') data were collected, Fourier transformed and internally mass calibrated. Only mass spectral peaks with a signal-to-noise ratio above 3.5 were retained. Mass spectra of the three technical replicates for each sample were filtered into a single peak list (with only those peaks present in ≥ 2 of the 3 spectra retained). Each filtered peak list (one per sample) was then further filtered to retain only those peaks that were present in 80% of all biological samples in the entire dataset, and missing values were imputed using the k-nearest neighbours (KNN) algorithm. The resulting matrices of peak intensity data (termed "DIMS dataset") were normalised by the probabilistic quotient (PQN) method prior to statistical analyses.

For univariate statistical analysis, one way ANOVA (or t-test) with Benjamini-Hochberg correction was conducted on the peaks in the normalised DIMS datasets to determine whether they changed intensity significantly between control and FRs or other treatment groups (at a false discovery rate (FDR) $< 10\%$ to correct for multiple hypothesis testing). For multivariate statistical analysis, the normalized DIMS datasets were generalized log transformed and principal component analysis performed using PLS_Toolbox (Eigenvector Research, Wenatchee, USA) in MatLab (version 7, the Math-Works, MA, USA). ANOVA (or t-test) with a Tukey-Kramer's post-hoc test was conducted on the PC scores for the top few principal components from each model (with an FDR of $<10\%$) to evaluate the statistical significance of the treatments on the basis of the overall metabolic profiles.

2.5.3 Putative annotation and Pathway analysis

For significantly changed DIMS peaks, putative empirical formulae and metabolite names were assigned by searching against the Human Metabolome Database (HMDB) and Kyoto Encyclopedia of Genes and Genomes (KEGG) and/or LIPIDMAPS database, using the metabolite annotation package MI-Pack (Weber and Viant, 2010) with an error window of 1 ppm.

Putative annotated metabolite names of significant DIMS peaks from the above databases were combined together, generating a list of significantly changed DIMS peaks from polar metabolomics dataset with one or more putative metabolite names. A list of annotated metabolites names was then submitted into IMPaLA (Kamburov et al., 2011) in compound list format using Fisher's Exact test for pathway over-representation analysis. Putative annotation of significantly changed DIMS peaks from non-polar DIMS dataset was not subjected to pathway over-representation analysis due to the less reliable annotation results.

2.6 Quantification of FRs in HepG2/C3A cells and in cell media

(work conducted by Dr. Mohamed Abou-Elwafa Abdallah, University of Birmingham)

2.6.1 Quantification of HBCD levels in HepG2/C3A cells and cell media after exposure

To measure the cellular uptake of HBCD after exposure, their concentrations were measured in treated cells and media (both with and without fetal bovine serum) after 24 hours using LC-MS/MS (Van den Eede et al., 2012). Briefly, 10 ng of each of ¹³C-labelled α - and β -HBCDs and 25 ng ¹³C-labelled γ -HBCD (supplied in 10 μ L

methanol) were added as internal (surrogate) standards while the samples were extracted from weighed cell pellets and cell media using liquid-liquid extraction with hexane:dichloromethane (DCM) (3:2) mixture. Chromatographic separation of the target analytes was achieved using a dual pump Shimadzu LC-20AB Prominence LC equipped with a SIL-20A autosampler, a DGU-20A3 vacuum degasser and an Agilent Pursuit XRS3 C₁₈ reversed phase analytical column (150 mm × 2 mm i.d., 3 μm particle size). Mass spectrometric analysis was performed using a Sciex API 2000 triple quadrupole mass spectrometer operated in negative electrospray ionisation mode.

The concentrations of HBCD diastereomers in the samples were calculated according to the response factors of the respective ¹³C-labelled internal standard for each diastereomer. The recovery ratios were calculated from the total amount of α-, β- and γ-HBCDs (ΣHBCDs) in the cell pellets after exposure, divided by the nominal amount that was added into the exposure media. Average concentrations of ΣHBCDs detected in the cell media were also calculated where each treatment group included three biological replicates.

2.6.2 Quantification of TDCIPP, TCIPP, TCEP and HBCD levels in HepG2/C3A cells and cell media

To evaluate the cellular uptake of FRs after exposure, their concentrations were measured in treated cells and cell media after 24 hours or 72 hours using LC-MS/MS according to a previously reported method (Abdallah et al., 2015b). Briefly, 10 ng of each of ¹³C- α-, β-, γ-HBCDs and d₁₅-TPhP (supplied in 10 μl methanol) were added as internal (surrogate) standards. Samples were extracted from weighted cell pellets and cell media using liquid-liquid extraction with hexane:ethylacetate (1:1) mixture.

Chromatographic analysis was conducted using a dual pump Shimadzu LC-20AB Prominence liquid chromatography equipped with SIL-20A autosampler, a DGU-20A3 vacuum degasser and an Accucore™ RP-MS column (100 x 2.1 cm, 2.6 µm, ThermoScientific, Bremen, Germany). Mass spectrometric analysis was performed using a Sciex API 4000 triple quadrupole mass spectrometer equipped with an electrospray ionization source and operated in MS/MS multiple reaction monitoring mode. Source and compound specific parameters were adjusted for each target FR (i.e. HBCDs, TCEP, TCIPP and TDCIPP) via direct infusion experiments (2 ng µL⁻¹ standard solution each, in methanol) using a built-in Harvard syringe pump at a flow rate of 10 µL min⁻¹.

The recovery ratios were calculated from the total amount of four individual FRs in the cell pellets after exposure, divided by the nominal amount that were added into the exposure media. Average concentrations of four FRs detected in the cell media were also calculated where each treatment group included three biological replicates.

CHAPTER 3 Transcriptomic and metabolomic approaches to investigate the molecular responses of human cell lines exposed to the flame retardant hexabromocyclododecane (HBCD)*

*The content of this chapter has been submitted to *Toxicology in vitro*: Zhang, J., Williams, T.D., Abdallah Abou-Elwafa, M., Harrad, S., Chipman, J.K., Viant, M.R., 2015. Transcriptomic and metabolomic approaches to investigate the molecular responses of human cell lines exposed to the flame retardant hexabromocyclododecane (HBCD).

3.1 Introduction

Hexabromocyclododecane (HBCD) is one of the most widely used classes of brominated flame retardant (Covaci et al., 2006; Marvin et al., 2011). Like other additive flame retardants, HBCD is anticipated to migrate into the environment during various stages of their manufacture, use and disposal (Harrad et al., 2010). Studies have shown that HBCD is persistent, bioaccumulative and is capable of long-range atmospheric transport (Marvin et al., 2011). HBCD has been detected in various environmental media including indoor air and dust, which thus represent sources of human exposure (Roosens et al., 2009). Human exposure to HBCD has been confirmed by its presence in breast milk, adipose tissue and blood (Marvin et al., 2011; Rawn et al., 2014a). For instance, HBCD levels detected in human milk samples in Spain were up to 188 ng/g lipid weight, with a median value of 27 ng/g (Eljarrat et al., 2009). A recent study (Rawn et al., 2014a) reported concentrations of HBCD in fetal liver (median 29 ng/g lipid) and placental tissues (median 49 ng/g lipid) collected between 1998 and 2010 in Canada. Weiss et al. (2004) detected HBCD in both maternal and cord blood (average values of 1.1 ng/g and 1.7 ng/g lipid weight, respectively) in the Netherlands. It has also been reported that the concentration of HBCD in human serum was up to 856 ng/g lipid (Thomsen et al., 2007). These studies confirm that human exposures are widespread across the globe.

To respond to the environmental and human health concerns regarding exposure to HBCD, toxicity studies have investigated and reported potentially adverse effects of HBCD in animal models and human cell lines (Marvin et al., 2011). Disruption of thyroid function has been found in rats (van der Ven et al 2006; Ema et al 2008;), fish (Palace et al., 2010, 2008) and chicken (Crump et al., 2008) following exposure to

HBCD. Low micromolar concentrations of HBCD have been shown to give rise to neurotoxic effects in *in vitro* cultured neuronal cells (e.g. PC12 cells (Dingemans et al., 2009) and SH-SY5Y cells (Al-Mousa and Michelangeli, 2012)) by interfering with calcium (Ca^{2+}) homeostasis and intracellular signalling pathways. Hepatotoxicity of HBCD has been reported in a wide range of studies, which showed that liver is a major main target organ (Hakk et al., 2012; Marvin et al., 2011). Long term exposure to HBCD at a relatively high dose (30 mg/kg/day, 28 days) increased liver weight in female rats (van der Ven et al., 2006) and induced hepatic cytochrome P450 (CYP) enzyme activities (CYP2B1 and CYP3A1) in rats (Cantón et al., 2008; Germer et al., 2006). In juvenile rainbow trout (Ronisz et al., 2004) and Chinese rare minnow (Zhang et al., 2008), HBCD inhibited activities of cytochrome P450s (CYPs) in the liver after 28-day exposure. The mRNA expression of CYPs (CYP2H1 and CYP3A37) were up-regulated in chicken (*Gallus gallus*) hepatocytes exposed to $\geq 1\mu\text{M}$ HBCD for 24 and 36 hours (Crump et al., 2008).

In several *in vitro* studies, induction of cell apoptosis by exposure to high concentrations of HBCD in HepG2 cells (An et al., 2014; Hu et al., 2009) and human L02 hepatocytes (An et al., 2013) has been suggested to result from increased production of reactive oxygen species (ROS). However, a slight increase in ROS has also been observed after low concentration (10^{-7} – 10^{-1} μM) exposures in human L02 hepatocytes, while there was no acute toxic effect reported (An et al., 2013). More studies are necessary to better understand whether any molecular changes result from concentrations that are realistic to likely human exposures to HBCD.

The aim of this chapter was to apply 'omics approaches to investigate the potential molecular toxicity of HBCD under as realistic experimental conditions as possible with

in vitro cell line models, i.e. including serum within the cell culture media. A wide range of sub-lethal exposure concentrations of a commercial mixture of HBCD was investigated including levels comparable to those reported previously in human serum. Specifically, oligonucleotide microarray based transcriptomics and direct infusion mass spectrometry (DIMS) based metabolomics were applied to determine gene expression and metabolic profiles of A549 and HepG2/C3A cells exposed to HBCD, respectively. Used in combination, these 'omics approaches can inform on both upstream regulatory processes as well as downstream functional molecular responses, providing insights into potential adverse effects of HBCD.

3.2 Materials and Methods

3.2.1 Chemicals and reagents

All chemicals, including 1,2,5,6,9,10-hexabromocyclododecane (CAS Number: 3194-55-6, purity >95%) were obtained from Sigma-Aldrich (Dorset, UK) unless otherwise stated.

3.2.2 Cell culture

The methods of A549 cells and HepG2/C3A cells culture were described in Section 2.2.

3.2.3 Cytotoxicity assays

3.2.3.1 MTT assay

The cytotoxicity of HBCD to A549 cells was assessed by the MTT assay. A549 cells were seeded in 96-well plates (5×10^3 cells per well) and incubated at 37°C with a humidified atmosphere containing 5% CO₂ for 24 hours. Then, cells were treated with HBCD at various concentrations (0.1, 1, 5, 10, 25, 50 and 100 µM; with six replicates

at each concentration) for 24 hours. The percentage of viable A549 cells was calculated. Concentration-response curves were plotted and the half maximal effective concentration (EC_{50}) values were then calculated. The procedure of MTT assay was described in Section 2.3.1.

3.2.3.2 CCK-8 assay

The cytotoxicity of HBCD to HepG2/C3A cells was evaluated by the CCK-8 assay using a commercial kit, according to the manufacturers' instructions (Dojindo Laboratories, Kumamoto, Japan). Briefly, HepG2/C3A cells (2×10^4 cells per well) were cultured in a 96-well plate overnight and the cells were treated in six replicates with several concentrations (0.1, 1, 5, 10, 25, 50 and 75 μ M) of HBCD in culture medium for 24 hours. The viability of cells in the CCK-8 assays, in terms of EC_{50} values, was calculated using the same approach as that used for the MTT assay. The details of CCK-8 assay were available in Section 2.3.2.

3.2.4 HBCD exposure experiments and sample preparation for metabolomics and transcriptomics

3.2.4.1 A549 cells

A549 cells were exposed to several HBCD concentrations: 2 nM (nominal concentration in the media, termed *Very low* concentration group), 20 nM (termed *Low* concentration group), 200 nM (termed *Medium* concentration group) and 2 μ M (termed *High* concentration group). In the control group, a concentration of 0.5% DMSO was used as a vehicle in the treated samples. Each concentration group included six or eight replicates. After 24-hour exposure, cells were rapidly quenched and harvested as described in. The extraction of metabolites employed liquid-liquid extraction approach with the ration of methanol/chloroform/water was 1:1:0.9 (v/v/v)

as described in Section 2.5.1.1.

Total RNA of quenched cells was isolated using Qiagen's mini RNeasy Kit and QIAshredder (Qiagen, Crawley, UK) according to the manufacturer's protocol. RNA was quantified with a NanoDrop 1000 spectrophotometer (Thermo Scientific, Waltham, MA), and the integrity of RNA was verified with a 2100 Bioanalyzer (Agilent Technologies, Santa Clara, CA). This was described in Section 2.4.1.

3.2.4.2 HepG2/C3A cells

Similar methodologies were used to culture, expose and harvest HepG2/C3A cells as above, with some subtle modifications to maximise the recovery of RNA and metabolites. Specifically, the HepG2/C3A cells were exposed to 4 μ M HBCD or 10 μ M 7,12-dimethylbenz[a]anthracene (DMBA) for 24 hours; 10 μ L DMSO as vehicle was added into the control samples (final concentration of DMSO was 0.5% (v/v) in all treatments). Each treatment group consisted of six replicates. Following the exposures, the cells were harvested and the metabolites (Section 2.5.1.2) and RNA (Section 2.4.1) were extracted in a similar manner to that described above.

3.2.5 Direct infusion mass spectrometry (DIMS) analysis

The dried polar extracts of cells were re-suspended in 150 μ L 80:20 (v/v) methanol:water (HPLC grade) with 20 mM ammonium acetate, vortexed and centrifuged at 14000 rpm, 4°C for 10 mins. Each sample was loaded into three wells of a 96-well plate (10 μ L per well) and then analysed (in triplicate) using direct infusion Fourier transform ion cyclotron resonance mass spectrometry in negative ion mode (LTQ FT Ultra, Thermo Fisher Scientific, Germany, coupled to a Triversa nanoelectrospray ion source, Advion Biosciences, Ithaca, NY, USA). Mass spectra

were recorded utilizing the selected ion monitoring (SIM) stitching approach from m/z 70 to 590 (Southam et al., 2007) and then processed using custom-written Matlab scripts as previously reported (Southam et al 2007; Kirwan et al 2014). The procedure of data processing and statistical analysis of DIMS data were described as earlier in Section 2.5.2.

3.2.6 Transcriptomic analysis

For RNA samples from A549 cells, six replicates (randomly selected from the total of eight replicates, to reduce costs) were used for each of the HBCD treated groups (2 nM (*Very low*), 20 nM (*Low*), 200 nM (*Medium*) and 2 μ M (*High*)) while the solvent (DMSO) control group comprised of eight replicates. For RNA samples from HepG2/C3A cells, a total of 16 samples were subjected to microarray analyses, comprising six samples from the HBCD (4 μ M) treated group, six from the solvent (DMSO) control group, and the remaining four from the DMBA (10 μ M) positive control group.

The procedures for microarray analysis were performed following the manufacturer's protocols (Agilent Technologies, Santa Clara, CA) and the detailed procedures were described in Section 2.4.2. Quantitative real time-PCR analysis (see Section 2.4.3) was performed to quantify the mRNA levels of a selected set of six genes in A549 or HepG2/C3A cells treated with HBCD or DMBA.

3.2.7 Quantification of HBCD in A549 and HepG2/C3A cells and cell media

(conducted by Dr. Mohamed Abou-Elwafa Abdallah, University of Birmingham)

To measure the cellular uptake of HBCD after exposure, A549 and HepG2/C3A cells were exposed to 2 μ M and 4 μ M HBCD, respectively, in both FBS-containing and

FBS-free media. Following 24-hour exposures, HBCD levels were quantified in both the cell pellets and media using the LC-MS/MS method (Van den Eede et al., 2012). The details of procedures can be found in Section 2.6.1. Average concentrations of Σ HBCDs (total amount of α -, β - and γ -HBCDs) detected in the cell media were also calculated where each treatment group included three biological replicates.

3.3 Results

3.3.1 Cytotoxicity of HBCD to A549 cells and HepG2/C3A cells

Concentration-dependent cytotoxicity of HBCD to A549 cells and HepG2/C3A cells after 24-hour treatments were observed (Figure 3.1). At relatively low concentration ranges from 0 to 10 μ M, HBCD exhibited minimal cytotoxicity with the viability of HepG2/C3A cells remaining greater than 90%, while for the A549 cells the viability remained greater than 80%. The EC_{50} values of cytotoxicity of HBCD to A549 and HepG2/C3A cells were 27.4 μ M and 63.0 μ M, respectively, in the presence of serum in the exposure media.

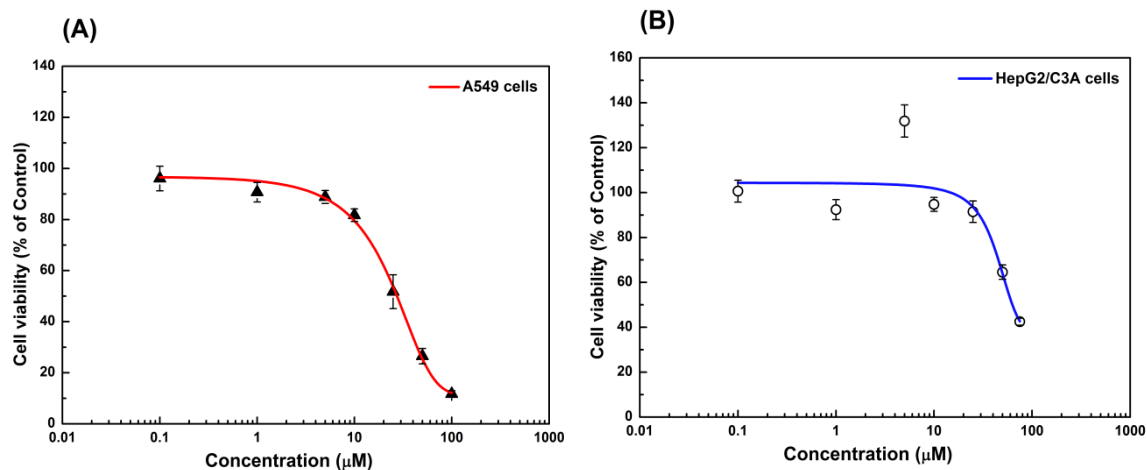


Figure 3.1 Cytotoxic effects of HBCD to A549 cells and HepG2/C3A cells. Cell viability of A549 cells (A) and HepG2/C3A cells (B) was examined using the MTT assay and CCK-8 assay, respectively, after exposure to different concentrations (0-100 μM for A549 cells; 0-75 μM for HepG2/C3A cells) of HBCD for 24 hours. Results are expressed as the percentage (mean ± SD, n=6) of cell viability compared to controls treated with the appropriate vehicle (DMSO).

In order to explore potential molecular events in cells at sub-toxic concentrations, 2 μM was selected as the highest concentration for exposure of A549 cells to HBCD, more than 10-fold lower concentration than the EC₅₀ value. Three additional treatment groups were included, each 10-fold lower in concentration. The experimental design therefore consisted of exposing A549 cells to HBCD at 2 nM, 20 nM, 200 nM and 2 μM, with the appropriate vehicle (DMSO) as a control group, so as to maximise the relevance of our findings to likely human exposure levels. Following a similar strategy for the HepG2/C3A cells, 4 μM was used as the exposure concentration for the 'omics studies. DMBA at 10 μM was employed as a reference treatment (positive control) for the gene expression study.

3.3.2 Molecular responses of A549 cells exposed to HBCD

3.3.2.1 Gene expression profiles of A549 cells exposed to HBCD

Oligonucleotide microarrays were employed to evaluate gene expression profiles of A549 cells after 24-hour exposures to four concentrations of HBCD, as detailed above. There was no clear separation of gene expression profiles between different treatment groups in A549 cells in PCA scores plot (Figure 3.2 A).

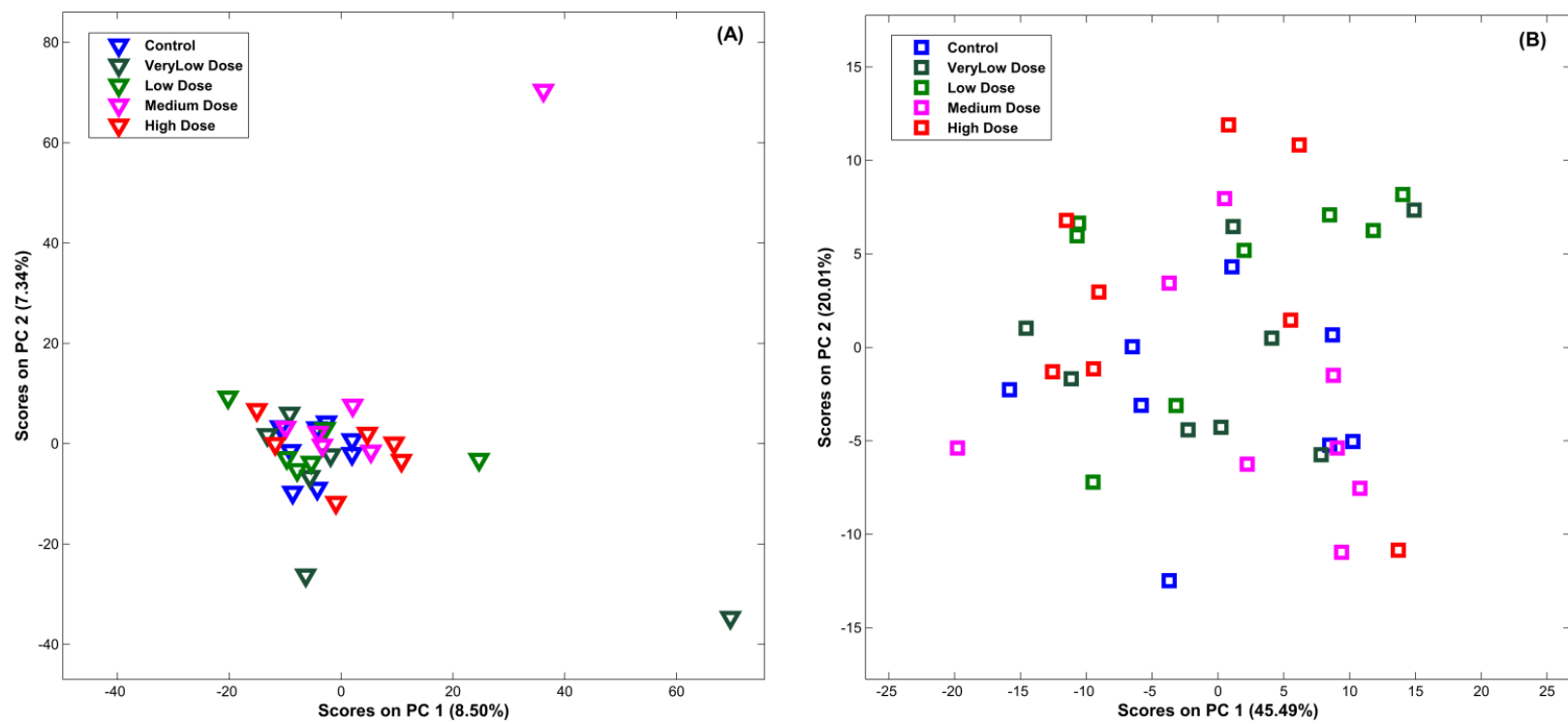


Figure 3.2 PCA scores plots of microarray dataset (A) and DIMS dataset (B) in A549 cells exposed to HBCD for 24 hours. Legend: controls (blue), Very low concentration (2 nM) group (dark green), Low concentration (20 nM) group (green), Medium concentration (200nM) group (pink) and High concentration (2 μ M) group (red). Biological replication comprised n=6 (microarray) and n=8 (DIMS) in HBCD treatment groups; n=8 in the control group.

The ANOVAs of the top four PC scores combined with a Tukey-Kramer's post hoc test (Table 3.1) also showed that there were no significant differences in the gene expression profiles between control and HBCD treated groups in A549 cells. Significance analysis of microarrays (SAM) found no significantly altered individual genes compared to controls, which is consistent with the results from the PCA of the gene expression dataset. Gene Set Enrichment Analyses also indicated there were no significantly enriched gene sets involving KEGG pathways in HBCD treated groups.

Table 3.1 Summary of the principal component (PC) analyses of both the microarray and DIMS datasets of A549 cells and HepG2/C3A cells following exposure to HBCD.

Dataset		PC1	PC2	PC3	PC4
A549_Microarray_24h	variance	8.50%	7.34%	6.17%	5.66%
	p value	0.777	0.114	0.924	0.817
A549_DIMS_24h	variance	45.49%	20.01%	4.87%	4.11%
	p value	0.943	0.089	0.005	0.700
HepG2/C3A_Microarray_24h	variance	42.21%	12.75%	9.15%	6.36%
	p value	2.90E-07	0.502	0.272	0.962
HepG2/C3A_DIMS_24h	variance	37.51%	25.50%	9.95%	6.20%
	p value	0.251	0.140	0.780	0.873

(Groups in A549 cells: Control, *Very Low* concentration, *Low* concentration, *Medium* concentration and *High* concentration; groups in HepG2/C3A cells: Control, HBCD and DMBA). The variance explained (%) by PCs 1-4 are listed together with p values from ANOVAs (or t-tests) of these PC scores across all treatments (values in bold indicate significance at a false discovery rate (FDR) <10%).

Quantitative RT-PCR analysis of six genes of interest (*CYP1A1* and *CYP3A4*: related to xenobiotic metabolism, *CDK2*: cell division/growth, *EEF1A1*: protein biosynthesis,

GSR: oxidative stress response, and *GJB1*: cell communication) revealed that only expression of *CYP3A4* in A549 cells treated with 20 nM (Low concentration) and 200 nM (Medium concentration) HBCD was slightly down-regulated (Figure 3.3 A), while no significant changes were observed in the microarray analysis after exposure to the different concentrations of HBCD for 24 hours. The expression levels of the other five genes were not significantly altered, in agreement with the results of the microarray analysis.

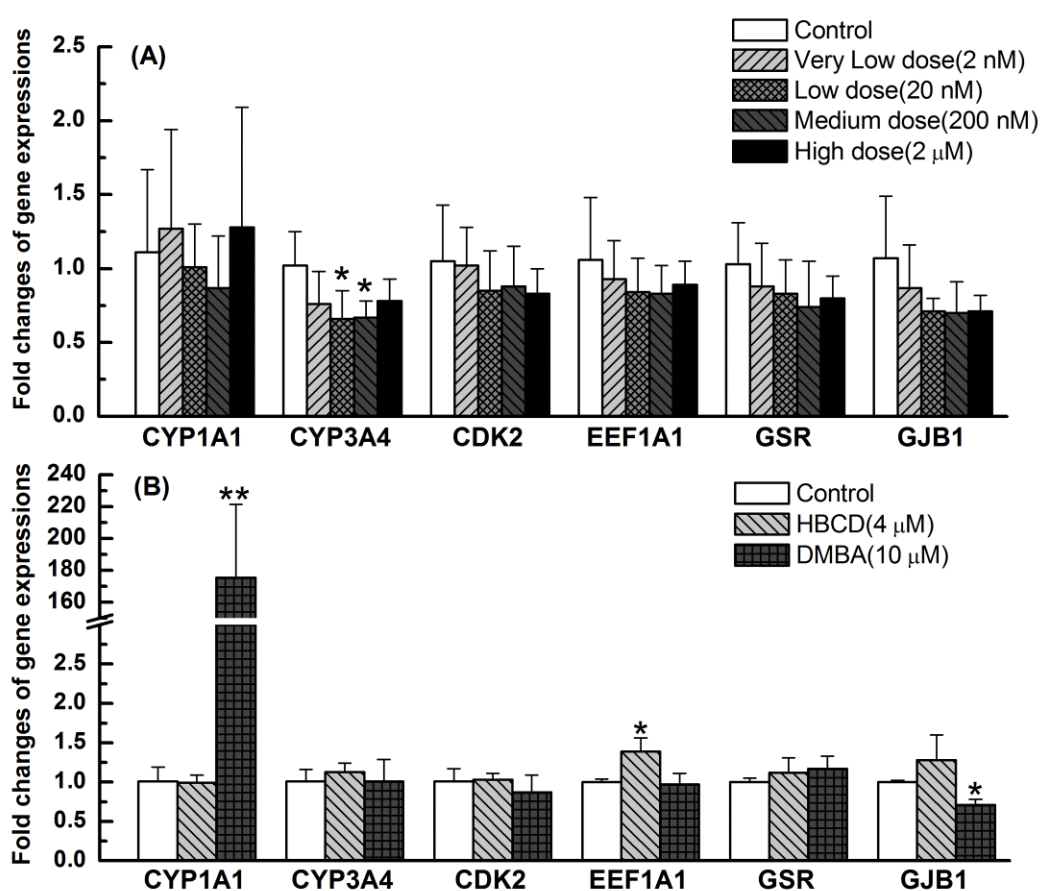


Figure 3.3 qPCR analysis of mRNA expression of six selected genes in A549 cells (A) and in HepG2/C3A cells (B) following HBCD or DMBA treatments. Data were obtained from quadruplicate PCR reactions of four biological replicates. Differences to the solvent control were tested by one-way ANOVA or t-test (* $P < 0.05$). Results are presented as mean \pm standard deviation.

3.3.2.2 Metabolic responses of A549 cells exposed to HBCD

Polar metabolites extracted from HBCD-exposed A549 cells were analysed by direct infusion mass spectrometry based metabolomics. After spectral processing, the DIMS dataset comprised of a total of 1457 mass spectral peaks that were subjected to PCA to visualize the similarities and differences of the metabolic profiles between control and HBCD-treated groups. The PCA scores plot (Figure 3.2 B) showed no separation in the metabolic profiles measured from HBCD-treated and control groups for PC1 vs. PC2, an observation that was supported by ANOVA of the top four PC scores data and subsequent analysis using Tukey-Kramer's post hoc tests. These results (Table 3.1) indicate no separation along PC1, PC2 and PC4, though HBCD-treated and control samples separated along the PC3 axis (representing 4.8% of variance in DIMS dataset) ($p = 0.005$). However, univariate statistical analyses of all 1457 peaks revealed that none changed significantly in response to HBCD across all four concentration groups (FDR < 10%).

3.3.3 Molecular responses of HepG2/C3A cells exposure to HBCD

3.3.3.1 Gene expression profiles of HepG2/C3A cells exposed to HBCD

Since no significant molecular changes had been discovered in A549 cells after exposure to the subtoxic HBCD concentration, HepG2/C3A cells, representing a system with a relatively higher xenobiotic metabolic activity, were exposed to 4 μM HBCD (less than 10% of EC_{50}) and 10 μM DMBA (as a positive control to induce gene expression). DMBA is a polycyclic aromatic hydrocarbon with carcinogenic properties and a CYP1A1 -substrate. The PCA scores plot indicated no separation of the gene expression profiles between HBCD treated group and the control group, whereas the analyses distinguished marked differences between DMBA group and the rest groups

(Figure 3.4A).

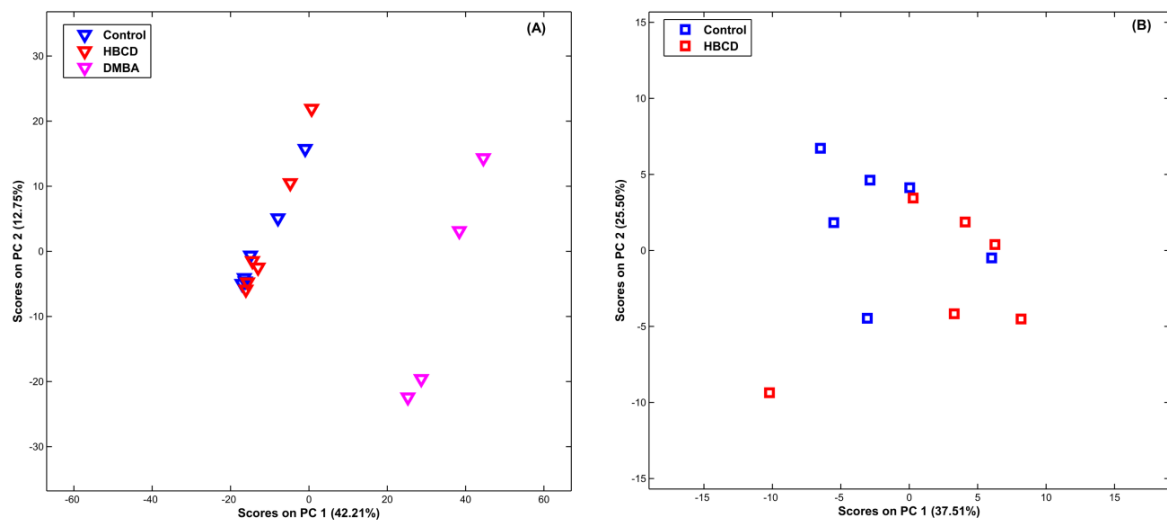


Figure 3.4 PCA scores plots of microarray dataset (A) and DIMS dataset (B) in HepG2/C3A cells exposed to 4 μ M HBCD and 10 μ M DMBA for 24 hours. Legend: controls (blue), 4 μ M HBCD group (red) and 10 μ M DMBA group (pink). Biological replication comprised n=6 (microarray) and n=6 (DIMS) in the control group and HBCD treatment groups; n=4 in 10 μ M DMBA group (as positive control in microarray analysis).

The statistical significance of the top four PC scores was verified by a t-test; no significant differences between the HBCD and control group existed, but the DMBA and control samples were significantly different along PC1 (representing 53.1% of the variance in the dataset, $p=8.62 \times 10^{-6}$). In addition, SAM of individual genes showed that there was no significant modulation of gene expression in the HBCD-treated group compared to the control group, while more than 300 probe sets changed in the DMBA treated group in HepG2/C3A cells (File 3.1, in Appendix).

The functional annotation tool (DAVID) was employed to determine the most relevant pathway(s) or process(es) involved in these significantly dysregulated genes in the DMBA-treated group identified by SAM. The results (Table 3.2) suggest that p53 signalling and apoptosis are the most significantly altered pathways in DMBA-treated

HepG2/C3A cells.

Table 3.2 DAVID analysis of genes modulated in HepG2/C3A cells exposed to DMBA.

Category	Term	Count	%	P-value	FDR (%)
KEGG_PATHWAY	hsa04115:p53 signaling pathway	12	4.84	1.69E-09	1.85E-06
GOTERM_BP_FAT	GO:0043065~positive regulation of apoptosis	19	7.66	1.17E-05	0.0197573
GOTERM_BP_FAT	GO:0043068~positive regulation of programmed cell death	19	7.66	1.29E-05	0.0217055
GOTERM_BP_FAT	GO:0010942~positive regulation of cell death	19	7.66	1.37E-05	0.0230983
GOTERM_BP_FAT	GO:0008284~positive regulation of cell proliferation	18	7.26	2.65E-05	0.0447051
GOTERM_BP_FAT	GO:0042981~regulation of apoptosis	26	10.48	3.92E-05	0.0660398
GOTERM_BP_FAT	GO:0043067~regulation of programmed cell death	26	10.48	4.61E-05	0.0776549
GOTERM_BP_FAT	GO:0010941~regulation of cell death	26	10.48	4.90E-05	0.082465
UP_SEQ_FEATURE	domain:Leucine-zipper	9	3.63	6.28E-05	0.0997848
GOTERM_BP_FAT	GO:0042127~regulation of cell proliferation	25	10.08	7.71E-05	0.1298289
INTERPRO	IPR000837:Fos transforming protein	4	1.61	1.15E-04	0.1655659
SP_PIR_KEYWORDS	Apoptosis	15	6.05	2.63E-04	0.3452098
GOTERM_BP_FAT	GO:0006979~response to oxidative stress	10	4.03	2.81E-04	0.4723701
INTERPRO	IPR004827:Basic-leucine zipper (bZIP) transcription factor	6	2.42	6.05E-04	0.8705805
GOTERM_BP_FAT	GO:0008629~induction of apoptosis by intracellular signals	6	2.42	6.48E-04	1.0862681
SMART	SM00338:BRLZ	6	2.42	6.92E-04	0.79229
GOTERM_BP_FAT	GO:0009612~response to mechanical stimulus	6	2.42	7.67E-04	1.2838372
GOTERM_BP_FAT	GO:0006915~apoptosis	19	7.66	8.06E-04	1.3499357
GOTERM_BP_FAT	GO:0042771~DNA damage response, signal transduction by p53 class mediator resulting in induction of apoptosis	4	1.61	8.63E-04	1.444984
GOTERM_BP_FAT	GO:0006917~induction of apoptosis	13	5.24	9.38E-04	1.5691692
GOTERM_BP_FAT	GO:0012501~programmed cell death	19	7.66	9.56E-04	1.5979897
GOTERM_BP_FAT	GO:0012502~induction of programmed cell death	13	5.24	9.64E-04	1.6117425
GOTERM_BP_FAT	GO:0009628~response to abiotic stimulus	14	5.65	0.001002	1.6753724
GOTERM_BP_FAT	GO:0051412~response to corticosterone stimulus	4	1.61	0.001053	1.7589655
UP_SEQ_FEATURE	short sequence motif:BH3	4	1.61	0.001085	1.7122901
GOTERM_BP_FAT	GO:0009636~response to toxin	6	2.42	0.001134	1.8928186
GOTERM_BP_FAT	GO:0007586~digestion	7	2.82	0.001156	1.9297183
PIR_SUPERFAMILY	PIRSF001719:fos transforming protein	3	1.21	0.001462	1.6575802
GOTERM_BP_FAT	GO:0042537~benzene and derivative metabolic process	3	1.21	0.001622	2.697796
GOTERM_MF_FAT	GO:0005543~phospholipid binding	9	3.63	0.001826	2.5017966
GOTERM_BP_FAT	GO:0051385~response to mineralocorticoid stimulus	4	1.61	0.002063	3.4198182
GOTERM_BP_FAT	GO:0001836~release of cytochrome c from mitochondria	4	1.61	0.002384	3.9421188
GOTERM_BP_FAT	GO:0008219~cell death	20	8.06	0.00243	4.0171447
GOTERM_BP_FAT	GO:0016265~death	20	8.06	0.002625	4.332755
INTERPRO	IPR000712:Apoptosis regulator Bcl-2, BH	4	1.61	0.00276	3.9121503
GOTERM_BP_FAT	GO:0033554~cellular response to stress	17	6.85	0.002774	4.5730517
GOTERM_BP_FAT	GO:0000302~response to reactive oxygen species	6	2.42	0.002845	4.686406

GSEA showed similar results (Table 3.3) that cytokine-cytokine receptor interaction, p53 signalling pathway, apoptosis and metabolism of xenobiotics by CYPs are the top enriched gene sets in the DMBA group, while no significant enrichment of gene sets were identified in the HBCD-treated groups. In HepG2/C3A cells, the mRNA expression of six selected genes was analysed by quantitative RT-PCR. This revealed similar trends as measured by microarray; including a remarkable up-regulation of *CYP1A1* (175-fold, $p < 0.0001$) and down-regulation of *GJB1* (0.7-fold, $p < 0.0001$) in the DMBA group, while there was no significantly altered expression of genes in cells treated with 4 μM HBCD, except a slightly increased expression of *EEF1A1* (1.4-fold, $p = 0.004$) (Figure 3.3B).

Table 3.3 Gene Set Enrichment Analysis of up-regulated gene sets in HepG2/C3A cells exposed to DMBA.

NAME	SIZE	ES	NES	NOM p-value	FDR q-value	FWER p-value
KEGG_CYTOKINE_CYTOKINE_RECEPTOR_INTERACTION	127	-0.52375	-2.17585	0.00000	0.00300	0.00000
KEGG_P53_SIGNALING_PATHWAY	62	-0.66124	-1.85655	0.00000	0.02298	0.04400
KEGG_METABOLISM_OF_XENOBIOTICS_BY_CYTOCHROME_P450	43	-0.50792	-1.78627	0.00906	0.05696	0.13500
KEGG_PRIMARY_IMMUNODEFICIENCY	24	-0.60144	-1.76441	0.02938	0.05375	0.15150
KEGG_APOPTOSIS	71	-0.46885	-1.74278	0.00000	0.05778	0.19000
KEGG_RETINOL_METABOLISM	31	-0.50028	-1.73649	0.00000	0.05373	0.21050
KEGG_HYPERTROPHIC_CARDIOMYOPATHY_HCM	50	-0.47004	-1.70432	0.00000	0.05887	0.26100
KEGG_LINOLEIC_ACID_METABOLISM	15	-0.61563	-1.62442	0.00000	0.12470	0.42950
KEGG_JAK_STAT_SIGNALING_PATHWAY	95	-0.41786	-1.61206	0.00000	0.12402	0.44800
KEGG_RIG_I_LIKE_RECEPTOR_SIGNALING_PATHWAY	49	-0.47164	-1.6064	0.00000	0.11672	0.45300
KEGG_STEROID_HORMONE_BIOSYNTHESIS	26	-0.45628	-1.60274	0.00000	0.11111	0.46000
KEGG_ECM_RECEPTOR_INTERACTION	57	-0.39068	-1.60079	0.00000	0.10318	0.47550
KEGG_NATURAL_KILLER_CELL_MEDIATED_CYTOTOXICITY	79	-0.35666	-1.58214	0.02911	0.11701	0.51100
KEGG_ARACHIDONIC_ACID_METABOLISM	34	-0.44116	-1.54699	0.02346	0.14894	0.60600
KEGG_B_CELL_RECEPTOR_SIGNALING_PATHWAY	57	-0.38727	-1.53047	0.00000	0.16431	0.66300
KEGG_TOLL_LIKE_RECEPTOR_SIGNALING_PATHWAY	63	-0.4496	-1.52228	0.01902	0.16600	0.69050
KEGG_HEMATOPOIETIC_CELL_LINEAGE	45	-0.38302	-1.49561	0.02933	0.18765	0.74150
KEGG_ARGININE_AND_PROLINE_METABOLISM	48	-0.3505	-1.49273	0.01207	0.18007	0.74600
KEGG_ARRHYTHMOGENIC_RIGHT_VENTRICULAR_CARDIOMYOPATHY_ARVC	47	-0.38134	-1.48343	0.02698	0.18311	0.76800
KEGG_DILATED_CARDIOMYOPATHY	52	-0.38974	-1.45306	0.06594	0.22010	0.80950
KEGG_DRUG_METABOLISM_CYTOCHROME_P450	43	-0.37794	-1.44691	0.02231	0.21819	0.82050
KEGG_PATHOGENIC_ESCHERICHIA_COLI_INFECTION	49	-0.41424	-1.43803	0.08656	0.22318	0.83800
KEGG_GLYCEROLIPID_METABOLISM	36	-0.36444	-1.4322	0.06230	0.22417	0.84500
KEGG_EPITHELIAL_CELL_SIGNALING_IN_HELICOBACTER_PYLORI_INFECTION	53	-0.42713	-1.42946	0.07802	0.21943	0.85550
KEGG_MAPK_SIGNALING_PATHWAY	185	-0.29509	-1.3726	0.00601	0.26992	0.90150

22 gene sets (names in Bold) are significantly enriched at nominal p-value < 0.05. 24 gene sets are significantly enriched at FDR < 25%.

3.3.3.2 Metabolomics analysis of HepG2/C3A cells exposed to HBCD

Polar metabolome of HepG2/C3A cells exposed to 4 μ M HBCD were measured by DIMS. A total of 2128 mass spectral peaks were subjected to PCA and univariate analysis. No distinct separation was observed in the PCA scores plot (Figure 3.4 B) of which the top four PC scores were evaluated by t-test, confirming no significant differences (Table 3.1). Further t-tests on each of the 2128 individual peaks in the HBCD exposed group compared to the control group confirmed that there was no significant metabolic change in HepG2/C3A cells exposed to 4 μ M HBCD for 24 hours. However, after extended HBCD exposure to 72 hours, the subtle metabolic changes were found in DIMS dataset in which there were 85 (of total 3412) MS peaks significantly changed (Table 3.4) which is likely to be the results of extension of exposure time or the delayed effects of 24 hours exposure.

Table 3.4 Significant MS peaks in DIMS dataset from HepG2/C3A cells exposed to HBCD for 72hours.

<i>m/z</i>	Intensity	Fold changes	p value	Adjusted p value	Empirical formula	Ion form	Mass error (ppm)	HMDB	KEGG_COMPOUND
124.00729	28262.31	0.38	1.01E-06	0.0011485	C2H7NO3S	[M-H]-	-0.8	Taurine	Taurine
127.05122	19331.709	0.61	0.0002001	0.0273072	C5H8N2O2	[M-H]-	-0.64	5,6-Dihydrothymine'	5,6-Dihydrothymine', 'alpha-Amino-gamma-cyanobutanoate', 'gamma-Amino-gamma-cyanobutanoate
166.99614	19835.911	0.69	0.000962	0.0455611	C5H6O5	[M+Na-2H]-	-0.32	2-Oxoglutarate',	2-Oxoglutarate', '5-Hydroxy-2,4-dioxopentanoate', 'Dehydro-D-arabinono-1,4-lactone', 'Methyloxaloacetate', 'Oxaloacetate 4-methyl ester
171.02744	43481.266	0.85	0.0008032	0.0434989	C5H10O5	[M+Na-2H]-	-0.31	2-Deoxyribonic acid', 'D-Ribose', 'D-Ribulose', 'D-Xylose', 'D-Xylulose', 'L-Arabinofuranose', 'L-Arabinose', 'Acetylglycine', 'L-2-Amino-3-oxobutanoic acid', 'L-Aspartate 4-semialdehyde	
176.0564	7663.2379	0.56	0.001017	0.0456515	C4H7NO3	[M+Hac-H]-	-0.27		2-Amino-3-oxobutanoate', 'L-2-Amino-3-oxobutanoic acid', 'L-Aspartate 4-semialdehyde
181.96597	3949.5365	0.55	0.0001011	0.0247906					
195.94999	6119.1374	0.74	0.0006189	0.0430959					
196.06033	2625.4167	1.02	0.0006726	0.0434989	C8H9N5	[M+Na-2H]-	-0.68		
202.97286	13209.369	0.65	0.0001768	0.0262212	C4H7O6P	[M+Na-2H]-	0.81		
206.01044	11861.708	0.33	5.53E-07	0.0011485					
212.06528	70909.693	0.53	0.0003918	0.036907					
213.06865	5627.8504	0.56	0.0006466	0.0432605	C11H14O2	[M+Cl]-	-0.62	'5-Phenylvaleric acid',	1,1-Dimethylethyl benzoate', '1-Phenylpropyl acetate', '2-Phenylpropyl acetate', '3,5-Dimethoxyallylbenzene', '3-Phenylpropyl acetate', '4-t-Butylbenzoic acid',
222.97972	7618.9158	1.35	5.53E-06	0.0037752					

228.86057	24274.267	0.87	0.0007974	0.0434989					
230.85763	15876.586	0.96	0.0007948	0.0434989					
241.13622	11836.346	0.45	0.0009832	0.0455611					
243.97417	3979.8865	0.55	3.22E-06	0.0027488					
248.97804	5040.7756	0.59	0.0001043	0.0247906					
248.99906	15353.659	0.66	0.0011846	0.0475518					
250.02082	7117.1873	0.69	0.0010705	0.0462333					
252.90499	118476.97	0.86	0.0009056	0.0454414					
254.902	43332.246	0.86	0.0001118	0.0247906					
256.04359	25039.934	0.65	0.0011234	0.0475518					
269.00426	7401.5741	0.67	0.0011405	0.0475518	C12H10O3S	[M+Cl]-	-0.78		
269.97585	41616.794	0.84	0.000361	0.036907					
270.02362	13463.02	0.74	0.0004	0.036907	C8H16N3OPS	[M+K-2H]-	-0.59		
278.02553	17622.736	0.72	0.0003701	0.036907					
287.9864	100026.02	0.87	0.0004829	0.0398421					
294.06779	18674.228	0.4	0.0003731	0.036907	C10H15N3O5	[M+(37Cl)]-	0.57		5-Methylcytidine
303.93145	13542.97	0.57	0.000742	0.0434989					
303.9604	23329.424	0.52	0.0007767	0.0434989					
305.07289	12985.946	0.62	0.0003938	0.036907					
307.94721	6798.1515	0.57	0.0001595	0.0249404					
309.96842	50017.327	0.77	0.0006335	0.043232					
336.90502	64825.242	0.95	0.0009553	0.0455611					
348.81943	49523.333	0.83	0.0001217	0.0247906					
350.8164	28170.606	0.83	0.0001235	0.0247906					
353.22759	9859.4717	0.7	0.0008259	0.0436666	C18H36O4	[M+(37Cl)]-	-0.63	'MG(0:0/15:0/0:0)', 'MG(15:0/0:0/0:0)	'(9R,10R)-Dihydroxyoctadecanoic acid', '(9S,10S)-9,10-Dihydroxyoctadecanoate',
358.013	5644.423	0.6	0.0007154	0.0434989					
358.95256	128404.21	0.66	0.0011591	0.0475518					
359.95573	8454.0662	0.71	0.0006016	0.0427646					

395.24403	11680.977	0.47	0.0011733	0.0475518	C22H36O6	[M-H]-	0.29		
421.15545	33618.278	0.46	0.0004909	0.0398421					
437.30385	26265.913	0.49	0.0002997	0.036907	C27H44O3	[M+Na-2H]-	0.31	'23S,25-dihydroxyvitamin D3', '24,25-Dihydroxyvitamin D', '24R,25-Dihydroxyvitamin D3', '7 alpha,24-Dihydroxy-4-cholesten-3-one',	'(25S)-5beta-Spirostan-3beta-ol', '1-alpha,24(R)-Dihydroxyvitamin D3', '3beta-Hydroxy-5-cholestenoate', '4-Cholesten-7alpha,12alpha-diol-3-one', '5,6-24(S),25-Diepoxycholesterol', '7alpha,24-Dihydroxy-4-cholesten-3-one',
438.30725	6840.7002	0.55	0.0001913	0.0271896					
439.30077	8120.3434	0.54	0.0003219	0.036907					
441.89656	12866.54	0.94	0.0009647	0.0455611					
445.91878	6475.9051	0.66	0.0003712	0.036907					
447.99842	3753.6685	0.86	0.0008644	0.0446863					
448.97661	6553.6893	2.02	0.0001471	0.0249404	C16H12O11S	[M+(37Cl)]-	0.27		
450.00437	8486.3231	0.81	0.0009895	0.0455611					
453.98398	5791.1309	0.61	0.0010015	0.0455611					
457.98032	9909.2953	1.23	0.0005286	0.0401185					
460.20575	11499.996	0.46	0.0010671	0.0462333					
471.99569	87957.722	0.93	3.66E-05	0.0138904					
473.02089	13849.121	1.61	8.56E-07	0.0011485					
473.21805	598675.56	0.49	0.0007112	0.0434989	C26H34O8	[M-H]-	-0.09		
473.99287	24843.642	0.95	0.0002493	0.0327196					
474.21511	6554.4147	0.57	0.0004002	0.036907					
474.22144	170314.69	0.5	0.0006826	0.0434989					
475.98259	34399.367	1.05	0.0001369	0.0249404					
477.97967	20608.562	1.12	0.0003051	0.036907					
479.22401	14651.462	0.43	0.0004166	0.0374101					
480.85739	13041.855	1.16	0.0010302	0.0456515					
485.94031	9478.8956	1.27	0.0008319	0.0436666					

486.80237	44937.066	1.05	4.59E-05	0.0156771			
488.79947	59053.404	1.03	6.51E-05	0.0201971			
490.00212	58228.917	1.03	0.000698	0.0434989			
490.79667	30802.862	1.08	1.20E-05	0.0068249			
493.97226	11467.519	1.24	0.0005021	0.0398421			
501.85201	14352.645	1.27	0.0007619	0.0434989			
504.02192	6821.8271	0.82	3.66E-05	0.0138904			
504.90183	9945.2867	1.26	0.0004455	0.0389774			
511.17404	9645.0131	0.55	0.0004921	0.0398421	C26H34O8	[M+K-2H]-	0.12
523.88112	33430.563	0.92	3.57E-05	0.0138904			
530.98007	5073.837	2.17	0.0009995	0.0455611			
533.96726	21740.72	1.05	0.0008839	0.0450127			
546.75824	45820.229	1.21	0.000733	0.0434989			
555.02414	9655.512	1.47	8.35E-05	0.0237542			
555.22117	11713.545	0.57	0.0005291	0.0401185			
555.99611	12532.507	0.81	0.00014	0.0249404			
557.9857	18065.501	0.96	0.0005515	0.0405234			
561.9805	8191.8178	1.1	0.0011624	0.0475518			
562.86044	9499.8975	1.04	0.0001608	0.0249404			
570.80277	56395.698	0.92	0.0005582	0.0405234			

3.3.4 Uptake of HBCD into A549 and HepG2/C3A cells

The recovery of HBCD from cell pellets and the concentrations of HBCD in the cell media were evaluated, with the objective to facilitate comparisons between the concentrations of HBCD in the present study and those reported in human tissue and biofluids.

The results (Figure 3.5) show that when cultured in FBS-containing media, an average of 12.4% of the nominal amount of HBCD added to the exposure system was detected in A549 cell pellets, while in those cell pellets collected from the FBS-free media, approximately double the amount (20.9%) was measured in the cells. In HepG2/C3A cells, recoveries of HBCD from cell pellets exposed in FBS-containing or FBS free media were considerably higher, and similar, 50.7% and 48.1% respectively. This suggested that the capacity for HepG2/C3A cells to uptake HBCD was higher than for A549 cells. As shown in Table 3.5, the average concentrations of HBCD in A549 cell pellets were 15.9 and 27.5 ng mg⁻¹ (wet weight) from FBS-containing exposure media and FBS-free media, respectively. However, the average concentrations of HBCD in HepG2/C3A cells from FBS-containing media and FBS-free media were 96.2 and 99.0 ng mg⁻¹ (wet weight) respectively, which were much higher than in A549 cells.

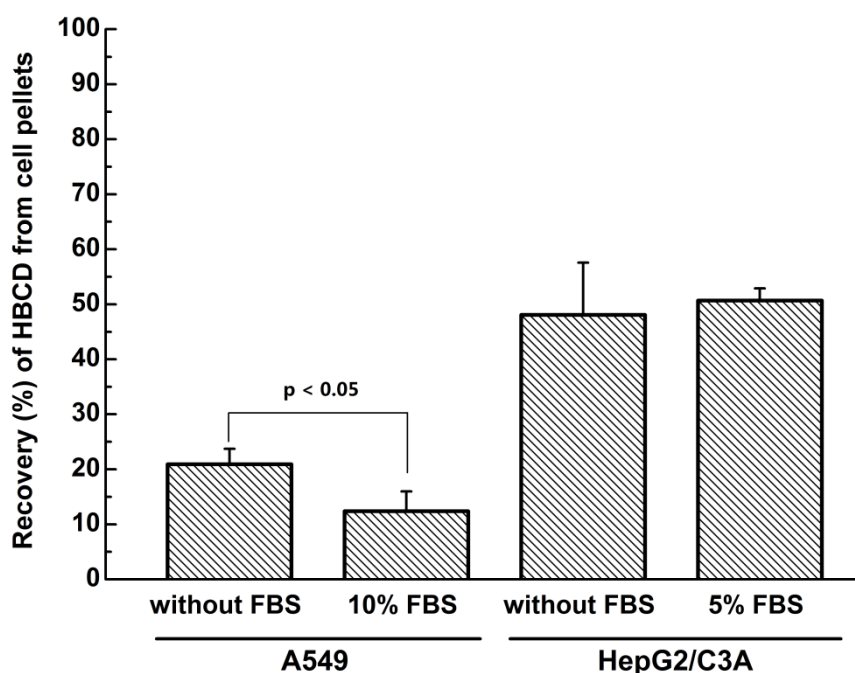


Figure 3.5 Recovery of HBCD from cell pellets in A549 cells and HepG2/C3A cells exposed to HBCD for 24 hours. A549 cells and HepG2/C3A cells were treated with 2 μ M and 4 μ M HBCD, respectively, in both serum (FBS)-containing media and serum-free media (without FBS). Recoveries are expressed as the percentage of detectable amount of HBCD from cell pellets and cell media after exposure, relative to the total nominal amount of HBCD added to the exposure media \pm standard deviation (n=3).

Table 3.5 Concentration of Σ HBCDs in cell pellets and cell media of A549 and HepG2/C3A cells after 24-hour exposure

Cell types	Types of Exposure Media	Nominal concentration of Σ HBCDs in exposure media	Average wet weight of cell pellets (mg)	Concentration of Σ HBCDs in cell pellets (ng/mg)	Total amount of Σ HBCDs in cell pellets (ng)	Concentration of Σ HBCDs in cell media after exposure (ng/mL)
A549	No FBS	2 μ M (1283.4 ng/mL)	19.8 \pm 3.3	27.5 \pm 5.0	535.6 \pm 71.2	46.9 \pm 7.4
	10% FBS	2 μ M (1283.4 ng/mL)	19.8 \pm 4.0	15.9 \pm 1.7	319.2 \pm 93.2	1133.7 \pm 26.8
HepG2/C3A	No FBS	4 μ M (2566.8 ng/mL)	25.4 \pm 3.1	99.0 \pm 26.0	2470.8 \pm 488.7	409.9 \pm 77.8
	5% FBS	4 μ M (2566.8 ng/mL)	27.2 \pm 2.8	96.2 \pm 10.5	2601.7 \pm 115.2	939.7 \pm 124.3

In addition to affecting uptake in A549 cells, the presence of FBS in the media also

affected the post-exposure concentrations of HBCD in the cell media itself. In A549 cells, following the 24-hour exposures, the concentration of HBCD in 10% FBS-containing media was 1133.7 ng/mL (Table 3.5), which is more than 20 times higher than HBCD measured in the FBS-free media. There was a similar difference in HepG2/C3A cell media (Table 3.5) where the concentration of HBCD in 5% FBS-containing media were considerably higher than in FBS-free media (939.7 ng/mL versus 409.9 ng/mL, respectively).

3.4 Discussion

The widespread use of HBCD has given rise to increasing health concerns following human exposure via various routes. Inhalation has been considered as one (albeit minor) pathway of human exposure to HBCD (Marvin et al., 2011). There is therefore a particular interest in investigating effects in lung cells as this organ has relatively high exposure and in liver cells that play a critical role in the detoxification (or activation) of xenobiotic chemicals and in which protective compensatory changes are often seen. A549 lung epithelial cells and HepG2/C3A liver cells were thus selected as *in vitro* models to investigate the potential toxic effects of HBCD in this study.

The EC₅₀ value of cytotoxicity of HBCD to HepG2/C3A cells in this study (63.0 µM) was similar to the value observed in HepG2 cells exposed to HBCD (ca. 50 µM)(Hu et al., 2009)), with both studies conducted containing serum in the exposure media.

Furthermore, in the immortalised human hepatocyte L02 cell line, the EC₅₀ for a 24-hour exposure to HBCD was reported as ca. 60 µM (An et al., 2013). Hence, the EC₅₀ value for this hepatic cell line treated with HBCD is consistent with previously published values, for the case of exposures conducted in the presence of serum which

more closely reflects the *in vivo* situation.

However, in the absence of FBS in the exposure media, the EC₅₀ values of HBCD was reported as being as low as ca. 3 µM in neuronal cell lines (Al-Mousa and Michelangeli, 2012; Reistad et al., 2006). The discrepancy between these reported EC₅₀ values might be explained by differences in the cell type or different levels of serum in the exposure media. The higher serum protein levels could result in a reduction in the free concentration of xenobiotic such as phenanthrene, a hydrophobic polycyclic aromatic hydrocarbon (PAH), accompanied by an increase in the EC₅₀ (Kramer et al., 2012). Free concentrations of compounds are believed to be appropriate to characterise the toxic potency of a chemical *in vitro* which may be used for *in vivo* extrapolation (Gülden et al., 2013). In the present study, the concentrations of HBCD in cell pellets and cell media after exposure were quantified by LC-MS/MS. The lowest concentration of HBCD detected in A549 cell pellets after exposure was ca. 15 ng/mg cell pellet (wet weight) (Table 3.5), which is equal to 750,000 ng/g lipid (assuming 2% lipids in cell pellets which is similar to the lipid content in human liver (Rawn et al., 2014a)). This is several hundred times higher than the highest concentrations reported in human fetal liver (4,500 ng/g lipid, median value: 29 ng/g lipid) and placental tissue (5,600 ng/g lipid, median value: 49 ng/g lipid)(Rawn et al., 2014a). Thus, taking account of the EC₅₀ values of HBCD in cells (63 µM in HepG2/C3A cells in this study), the concentrations achieved in cells that cause cytotoxicity are vastly higher than those reported in human tissues. In addition, mitochondrial reductive activity (MTT assay) and the integrity of the cell membrane (AK assay) in proliferating cells were disrupted by 60 µM HBCD to a greater extent than in confluent cells (Figure 3.6 A and B). However, cell protein content was not significantly changed in the group exposed to 60 µM HBCD for 24 hours

compared to the control group in either proliferating cells or confluent cells (Figure 3.6 C). This suggests that 60 μM HBCD has no significant effects on cell proliferation of HepG2/C3A cells but that proliferating cells were more susceptible to HBCD toxicity.

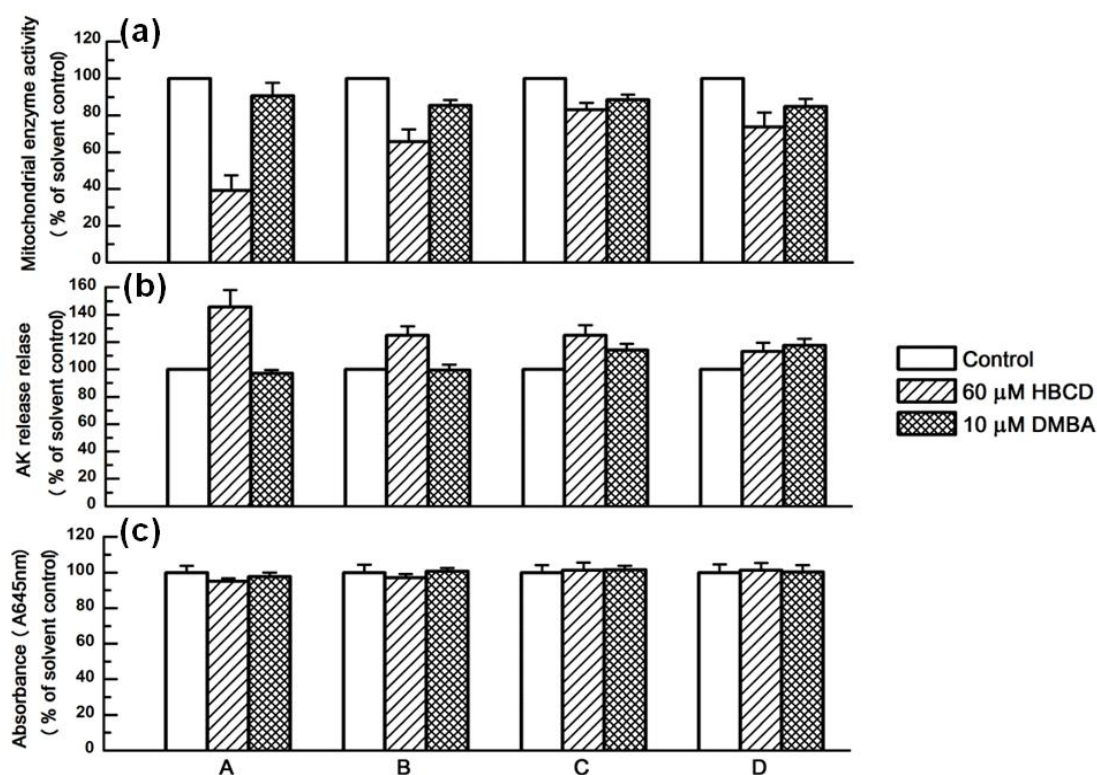


Figure 3.6 Cytotoxic effects of proliferating and confluent HepG2/C3A cells exposed to 60 μM HBCD and 10 μM DMBA for 24 hours. HepG2/C3A cells at various seeding density (A: 10,000cells/well; B: 20,000cells/well; C: 40,000cells/well and D: 60,000cells/well) were exposed to 60 μM HBCD or 10 μM DMBA for 24 hours. Mitochondrial enzyme activity and AK release of different density cells were measured by CCK-8 assay (a) and AK assay (b) (each bar represent at least three independent experiments). Total protein content was evaluated by BioRad DC Protein Assay (c) (each bar represents six replicates). Results of the CCK-8 assay, AK assay and protein assay were expressed as the percentage of the unexposed control \pm standard error (SE). Solvent control values were set as 100%.

Molecular responses in terms of transcriptomic and metabolic levels were also assessed. Particular attention was given to cytochrome P450 monooxygenases (CYPs) that play critical roles in biotransformation activities and the induction of which is a common response to organic toxicants (Danielson, 2002). Forty probe sets

(representing 35 mRNAs of CYPs) were detected in the A549 microarray dataset (Table 3.6), whereas 43 probe sets (representing 33 mRNAs of CYPs) in HepG2/C3A microarray dataset (Table 3.7). CYP1A1 and CYP3A4 are two particularly important members in phase I metabolism of aromatic hydrocarbons. The induction of *CYP1A1* mRNA expression has been used as an indicator of exposure to PAH (Castorena-Torres et al., 2008). In the present study, HBCD did not induce mRNA expression for either of these CYP genes in A549 cells or HepG2/C3A cells after a 24-hour exposure in contrast to the marked induction of *CYP1A1* (175-fold) observed in response to DMBA treatment in HepG2/C3A cells.

Table 3.6 Gene expression of CYPs in A549 cells exposed to HBCD for 24 hrs from microarray dataset.

Gene Symbol	Accession No.	Control	Very Low	Low	Medium	High
CYP11A1 transcript variant 1	[NM_000781]	1.00±0.13	1.13±0.13	1.14±0.11	1.14±0.14	1.15±0.13
CYP11B1 transcript variant 1	[NM_000497]	1.00±0.51	0.86±0.20	1.14±0.62	1.00±0.27	0.99±0.31
CYP11B2	[NM_000498]	1.00±0.15	0.99±0.12	0.97±0.19	1.25±0.34	1.11±0.39
CYP17A1	[NM_000102]	1.00±0.10	1.08±0.06	1.09±0.06	1.00±0.08	1.12±0.12
CYP19A1 transcript variant 2	[NM_031226]	1.00±0.25	0.89±0.13	0.91±0.23	0.92±0.18	0.94±0.13
CYP19A1 transcript variant 2	[NM_031226]	1.00±0.64	0.67±0.15	0.62±0.21	1.43±1.58	0.61±0.11
CYP21A2 transcript variant 1	[NM_000500]	1.00±0.10	0.93±0.08	0.96±0.11	0.96±0.07	1.07±0.16
CYP21A2 transcript variant 2	[NM_001128590]	1.00±0.13	1.08±0.16	1.05±0.12	1.08±0.09	1.09±0.16
CYP24A1	[NM_000782]	1.00±0.09	0.94±0.19	0.99±0.08	0.89±0.21	1.00±0.08
CYP26B1	[NM_019885]	1.00±0.12	0.98±0.08	0.90±0.16	1.20±0.17	1.05±0.13
CYP27A1	[NM_000784]	1.00±0.24	1.02±0.34	0.99±0.22	1.00±0.28	1.13±0.55
CYP27C1	[NM_001001665]	1.00±0.19	1.32±1.02	0.91±0.27	1.16±0.42	1.12±0.55
CYP2A13	[NM_000766]	1.00±0.07	1.02±0.08	1.06±0.04	1.04±0.16	1.12±0.19
CYP2A7 transcript variant 1	[NM_000764]	1.00±0.19	0.96±0.26	0.99±0.23	0.89±0.24	1.11±0.53
CYP2B6	[NM_000767]	1.00±0.06	1.05±0.15	1.01±0.07	0.96±0.13	1.01±0.10
CYP2C18 transcript variant 1	[NM_000772]	1.00±0.17	1.00±0.23	0.92±0.23	0.76±0.07	0.88±0.13
CYP2C19	[NM_000769]	1.00±0.47	0.87±0.04	0.95±0.17	0.87±0.07	0.88±0.06
CYP2C8 transcript variant 1	[NM_000770]	1.00±0.51	0.91±0.24	0.85±0.11	0.87±0.06	0.81±0.07
CYP2C9	[NM_000771]	1.00±0.17	0.96±0.30	0.89±0.20	0.88±0.27	0.94±0.18
CYP2D6 transcript variant 1	[NM_000106]	1.00±0.12	1.06±0.28	0.96±0.10	0.96±0.18	1.00±0.10
CYP2D6 transcript variant 1	[NM_000106]	1.00±0.12	1.04±0.14	1.16±0.14	1.03±0.11	1.07±0.09
CYP2F1	[NM_000774]	1.00±0.21	0.95±0.08	1.17±0.22	1.07±0.43	1.27±0.40
CYP39A1	[NM_016593]	1.00±0.45	0.75±0.12	0.77±0.22	0.78±0.18	0.64±0.14
CYP3A4 transcript variant 1	[NM_017460]	1.00±0.10	1.00±0.08	0.98±0.11	0.95±0.12	1.03±0.14
CYP3A43 transcript variant 1	[NM_022820]	1.00±0.18	1.20±0.39	0.91±0.24	0.89±0.11	1.11±0.38
CYP3A5 transcript variant 2	[NM_001190484]	1.00±0.19	0.95±0.22	1.06±0.06	1.15±0.22	1.16±0.65
CYP46A1	[NM_006668]	1.00±0.25	1.07±0.22	0.96±0.12	0.99±0.29	0.98±0.14
CYP4A11	[NM_000778]	1.00±0.04	1.17±0.17	1.21±0.17	1.17±0.18	1.19±0.29
CYP4A11	[NM_000778]	1.00±0.09	0.97±0.05	0.93±0.10	0.94±0.06	0.92±0.09
CYP4A22	[NM_001010969]	1.00±0.18	1.16±0.13	1.12±0.13	1.21±0.18	0.98±0.20

CYP4B1 transcript variant 2	[NM_000779]	1.00±0.37	2.44±2.15	1.48±1.32	2.50±2.38	2.50±2.69
CYP4F11 transcript variant 1	[NM_021187]	1.00±0.08	0.91±0.11	0.90±0.09	0.97±0.09	0.98±0.13
CYP4F2	[NM_001082]	1.00±0.12	0.95±0.06	0.89±0.10	0.93±0.10	0.88±0.10
CYP4F2	[NM_001082]	1.00±0.46	0.88±0.20	0.80±0.31	0.86±0.51	1.49±1.44
CYP4F22	[NM_173483]	1.00±0.84	0.90±0.42	0.90±0.46	0.78±0.20	0.93±0.45
CYP4V2	[NM_207352]	1.00±0.13	0.91±0.14	0.94±0.17	0.98±0.14	0.99±0.17
CYP4Z1	[NM_178134]	1.00±0.86	7.52±10.50	1.50±1.99	0.31±0.06	0.67±0.91
CYP4Z1	[NM_178134]	1.00±0.2	1.00±0.07	0.89±0.12	0.94±0.20	1.03±0.09
CYP7A1	[NM_000780]	1.00±0.07	1.00±0.15	0.98±0.11	0.94±0.16	0.96±0.10
CYP8B1	[NM_004391]	1.00±0.19	1.06±0.23	1.44±0.58	1.58±1.55	1.12±0.25

Table 3.7 Gene expression of CYPs in HepG2/C3A cells exposed to HBCD and DMBA for 24 hours from microarray dataset.

Gene Symbol	Accession No.	Control	HBCD	DMBA
CYP2A13	[AY513606]	1.00 ±0.08	0.89 ±0.42	1.16 ±0.13
CYP1A1	[NM_000499]	1.00 ±0.27	0.78 ±0.27	26.26±3.10
CYP1A2	[NM_000761]	1.00 ±0.07	0.88 ±0.40	2.14 ±0.09
CYP11A1,transcript variant 1	[NM_000781]	1.00 ±0.05	0.92 ±0.44	0.99 ±0.08
CYP17A1	[NM_000102]	1.00 ±0.10	0.85 ±0.38	0.98 ±0.11
CYP19A1, transcript variant 2,	[NM_031226]	1.00 ±0.05	0.86 ±0.41	1.16 ±0.07
CYP19A1, transcript variant 2	[NM_031226]	1.00 ±0.12	0.81 ±0.36	0.91 ±0.04
CYP2A13	[NM_000766]	1.00 ±0.08	0.86 ±0.41	0.94 ±0.08
CYP2B6	[NM_000767]	1.00 ±0.07	0.98 ±0.45	1.62 ±0.08
CYP2B6	[NM_000767]	1.00 ±0.03	0.88 ±0.43	1.07 ±0.05
CYP2D6, transcript variant 1	[NM_000106]	1.00 ±0.10	0.86 ±0.38	0.92 ±0.08
CYP2D6, transcript variant 1,	[NM_000106]	1.00 ±0.13	0.91 ±0.41	0.95 ±0.18
CYP2J2	[NM_000775]	1.00 ±0.10	0.88 ±0.39	1.10 ±0.08
CYP2R1	[NM_024514]	1.00 ±0.10	0.81 ±0.36	1.14 ±0.07
CYP2S1	[NM_030622]	1.00 ±0.12	0.93 ±0.39	1.29 ±0.15
CYP2S1	[NM_030622]	1.00 ±0.07	0.93 ±0.43	1.37 ±0.10
CYP2W1	[NM_017781]	1.00 ±0.06	0.81 ±0.37	0.87 ±0.07
CYP20A1	[NM_177538]	1.00 ±0.06	0.84 ±0.39	1.00 ±0.17
CYP20A1	[NM_177538]	1.00 ±0.04	0.84 ±0.39	0.96 ±0.08
CYP21A2, transcript variant 1	[NM_000500]	1.00 ±0.05	0.85 ±0.39	2.09 ±0.17
CYP21A2, transcript variant 2,	[NM_001128590]	1.00 ±0.06	0.76 ±0.35	1.06 ±0.31
CYP24A1,transcript variant 1,	[NM_000782]	1.00 ±0.08	0.91 ±0.44	1.39 ±0.11
CYP24A1,transcript variant 1,	[NM_000782]	1.00 ±0.15	0.93 ±0.39	1.82 ±0.55
CYP26A1, transcript variant 2,	[NM_057157]	1.00 ±0.26	1.08 ±0.48	1.86 ±0.28
CYP27A1	[NM_000784]	1.00 ±0.02	0.86 ±0.41	0.97 ±0.07
CYP27B1	[NM_000785]	1.00 ±0.06	0.84 ±0.38	0.98 ±0.07
CYP3A4, transcript variant 1	[NM_017460]	1.00 ±0.10	0.93 ±0.43	1.05 ±0.11
CYP3A5, transcript variant 1	[NM_000777]	1.00 ±0.04	0.88 ±0.41	1.60 ±0.09
CYP3A5, transcript variant 2	[NM_001190484]	1.00 ±0.22	1.01 ±0.43	1.66 ±0.22
CYP3A7	[NM_000765]	1.00 ±0.06	0.93 ±0.43	1.37 ±0.07
CYP3A7	[NM_000765]	1.00 ±0.09	0.89 ±0.40	1.42 ±0.07
CYP4A11	[NM_000778]	1.00 ±0.10	0.92 ±0.43	1.16 ±0.07
CYP4A11	[NM_000778]	1.00±0.12	0.76 ±0.33	0.80 ±0.10
CYP4F11, transcript variant 1	[NM_021187]	1.00 ±0.09	0.89 ±0.40	1.58±0.11
CYP4F11, transcript variant 1	[NM_021187]	1.00 ±0.10	0.90 ±0.41	1.44 ±0.26
CYP4F12	[NM_023944]	1.00 ±0.10	0.80 ±0.35	1.15 ±0.14
CYP4F2	[NM_001082]	1.00 ±2.14	0.16 ±0.06	0.14 ±0.03
CYP4F2	[NM_001082]	1.00 ±0.09	0.82 ±0.36	1.44 ±0.07
CYP4F3, transcript variant 1	[NM_000896]	1.00 ±0.08	0.83 ±0.37	1.43 ±0.11
CYP4F8	[NM_007253]	1.00 ±0.05	0.81 ±0.38	1.13 ±0.05
CYP4V2	[NM_207352]	1.00 ±0.09	0.80 ±0.37	0.98 ±0.15
CYP51A1, transcript variant 1	[NM_000786]	1.00 ±0.04	0.83 ±0.39	0.84 ±0.05
CYP8B1	[NM_004391]	1.00 ±0.07	0.89 ±0.41	0.91 ±0.03

Several studies have reported that *CYP3A4* is not expressed in A549 cells (Courcot et al., 2012; Hukkanen et al., 2000). However, in a recent study, the expression of *CYP3A4* was induced by 5 μ M of the PAH benzo[a]pyrene (B[a]P) in A549 cells exposed for 14 hours, but not in HepG2 cells (Genies et al., 2013). Fery et al. (2009) also reported that HBCD failed to induce CYP3A enzyme activity in HepG2 cells, but a significant induction was observed in primary cultured rat hepatocytes. In this study, mRNA expression of *CYP3A4* was detected in both A549 and HepG2/C3A cells, and this was slightly down-regulated after a 24-hour exposure to 20 nM and 200 nM HBCD in A549 cells while there were no significant changes in HepG2/C3A cells. These observations show a noticeable contrast between HBCD and DMBA in the induction of CYP expression.

The effects observed with DMBA are markedly different from those following HBCD exposure despite the latter showing intracellular accumulation. The extensive modification of the transcriptome as seen with DMBA includes evidence of a significant stress response at sub-toxic concentrations. These responses include the changes in CYP expression as mentioned above plus a range of other responses in the expression of genes involved in (e.g. apoptosis, regulation of cell proliferation, etc.). Neither two cell types showed this stress response to HBCD. This might be interpreted as a failure to react in a compensatory mode for protective purposes since no such response is seen right up to the concentrations that exhibit a toxic effect in the MTT assay or CCK-8 assay.

Few detectable transcriptomic and metabolomic responses after 24 hours exposure might be due to missing the time window of some defensive or protective events. It has been reported that levels of *CYP1A1* mRNA in A549 and HepG2 cells were modulated

by B[a]P at an early stage of exposure (less than 4 or 6 hours) but not beyond (Genies et al., 2013). Likewise, potential molecular responses after a relatively longer exposure may reflect potential chronic toxicity. van der Ven et al.(2006) reported that 28 days exposure to HBCD at a relatively high dose (30 mg/kg/day) increased liver weight in female rats and induced hepatic CYP enzyme activities (CYP2B1 and CYP3A1) in rats (Cantón et al., 2008; Germer et al., 2006). However, a 72-hour exposure at relative low concentration (2 to 200 nM) did not significantly change the survival rate and the malformation rate in zebrafish embryos (Wu et al., 2013). In the present study, additional DIMS analysis suggested possible metabolic changes (e.g. decrease of taurine) after 72hours exposure in HepG2/C3A cells exposed to 4 µM HBCD, which might be responsive to stress after longer exposure or the delayed effects of 24 hours exposure.

3.5 Conclusions

'Omics approaches were used to determine the potential molecular changes in two cell lines after exposure to HBCD over a wide range of concentrations in the presence of serum. Few molecular changes were observed in the 'omics data despite employing cellular concentrations of HBCD up to several hundred times higher than those reported in human tissues and concentrations that approached cytotoxic levels. In contrast to the findings for the PAH, there was little evidence of a compensatory stress response to HBCD such as elevation of CYP or antioxidant systems. This lack of compensatory response does not equate to a lack of protection since cytotoxicity (mitochondrial dysfunction and loss of cell integrity) was only observed in HepG2/C3A cells exposed to a high concentration of HBCD (60 µM), at which the cellular concentrations achieved exceeded, by several orders of magnitude, the tissue

concentrations observed in environmentally exposed organisms.

CHAPTER 4 Transcriptomic and metabolomic responses of human cell lines exposed to tris (1, 3-dichloro-2-propyl) phosphate (TDCIPP)*

*The content of this chapter has been accepted for publication in *Journal of Applied Toxicology*: Zhang, J., Williams, T.D., Chipman, J.K., Viant, M.R., 2015. Defensive and adverse energy-related molecular responses precede Tris (1, 3-dichloro-2-propyl) phosphate (TDCIPP) cytotoxicity. *Journal of Applied Toxicology*. DOI 10.1002/jat.3194.

4.1 Introduction

Tris (1,3-dichloro-2-propyl) phosphate (TDCIPP) is a high volume production PFR which is added to flexible polyurethane foam in the automotive upholstery, foams for household furniture and other commercial products, i.e. beddings (van der Veen and de Boer, 2012). Stapleton et al. (2012) reported that TDCIPP is one of the most abundant PFRs in foam from residential couches in the United States, with an average concentration of 44.87mg/g.

Similar to other additive FRs, TDCIPP is not chemically bound to the material it protects and can leach out from the products to the environment more easily than reactive FRs. TDCIPP has been detected in a wide range of environmental media, i.e. surface water, sediment, biota, air and dust (van der Veen and de Boer, 2012). For example, Carignan et al. (2013) found that the TDCIPP level in office dust samples from Boston, USA was up to 72 µg/g. The average concentration of TDCIPP in car dust in Germany was 130 µg/g (Brommer et al., 2012). The high prevalence of TDCIPP in dust samples suggests that it could contribute as a source of human exposure to TDCIPP within indoor or enclosed environments (Stapleton & Klosterhaus, 2009; van der Veen & de Boer, 2012), especially for toddlers who may have more dust exposure due to frequent hand-mouth behaviour (Butt et al., 2014). The half-life of TDCIPP in humans is believed to be as short as several hours or a few days (Carignan et al., 2013). However, because of the long lifespan of commercial products that contain FRs, human exposure is likely to last for years, even decades (Betts, 2013).

Although, in a risk assessment report, TDCIPP has been classified as a safe compound for its intended application (European Union, 2008), it has also been listed

as a carcinogen in the Proposition 65 list by the California Environmental Protection Agency (OEHHA, 2013). The evidence for TDCIPP's carcinogenicity via a genotoxic mechanism(s) has been building (OEHHA, 2011). For example, positive evidence for genotoxicity was found in *in vitro* tests including mutagenicity in multiple strains of *Salmonella* (Gold et al., 1978), chromosomal aberrations and sister chromatid exchanges in mouse (*Mus musculus*) lymphoma cells (Brusick et al., 1979) and weakly unscheduled DNA synthesis in rat (*Rattus norvegicus*) hepatocytes (Sederlund et al., 1985), though negative results were also found in most *in vivo* genotoxicity studies (OEHHA, 2011). As such, it has been suggested that there is insufficient information to date to determine whether or not TDCIPP induces cancer in humans (ATSDR, 2012). However, in rats, exposure to TDCIPP can increase the rate of formation of tumours at multiple sites (i.e. liver, kidney and testicles) (Freudenthal and Henrich, 2000).

Recent *in vitro* and *in vivo* studies have suggested that TDCIPP is likely to be endocrine disrupting and neurotoxic. Meeker and Stapleton (2010) reported that altered thyroxine levels and decreased semen quality in men might be linked to exposure to TDCIPP. Other studies found that exposure to TDCIPP can change thyroid hormone concentrations in chicken (*Gallus gallus*) embryos (Farhat et al., 2013) and zebrafish (*Danio rerio*) (Wang et al., 2013) and alter sex hormone levels in human H295R cell lines and zebrafish (Liu et al., 2012). Dysregulation of gene expression related to thyroid hormone metabolism was found in zebrafish (Wang et al., 2013) and avian hepatocytes (Crump et al., 2012). TDCIPP displays androgen receptor (AR), glucocorticoid receptor (GR) and pregnane X receptor (PXR) antagonistic activities in cell-based transactivation assays (Kojima et al., 2013). Concentration-dependent neurotoxicity was observed in rat PC12 cells. For example, oxidative stress increased

following 50 μ M TDCIPP treatment (Dishaw et al., 2011), while dysregulation of gene and protein expression related to apoptosis, neurite growth and synapse formation were observed after TDCIPP exposure which could disrupt neurodevelopment (Ta et al., 2014). Limited studies of the hepatic toxicity of TDCIPP were focussed on chicken embryonic hepatocytes or liver; in which phase I and II xenobiotic-metabolizing enzymes were elevated after TDCIPP exposure (Crump et al., 2012; Farhat et al., 2014a).

To assist in the assessment of effects following human exposure to TDCIPP, toxicogenomic responses of two human cell lines (HepG2/C3A and A549 cells) were investigated. Specifically, microarray based transcriptomics and direct infusion mass spectrometry (DIMS) based untargeted metabolomics were employed to explore the potential adverse effects of TDCIPP at sub-cytotoxic concentrations and to help elucidate the mechanisms of action of this PFR in these two human cell lines. Therefore, the aims of this chapter were (1) to examine the gene expression and metabolic profiles of these cell lines exposed to several concentrations of TDCIPP, and (2) to explore the molecular mechanisms of any toxicity in these human cell lines.

4.2 Materials and Methods

4.2.1 Chemicals and reagents

All chemicals, including tris (1, 3-dichloro-2-propyl) phosphate (CAS Number: 13674-87-8, purity >97%) were obtained from Sigma-Aldrich Chemical Company (Dorset, UK) unless otherwise stated.

4.2.2 Cell culture

HepG2/C3A cells were generously provided by Prof. R. Blust from the University of

Antwerp, Belgium. HepG2/C3A cells and A549 cells were cultured as described previously (Section 2.2).

4.2.3 Cytotoxicity assay

To assess the cytotoxicity of TDCIPP to HepG2/C3A cells and A549 cells, the CCK-8 assay, which assesses mitochondrial reductive activity, was applied following the manufacturers' instructions (Dojindo Laboratories, Kumamoto, Japan) as described in Section 2.3.2. Briefly, HepG2/C3A cells (2×10^4 cells per well) and A549 cells (1×10^4 cells per well) were seeded into 96-well plates overnight and the cells were treated in six replicates with various concentrations (1, 5, 10, 25, 50, 100, 200 and 500 μM) of TDCIPP in the media containing FBS for 24 hours or 72 hours. In parallel, a group of HepG2/C3A cells were exposed to the same concentrations of TDCIPP for 24 hours but in FBS-free media. The solvent control group were treated with 0.5% DMSO (v/v) and considered 100% viable. The cell viability was calculated at each concentration of TDCIPP. The half maximal effective concentration (EC_{50}) values were calculated according to the plotted concentration-response curves.

4.2.4 Design of exposure experiment

HepG2/C3A cells and A549 cells were seeded into 6-well plates at cell density of 1×10^6 and 8×10^5 cells/well respectively. After overnight acclimatisation, cells were exposed to different concentrations of TDCIPP (*Low Concentration*: 1 μM ; *Medium Concentration*: 10 μM and *High Concentration*: 100 μM) for 24 hours. In order to evaluate the effects of exposure time, 72-hour exposures were also conducted for HepG2/C3A cells using the same TDCIPP concentrations. In addition, a batch of HepG2/C3A cells was exposed to the same concentrations of TDCIPP for 24 hours employing FBS-free media.

For metabolomics analysis, eight biological replicates were used in each concentration group per treatment condition. For transcriptomics analysis, only HepG2/C3A cells and A549 cells exposed to 10 μM (*Medium concentration*) and 100 μM (*High concentration*) in the FBS-containing media for 24 hours were analysed (n=4). The solvent control groups in each treatment condition were treated with 0.5% DMSO (v/v) with the same number of replicates for omics analyses (Table 4.1).

Table 4.1 Experimental design of TDCIPP exposure experiment.

Groups (Cell lines/exposure time/media type)	<i>High Concentration</i> (100 μM)	<i>Medium Concentration</i> (10 μM)	<i>Low Concentration</i> (1 μM)	Solvent Control
A HepG2/C3A; 24h; + FBS	8 (4)	8 (4)	8	8 (4)
B A549 ; 24h; + FBS	8 (4)	8 (4)	8	8 (4)
C HepG2/C3A; 72h ; + FBS	8	8	8	8
D HepG2/C3A; 24h; - FBS	8	8	8	8

Numbers in this table indicate the biological replicates number in metabolomics analysis (n=8) and numbers in parentheses refer to the number of biological replicates in transcriptomics analysis (n=4).

4.2.5 Transcriptomics analysis

After 24 hours exposure, HepG2/C3A cells and A549 cells were harvested after rapid washing twice with PBS. Cell pellets were collected and quenched in liquid nitrogen for transcriptomics analysis. Total RNA of cells was extracted using Qiagen's mini RNeasy Kit and QIAshredder (Qiagen, Crawley, UK) as described in Section 2.4.1

The procedures for microarray analysis were performed following the manufacturer's protocols as described in Section 2.4.2. Microarray datasets of this study are available from the ArrayExpress database under accession number: E-MTAB-3323. Quantitative Reverse Transcription PCR (qPCR) analysis was performed to quantify the mRNA

expression of six selected genes in HepG2/C3A or A549 cells exposed to TDCIPP as described in Section 2.4.3.

4.2.6 Metabolomics analysis

After 24 hours or 72 hours exposure, cells were harvested and metabolites were extracted as described earlier in Section 2.5.1.2. Briefly, cells were quickly washed with PBS twice before the 6-well plates were quenched on liquid nitrogen. Then, metabolites were extracted by liquid-liquid extraction method (methanol: chloroform: water (v/v/v) was 1:1:0.9). After centrifuge, polar phases were collected and dried until for direct infusion mass spectrometry (DIMS) analysis which was described in Section 2.5.2 including statistical analysis of DIMS data. Putative annotation of significantly changed DIMS peaks were performed by using the metabolite annotation package MI-Pack (Weber and Viant, 2010) as described in 2.5.3.

4.3 Results

4.3.1 Cytotoxicity of TDCIPP to HepG2/C3A cells and A549 cells

The cytotoxicity of TDCIPP to HepG2/C3A cells and A549 cells was evaluated using the CCK-8 assay. Concentration-response curves are shown in Figure 4.1. The EC₅₀ values of TDCIPP to HepG2/C3A cells and A549 cells cultured in the FBS-containing media were 167.9 μ M and 193.1 μ M, respectively. In serum-free media, the EC₅₀ value in HepG2/C3A cells was 202.4 μ M,. However, after an extended exposure of 72 hours, the EC₅₀ value in HepG2/C3A cells (84.0 μ M) declined noticeably compared to a 24-hour exposure which indicates that the extended exposure enhances the cytotoxicity of TDCIPP. There were minimal cytotoxic effects at concentrations ranging from 1 to 100 μ M in both cell lines exposed to TDCIPP for 24 hours, but after a 72-hour

exposure, 100 μM TDCIPP caused obvious cytotoxic effects with an onset at ca. 10 μM in HepG2/C3A cells.

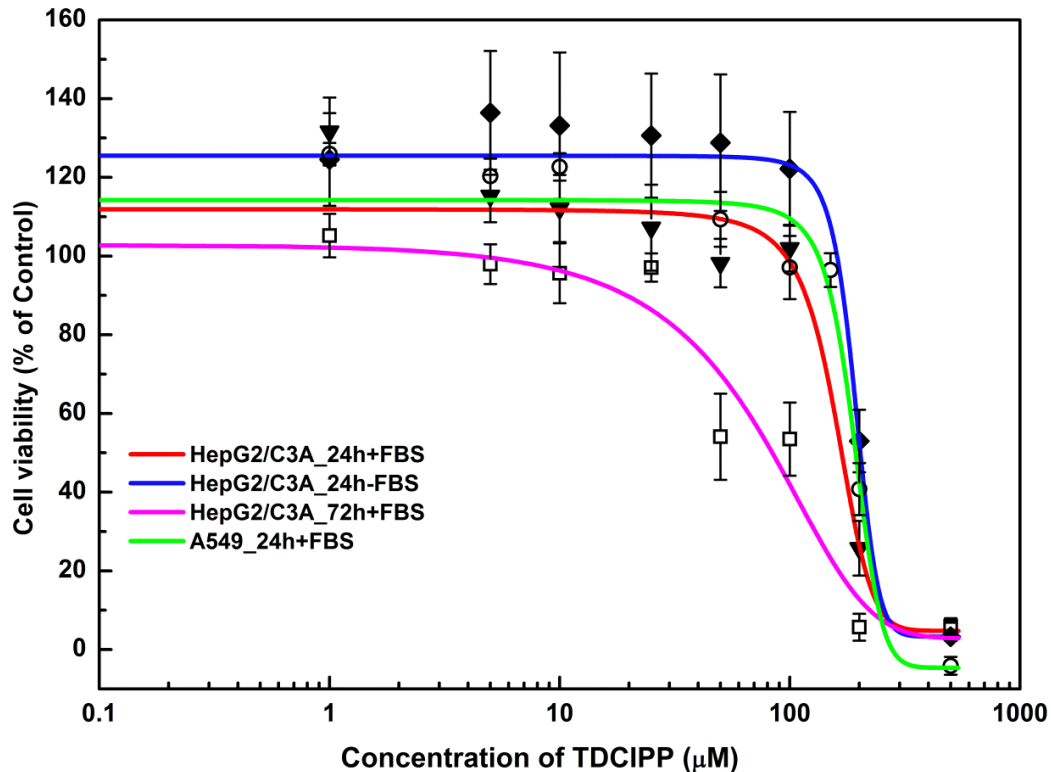


Figure 4.1 Cytotoxic effects of TDCIPP to HepG2/C3A cells and A549 cells. Cell viability of and HepG2/C3A and A549 cells was examined by using CCK-8 assays after exposure to different concentrations (1, 5, 10, 25, 50, 100, 200 and 500 μM) of TDCIPP in FBS-containing media or FBS-free media for 24 or 72 hours, respectively. Results are expressed as the percentage of cell viability compared to controls treated with the appropriate vehicle (0.5% DMSO (v/v)). Data represent mean \pm SD (n=6) (EC_{50} = 167.9 μM , 202.4 μM , 84.0 μM and 193.1 μM) (diamond represents HepG2/C3A_24hr-FBS; triangle represents HepG2/C3A_24hr +FBS; square box represents HepG2/C3A_72hr+FBS; circle represents A549_24hr+FBS.)

Using these concentration-response curves (Figure 4.1) and EC_{50} values, several concentrations were selected for the omics studies. These included *Low* (1 μM) and *Medium* (10 μM), which represent sub-cytotoxic concentrations in the present study, and a *High concentration* (100 μM) at which cytotoxic effects were known to occur by 72 hour.

4.3.2 Omics effects of TDCIPP on HepG2/C3A and A549 cells

4.3.2.1 Transcriptomic responses of HepG2/C3A and A549 cells exposed to TDCIPP for 24 hours

Oligonucleotide microarrays were employed to investigate the gene expression profiles of HepG2/C3A and A549 cells exposed to 10 μM (*Medium Concentration*) and 100 μM (*High Concentration*) TDCIPP for 24 hours. PCA analysis of these microarray datasets (Figure 4.2) showed a distinct difference between the *High concentration* group and all other groups in both cell lines.

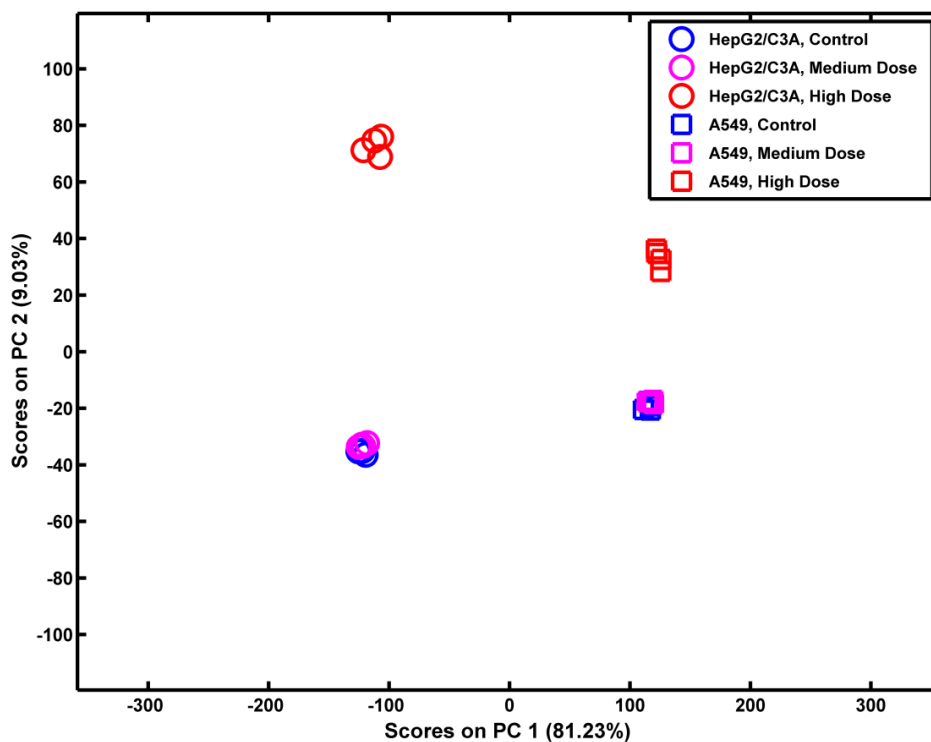


Figure 4.2 PCA scores plot of all genes of HepG2/C3A and A549 cells exposed to TDCIPP for 24 hours (n=4). Legend: circles represent HepG2/C3A cells treated with TDCIPP for 24 hours with FBS in the exposure media, squares represent A549 cells treated with TDCIPP for 24 hours in the presence of FBS, red represents the *High concentration* group, pink the *Medium concentration* group, and blue are the control group.

Similarly, the results of univariate analyses showed there were 5320 probes altered significantly at *High concentration* in HepG2/C3A cells and 2803 probes at *High*

concentration in A549 cells (File 4.1, in Appendix). However, there were no significant changes in individual gene expression in the *Medium concentration* group for either HepG2/C3A or A549 cells. DAVID analysis showed that the significantly differentially expressed genes in *High concentration* groups in HepG2/C3A cells were related to regulation of transcription, mitochondrion, lipid metabolism and amino acid metabolism related pathways (File 4.2, in Appendix). In A549 cells, DAVID analysis of significantly modulated genes revealed up regulation of apoptosis and down regulation of cell cycle related pathways (File 4.2, in Appendix) after exposure to *High concentration* TDCIPP.

Gene Set Enrichment Analysis was then employed to explore any potential changes of gene sets where the subtle changes of individual genes may not be significant in classic univariate statistical analysis. Interestingly, the results of GSEA (Table 4.2) revealed that genes involved in oxidative phosphorylation and cell cycle pathways were down-regulated subtly in the *Medium concentration* group in HepG2/C3A cells, and to a greater extent in *High concentration* groups, while the *Medium concentration* group of A549 cells shared similar results. However, xenobiotic metabolism related pathways (e.g. drug metabolism cytochrome P450 and ABC transporters) were up-regulated in the *Medium concentration* group of HepG2/C3A cells, but down-regulated in the *High concentration* group. Similar results were found in A549 cells, but these were not statistically significant in the *High concentration* group.

Table 4.2 Normalized Enrichment Scores of significant pathways in HepG2/C3A cells and A549 cells exposed to TDCIPP for 24 hours.

Pathways	HepG2/C3A		A549		Pathways	HepG2/C3A		A549	
	Medium	High	Medium	High		Medium	High	Medium	High
KEGG_ABC_TRANSPORTERS	1.550	NS	2.039	NS	KEGG_RNA_POLYMERASE	-1.521	NS	-1.927	NS
KEGG_RETINOL_METABOLISM	1.843	NS	NS	NS	KEGG_RNA_DEGRADATION	-1.644	NS	NS	NS
KEGG_LINOLEIC_ACID_METABOLISM	1.705	NS	NS	NS	KEGG_SELENOAMINO_ACID_METABOLISM	-1.517	NS	NS	NS
KEGG_DRUG_METABOLISM_CYTOCHROME_P450	1.647	-1.796	NS	NS	KEGG_N_GLYCAN_BIOSYNTHESIS	-1.516	NS	NS	NS
KEGG_TASTE_TRANSDUCTION	1.569	NS	NS	NS	KEGG_PEROXISOME	NS	-2.136	NS	NS
KEGG_ERBB_SIGNALING_PATHWAY	NS	1.916	NS	NS	KEGG_PROPANOATE_METABOLISM	NS	-2.130	NS	NS
KEGG_LYSOSOME	NS	NS	2.029	NS	KEGG_BETA_ALANINE_METABOLISM	NS	-2.038	NS	NS
KEGG_STEROID_BIOSYNTHESIS	NS	-2.124	2.227	NS	KEGG_FATTY_ACID_METABOLISM	NS	-1.992	NS	NS
KEGG_RIBOSOME	-1.719	1.838	-1.813	NS	KEGG_VALINE_LEUCINE_AND_ISOLEUCINE_DEGRADATION	NS	-1.973	NS	NS
KEGG_DNA_REPLICATION	-1.898	-2.318	-2.020	-2.867	KEGG_BUTANOATE_METABOLISM	NS	-1.948	NS	NS
KEGG_PARKINSONS_DISEASE	-1.866	-2.499	-1.729	-1.990	KEGG_GLUTATHIONE_METABOLISM	NS	-1.932	NS	NS
KEGG_SPLICEOSOME	-1.768	-1.640	-2.152	-2.624	KEGG_CARDIAC_MUSCLE_CONTRACTION	NS	-1.918	NS	NS
KEGG_MISMATCH_REPAIR	-1.806	-1.718	-1.667	-2.240	KEGG_PENTOSE_PHOSPHATE_PATHWAY	NS	-1.911	NS	NS
KEGG_CELL_CYCLE	-1.680	-1.652	-1.917	-2.475	KEGG_PYRUVATE_METABOLISM	NS	-1.904	NS	NS
KEGG_PROTEASOME	-1.998	-1.911	-1.831	NS	KEGG_BIOSYNTHESIS_OF_UNSATURATED_FATTY_ACIDS	NS	-1.874	NS	NS
KEGG_HUNTINGTONS_DISEASE	-1.761	-2.019	-1.820	NS	KEGG_GLYCINE_SERINE_AND_THREONINE_METABOLISM	NS	-1.804	NS	NS
KEGG_SYSTEMIC_LUPUS_ERYTHEMATOSUS	-1.578	-2.213	-2.547	NS	KEGG_O_GLYCAN_BIOSYNTHESIS	NS	-1.737	NS	NS
KEGG_OXIDATIVE_PHOSPHORYLATION	-1.774	-2.504	NS	-1.812	KEGG_GLYCOSAMINOGLYCAN_BIOSYNTHESIS_HEPATIC	NS	-1.626	NS	NS
KEGG_BASE_EXCISION_REPAIR	-1.542	-1.568	NS	-2.027	KEGG_ARGININE_AND_PROLINE_METABOLISM	NS	-1.552	NS	NS
KEGG_PYRIMIDINE_METABOLISM	-1.625	NS	-2.027	-2.046	KEGG_HISTIDINE_METABOLISM	NS	-1.548	NS	NS
KEGG_NUCLEOTIDE_EXCISION_REPAIR	-1.694	NS	-1.670	-1.799	KEGG_CITRATE_CYCLE_TCA_CYCLE	NS	-1.536	NS	NS
KEGG_ALZHEIMERS_DISEASE	-1.724	-2.206	NS	NS	KEGG_PATHOGENIC_ESCHERICHIA_COLI_INFECTION	NS	NS	-1.655	NS
KEGG_GLYCOSYLPHOSPHATIDYLINOSITOL_GPI_ANCHORING	-1.537	-1.670	NS	NS	KEGG_HOMOLOGOUS_RECOMBINATION	NS	NS	NS	-2.111
KEGG_GLYCOLYSIS_GLUCCONEOGENESIS	NS	-2.223	NS	-1.722	KEGG_OOCYTE_MEIOSIS	NS	NS	NS	-1.952
KEGG_PURINE_METABOLISM	NS	-1.536	NS	-1.723	KEGG_PROGESTERONE_MEDIATED_OOCYTE_MATURATION	NS	NS	NS	-1.895

Normalized enrichment scores (NES) of significantly changed gene sets/KEGG pathways (FDR <0.05) from both HepG2/C3A and A549 cell lines exposed to TDCIPP. Red colour donates enrichment amongst up-regulated genes, and green colour donates enrichment amongst down-regulated genes, NS denotes no significant change. (Detailed results of GSEA including FDR q-values are available in File 4.3, in Appendix.)

Since the gene expression profiles of both cell types showed concentration-response trends, we tested several genes in the *Medium concentration* group, which might represent the marginal effects on gene expression, by using qPCR. As shown in Table 4.3, the fold change of selected genes (*CYP1A1*: phase I xenobiotic metabolism; *ABCC2*: multi-drug transporter; *ATP5J2*, *NQO1* and *NDUFB3*: oxidative phosphorylation; *MT1L*: stress response) from *Medium concentration* groups were similar to those found by microarray analysis. In HepG2/C3A cells, the expression of *CYP1A1* gene showed an up-regulated trend (1.5-fold, but not significant in qPCR analysis) in the *Medium concentration* group, with a remarkable 38-fold up-regulation in the *High concentration* group. The expression of the *ABCC2* gene was statistically significantly slightly increased (1.3-fold in qPCR analysis) in the *Medium concentration* group and statistically significantly induced in the *High concentration* group (2.6-fold) in HepG2/C3A cells. None of the three selected genes (*ATP5J2*, *NQO1* and *NDUFB3*) involved in the oxidative phosphorylation pathway were significantly changed in the *Medium concentration* group in either qPCR or microarray analysis except for a slight increase of gene expression of *NQO1* (1.2-fold in qPCR analysis) in A549 cells. However, significant down-regulation of these genes was observed in the *High concentration* group in both cell lines. *MT1L* was 21-fold up-regulated in the *High concentration* group of HepG2/C3A cells, while in the *Medium concentration* group there was no significant change detected by qPCR analysis. In A549 cells, a slight (non-significant) increase was observed for the *High concentration* group and there was no significant change in *Medium concentration* group by either qPCR or microarray analysis.

Table 4.3 Fold changes of selected genes in HepG2/C3A and A549 cells exposed to 10 µM TDCIPP for 24 hours.

Genes	HepG2/C3A						A549					
	qPCR		Microarray				qPCR		Microarray			
	Medium concentration		Medium concentration		High concentration		Medium concentration		Medium concentration		High concentration	
	Fold change	p-value	Fold change	corrected p-value	Fold change	corrected p-value	Fold change	p-value	Fold change	corrected p-value	Fold change	corrected p-value
CYP1A1	1.47 ± 0.30	0.052	1.48 ± 0.75	0.622	37.58 ± 12.74	0.000	1.21 ± 1.04	0.714	1.15 ± 0.50	0.874	1.65 ± 0.67	0.426
ABCC2	1.30 ± 0.17	0.032	1.27 ± 0.18	0.581	2.58 ± 0.42	0.001	1.01 ± 0.25	0.926	1.16 ± 0.27	0.905	0.94 ± 0.19	0.648
ATP5J2	1.02 ± 0.37	0.903	0.89 ± 0.05	0.581	0.41 ± 0.04	0.000	1.14 ± 0.11	0.091	0.88 ± 0.25	0.893	0.55 ± 0.08	0.038
NQO1	0.92 ± 0.20	0.494	1.09 ± 0.14	0.73	0.56 ± 0.08	0.002	1.18 ± 0.05	0.004	0.99 ± 0.27	0.97	0.58 ± 0.18	0.032
NDUFB3	0.98 ± 0.36	0.933	0.88 ± 0.05	0.581	0.31 ± 0.04	0.000	1.22 ± 0.16	0.066	0.87 ± 0.23	0.889	0.38 ± 0.06	0.015
MT1L	0.88 ± 0.29	0.459	0.93 ± 0.14	0.76	20.50 ± 3.02	0.000	1.49 ± 0.63	0.217	1.01 ± 0.68	0.943	1.27 ± 0.34	0.487

In qPCR analysis, fold changes (mean ± SD) with p-values less than 0.05 by t-test (in Minitab 16) were considered as significant, while significance of fold changes in microarray analysis were tested by t-tests with corrected p-values using Benjamini-Hochberg method in Genespring (Agilent). Bold p-values or corrected p-values were less than 0.05.

4.3.2.2 Metabolomic responses of HepG2/C3A and A549 cells exposed to TDCIPP for 24 hours

PCA showed that the polar metabolome of HepG2/C3A cells in the *High concentration* group was separated remarkably from the rest of the groups (Figure 4.3).

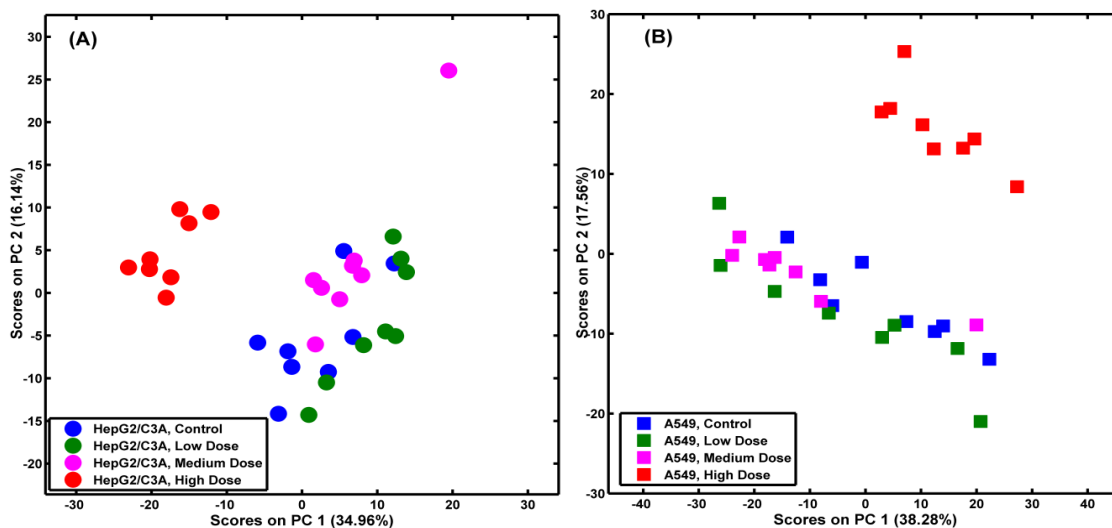


Figure 4.3 PCA scores plots of the polar metabolome of HepG2/C3A cells (A) and A549 cells (B) exposed to TDCIPP ($n=8$). Legend: red represents the *High concentration* group, pink the *Medium concentration* group, green the *Low concentration* group, and blue are controls.

ANOVA (and subsequent Tukey-Kramer's post hoc tests) of the top four PC scores confirmed that this group was significantly different along both PC1 and PC2 (representing 35.0% and 16.1% of the variance within the DIMS dataset, respectively) (Table 4.4).

Table 4.4 Summary of principal component (PC) analyses of microarray and DIMS datasets of A549 cells and HepG2/C3A cells exposed to TDCIPP.

Dataset		PC1	PC2	PC3	PC4
HepG2/C3A_24hrs_Microarray	variance	69.77%	5.93%	5.49%	4.85%
	p value	2.68E-13	0.472	0.966	0.922
A549_24hrs_Microarray	variance	53.11%	13.43%	8.40%	6.34%
	p value	2.26E-11	0.947	0.151	0.242
HepG2/C3A_24hrs_DIMS	variance	34.96%	16.14%	10.37%	5.21%
	p value	5.85E-11	0.015	0.33	0.307
A549_24hrs_DIMS	variance	38.28%	17.56%	8.27%	6.34%
	p value	0.008	8.47E-09	0.838	0.01
HepG2/C3A_without FBS_DIMS	variance	32.04%	12.96%	9.50%	4.69%
	p value	7.89E-13	1.57E-06	0.055	0.022
HepG2/C3A_72hrs_DIMS	variance	54.30%	10.84%	5.52%	4.83%
	p value	9.75E-26	6.96E-20	0.112	8.44E-11

(Groups in each dataset as described in section 4.2.4: Control, *Low* concentration, *Medium* concentration and *High* concentration). The variance explained (%) by PCs 1-4 are listed together with p values from ANOVAs of these PC scores across all treatments (values in bold indicate significance at a false discovery rate (FDR) <10%).

More than 2000 DIMS peaks were determined to change significantly in the *High* concentration group (corrected p-value < 0.05) by t-test (File 4.4, in Appendix). In the *Medium* concentration group, only 66 DIMS peaks changed significantly compared to the control group, of which 41 DIMS peaks were also significantly altered in the *High* concentration group. Only one DIMS peak was significantly changed in the *Low* concentration group.

Putative annotation of these significantly changed DIMS peaks was performed in MI-Pack by searching against the HMDB and KEGG databases. These results were then subjected to pathway over-representation analysis in IMPaLA, which indicated the dysregulation of several metabolic pathways related to ABC transporters, metabolism of amino acids and derivatives (i.e. arginine and proline metabolism,

cysteine and methionine metabolism, glycine and serine metabolism) and glutathione conjugation in the *High concentration* group (File 4.5, in Appendix).

Similarly, the *High concentration* group of A549 cells also showed distinct differences from all other groups in the PCA scores plot (Figure 3B). The significance tests of the PC scores confirmed that groups differed along PC1 (Table 4.4). There were more than 1000 significantly changed DIMS peaks in the *High concentration* group compared with the control (File 4.4, in Appendix). Although there were fewer significantly changed DIMS peaks in the *High concentration* group of A549 cells compared to that discovered for the *High concentration* group in HepG2/C3A cells, the pathway analysis of significant DIMS peaks with putatively annotated metabolite names showed similar disturbed metabolic pathways, which included ABC transporters, metabolism of amino acids and derivatives, and glutathione conjugation (File 4.5, in Appendix).

4.3.2.3 Metabolomic responses of HepG2/C3A exposed to TDCIPP for 72 hours

To evaluate the effects of increased exposure time on the toxicity of TDCIPP, the metabolome of HepG2/C3A cells treated with TDCIPP (1, 10 and 100 μM) for 72 hours were analysed. Following these extended exposures, the metabolic profiles of HepG2/C3A cells in the *High concentration* group was altered drastically compared with the controls (Figure 4.4), and the statistical significance of the top four PC scores were all verified by ANOVA and Tukey-Kramer's post hoc tests (Table 4.4).

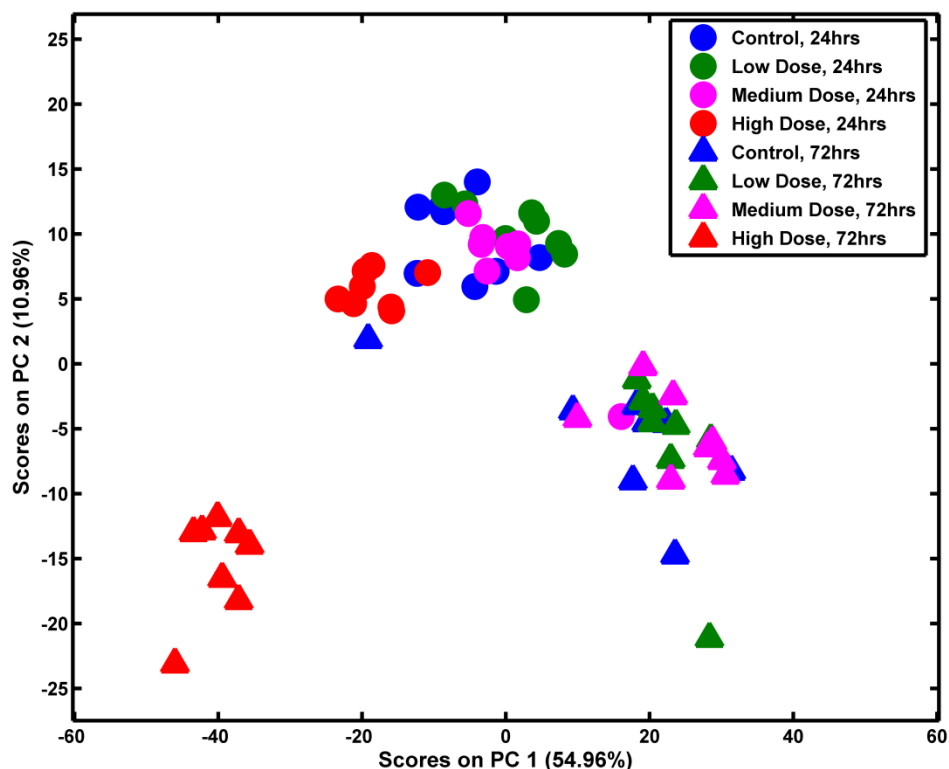


Figure 4.4 PCA scores plot of the polar metabolome of HepG2/C3A cells exposed to TDCIPP for 24 hours and 72 hours ($n=8$). Legend: circles represent the 24-hour exposure, triangles represent the 72-hour exposure, red represents the High concentration group, pink the Medium concentration group, green the Low concentration group, and blue are controls.

Further analyses revealed that more than 4000 DIMS peaks were significantly changed in the *High concentration* group after 72-hour exposures, double that of the *High concentration* group after 24-hour exposures (File 4.4, in Appendix). However, there were no significantly changed DIMS peaks in the *Medium concentration* group or the *Low concentration* groups, similar to the 24-hour exposures. Additional significant metabolic pathways (e.g. metabolism of nucleotides, glyoxylate and dicarboxylate metabolism, and fructose and mannose metabolism) were identified in the *High concentration* group after 72-hour exposures, but both 24-hour and 72-hour exposures shared some common pathways, e.g. ABC transporters, arginine and

proline metabolism, cysteine and methionine metabolism, glycine and serine metabolism, and glutathione conjugation (File 4.5, in Appendix).

4.4 Discussion

Although TDCIPP has been widely applied as an alternative flame retardant since PBDEs have been phased out from global FRs market, its molecular mechanisms of toxicity have not been extensively characterised. In the present study, unbiased transcriptomic and metabolomic approaches were employed to explore potential adverse effects and to help understand the mechanisms of action resulting from exposure to TDCIPP in two human cell lines (HepG2/C3A and A549 cells).

Concentration-dependent cytotoxicity of TDCIPP was observed in both cell lines (Figure 4.1). With FBS in the exposure media, the 24-hour EC_{50} of TDCIPP in HepG2/C3A cells was 167.9 μ M, which is similar to the cytotoxicity found in HepG2/C3A cells exposed in FBS-free media (EC_{50} = 202.4 μ M). Furthermore, DIMS analysis also showed similar metabolic profiles of HepG2/C3A cells treated with TDCIPP for 24 hours in FBS-containing media or FBS-free media (Figure 4.5). This indicates that FBS in the exposure media minimally affected the potency of TDCIPP to HepG2/C3A cells.

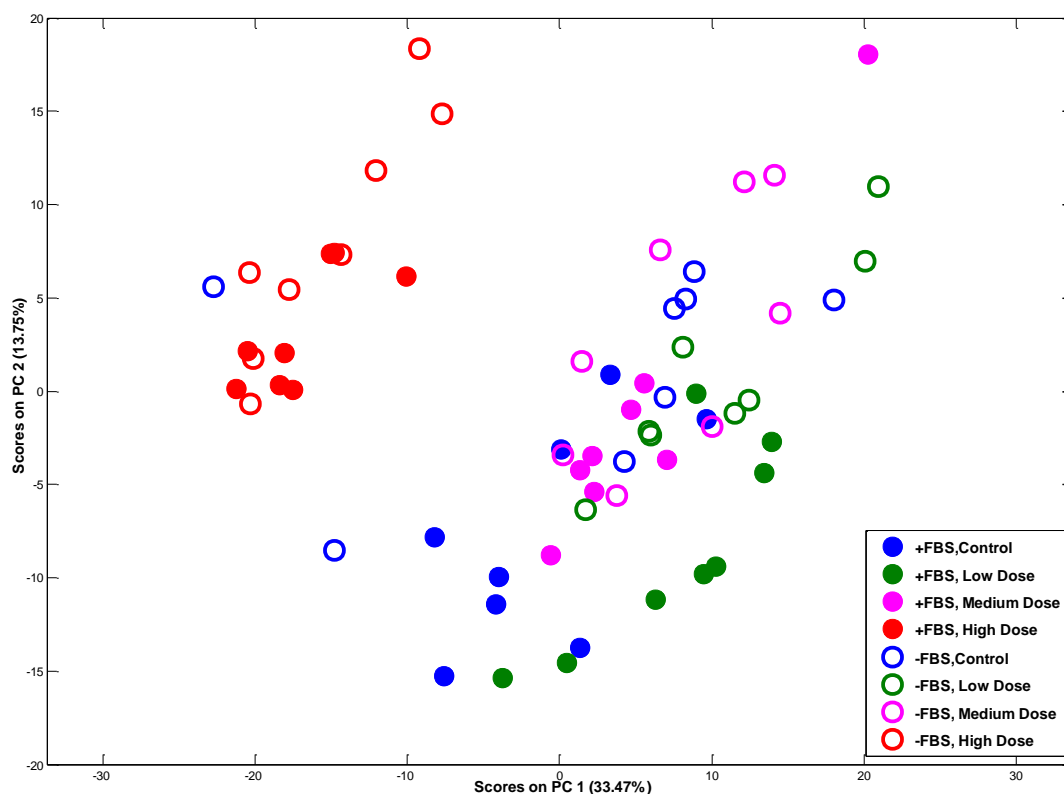


Figure 4.5 PCA scores plot of DIMS data of polar extracts of HepG2/C3A cells exposed to TDCIPP in FBS containing media or FBS-free media (n=8). Legend: closed round represent as HepG2/C3A cells treated with TDCIPP for 24 hours with FBS in the exposure media, while open round represent as HepG2/C3A cells treated with TDCIPP for 24hours without FBS in the exposure media; red represents the *High concentration* group, pink the *Medium concentration* group, green the *Low concentration* group and blues are the control group.

According to the concentration-response curve for TDCIPP, 10 μ M TDCIPP did not cause substantial cytotoxicity in either cell line after a 24-hour exposure, but transcriptional changes were observed that indicated a defensive response in HepG2/C3A cells including an up-regulation of genes involved in xenobiotic metabolism (i.e. cytochrome P450 and ABC transporters). Although the induction of *CYP1A1* gene expression in the *Medium concentration* group in HepG2/C3A cells was not statistically significant (1.5-fold, $p=0.052$), the tendency towards an

up-regulation was confirmed in the *High concentration* group with a 38-fold induction. CYP1A1 is a member of the cytochrome p450 superfamily; it plays a key role in primary xenobiotic metabolism and can be induced by polycyclic aromatic hydrocarbons (PAHs) (Ma and Lu, 2007). It has been reported that a *CYP1A1* gene orthologue was also induced in zebrafish embryos/larvae exposed to 4.64 μM TDCIPP (Liu et al., 2013), but suppression of *CYP1A4*, which is avian orthologue of human *CYP1A1*, was also observed in chicken embryonic hepatocytes (Farhat et al., 2014b). *ABCC2* is a member of the ATP-binding cassette transporters that play important roles in protection against xenobiotics by excreting phase II products out of cells in phase III of xenobiotic metabolism (Szakács et al., 2008). The up-regulation of *ABCC2* mRNA in HepG2/C3A cells exposed to 10 μM TDCIPP was confirmed by qPCR analysis. GSEA of microarray data also suggested that the ABC transporters as a group were up-regulated in cells exposed to *Medium concentration* TDCIPP, which may be part of the cell's protective response.

The genes associated energy metabolism pathways (i.e. oxidative phosphorylation) were down-regulated in HepG2/C3A cells exposed to 10 μM TDCIPP; this effect was concentration dependent with more significantly down-regulated individual genes involved in the oxidative phosphorylation pathway detected after exposure to 100 μM TDCIPP. For example, the expressions of *ATP5J2*, *NQO1* and *NDUFB3* genes were not significantly changed at 10 μM TDCIPP exposure in HepG2/C3A cells but were statistically significant in the *High concentration* group (Table 4.3). The disruption of oxidative phosphorylation may implicate mitochondrial dysfunction at 100 μM TDCIPP exposure, which may link to the cytotoxic effects in HepG2/C3A cells. It has

been reported that tetrabromobisphenol A (TBBPA), another flame retardant, could elicit cytotoxicity through mitochondrial dysfunction linked to oxidative phosphorylation at an early stage, and subsequently lipid peroxidation, in rat hepatocytes (Nakagawa et al., 2007). Here, down-regulated transcriptional responses relevant to peroxisome and lipid metabolism were also found in HepG2/C3A cells exposed to 100 μ M TDCIPP, but not in the 10 μ M group. Furthermore, pathways involved in cell proliferation (e.g. DNA replication, cell cycle) (Files 4.2 and 4.3, in Appendix) were also down regulated in transcriptomic analysis of HepG2/C3A cells treated with 10 or 100 μ M, which may also contribute to the observed cytotoxicity.

In the *High concentration* group, more adverse transcriptional responses of HepG2/C3A cells were observed (Files 4.2 and 4.3, in Appendix), e.g. pathways relevant to energy metabolism (oxidative phosphorylation, glycolysis/ gluconeogenesis, TCA cycle), xenobiotic activity (drug metabolism cytochrome P450, and glutathione metabolism) and cell cycle were down regulated while up-regulation of apoptosis pathway transcripts was also found. These transcriptional changes in the *High concentration* group suggest cellular damage subsequently resulting in cytotoxicity. TDCIPP has been reported as a potential carcinogen possibly through a genotoxic mechanism (OEHHA, 2011). In this study we found that DNA repair gene expression was generally repressed (File 4.1, in Appendix), whereas certain DNA-damage responsive transcripts (e.g. *DDIT3* and *DDIT4*) were induced. If TDCIPP indeed reduces base excision and mismatch DNA repair capacity this could indirectly enhance susceptibility to mutation.

Consistent with the transcriptional changes at 100 μM exposure, metabolomics analysis (File 4.5, in Appendix) also demonstrated that pathways related to ABC transporters and xenobiotic activity (represented by the glutathione conjugation pathway) were disturbed at the metabolic level. However, the metabolomics results did not provide any further support to the transcriptional changes observed at 10 μM TDCIPP exposure. Notably, several DIMS peaks were putatively annotated to be reduced glutathione (GSH) (File 4.4, in Appendix), which is a key cellular antioxidant and used in phase II conjugation reactions in xenobiotic metabolism. Glutathione concentration was increased (but not statistically significantly) in the *Low* and *Medium concentration* groups, but significantly decreased in the *High concentration* group in HepG2/C3A cells. This might imply a defensive response via glutathione oxidation or conjugation in *Low* and *Medium concentration* groups, which was overwhelmed in the *High concentration* group.

The adverse metabolic responses of HepG2/C3A cells after a 24-hour exposure to 100 μM TDCIPP were also observed after 72-hour exposures, with additional significantly changed DIMS peaks. This may be the result of the cytotoxic effects in HepG2/C3A cells after a 72-hour exposure to 100 μM TDCIPP. In addition, the shifting of the concentration-response curve from 24-hour to 72-hour exposures (Figure 4.1), thereby decreasing the EC_{50} value (at 72 hours) to 84.0 μM , confirms the impact of exposure time on HepG2/C3A cytotoxicity.

There are still some limitations in interpreting the molecular responses to TDCIPP in this study. First, the HepG2/C3A cell lines were selected as an *in vitro* model for hepatotoxicity, since these cells have been shown to provide many characteristics of

primary hepatocytes and have been valuable in previous studies (Jairaj et al., 2003; Kawata et al., 2009; Khalaf et al., 2009; Lu et al., 2000; Tian et al., 2008). However, various aspects of xenobiotic metabolising activity of HepG2/C3A cells are still limited compared to human primary culture hepatocytes (Gerets et al., 2012; Hart et al., 2010). It remains possible that a response in primary cells *in vivo* may not be fully recapitulated in cancer- derived cells due to different responsiveness of a particular biological pathway. Therefore, the extrapolation of current results to different cell types *in vivo* should be cautious.

Moreover, the lowest nominal observed effect concentration in this study is 10 μM (ca. 4300 ng/mL). This is an unlikely concentration can be achieved in humans via normal exposure routes. A few available studies reported that the level of TDCIPP in human body is approximate at ng/g lipid levels which is several orders of magnitude lower than concentrations used in the present study. For example, up to 252 ng/g lipid was detected in human adipose tissue samples (LeBel and Williams, 1986) and up to 162 ng/g lipid was reported in human breast milk (Kim et al., 2014) while the average concentration of BDCIPP (which is the primary metabolite of TDCIPP) in human urine was 0.12 ng/mL (Meeker et al., 2013).) There is a need is to gain more information on human exposure to TDCIPP, thus enabling a more robust risk assessment.

In addition, only polar metabolic profiles of the two cell lines were analysed using DIMS-based metabolomics. The non-polar part of the intracellular metabolome was not analysed and potentially could contribute novel insights into the lipidomic changes.

4.5 Conclusions

In summary, we have demonstrated concentration-dependent cytotoxicity of TDCIPP in HepG2/C3A and A549 cells after 24- or 72-hours exposures. Stress responses that reflect a defensive response (e.g. xenobiotic metabolism and ABC transporters) were observed at a transcriptional level following exposure to a sub-cytotoxic concentration of TDCIPP for 24 hours. The down-regulation of energy metabolism-related transcription (oxidative phosphorylation) was apparent at 10 μM , but more severe at a higher concentration (100 μM) exposure, accompanied by the suppression of pathways relevant to cell proliferation (e.g. cell cycle, DNA replication). Functional metabolic pathways (e.g. ABC transporters and metabolism of nucleotides) were disrupted after 72 hours in HepG2/C3A cells exposed to 100 μM TDCIPP that corresponded to the transcriptional and metabolic changes at 24 hours. Taken together, defensive changes to stress and energy-related responses preceded the cytotoxic effects of TDCIPP in HepG2/C3A cells.

CHAPTER 5 Toxicogenomic responses of HepG2/C3A cells exposed to environmental levels of flame retardants and indoor dust extracts*

*The content of this chapter has been submitted to *Chemosphere*: Zhang, J., Abdallah Abou-Elwafa, M., Williams, T.D., Harrad, S., Chipman, J.K., Viant, M.R., 2015. Gene expression and metabolic responses of HepG2/C3A cells exposed to flame retardants and dust extracts at concentrations relevant to indoor environmental exposures.

5.1 Introduction

Since additive FRs are not covalently bound to the treated materials, they can leach out of consumers products over time, particularly to the indoor environment. Studies have suggested that indoor dust is a sink for different types of FRs released from consumer products (Harrad et al., 2010; Rauert et al., 2014), where they are present as a complex mixture with other indoor contaminants (Butte and Heinzow, 2002). For example, the concentration of TDCIPP can reach up to 72 µg/g in office dust (Carignan et al., 2013) and HBCD was found in house dust in the USA at levels up to 130 µg/g (Stapleton et al., 2008).

The ingestion of indoor dust is one of primary routes for human exposure to mixed FRs while others include through diet, inhalation of air and direct dermal contact with dust or consumer products (Abdallah et al., 2015a; Harrad et al., 2010). Consequently, there are increasing concerns about the effects of human exposure to FRs, especially since different types of FRs have been detected in human serum and tissues (Darnerud, 2003; Frederiksen et al., 2009; Kim et al., 2014; Pulkrabová et al., 2009; Rawn et al., 2014a, 2014b; van der Veen and de Boer, 2012).

Toxicological studies have demonstrated that many FRs can be neurotoxic, and endocrine disruptive, both *in vitro* and *in vivo*. For example, PBDEs are neurotoxic to rat neuronal cells by altering the release of neurotransmitters and disturbing Ca²⁺ homeostasis (Dingemans et al., 2008), while PBDEs have been shown to alter serum thyroxine (T4) levels in pregnant women (Stapleton et al., 2011; Zota et al., 2011). It has also been shown that TBBPA can mimic estrogen to bind and inhibit a key hormone-metabolizing enzyme, human estrogen sulfotransferase (*SULT1E1*)

(Gosavi et al., 2013). Hepatotoxicity of FRs has also been described. Chronic exposure to HBCD at 30 mg/kg/day (for 28 days) increased liver weight in female rats (van der Ven et al., 2006) and induced hepatic cytochrome P450 (CYP) enzyme activities (CYP2B1 and CYP3A1) in these animals (Cantón et al., 2008; Germer et al., 2006). Besides the neurotoxic (Dishaw et al., 2011) and endocrine disruptive (Dishaw et al., 2014) properties of a number of OPFRs, some of them (e.g. TCEP, TCIPP and TDCIPP) have been suggested to possess carcinogenic potential (ATSDR, 2012; OEHHA, 2011; van der Veen and de Boer, 2012).

However, under realistic indoor conditions, humans are exposed to a complex mixture of chemicals including FRs. Toxicity screening of chemical mixtures might reflect the effects of exposure more accurately by including the potential interactions (i.e. additive, synergistic or antagonistic) of individual components in the complex formulation (Bandelet et al., 2012). Suzuki et al. (2013) reported that indoor dust extracts containing various FRs were agonistic to estrogen receptor α (ER α) and antagonistic to the androgen receptor (AR) and progesterone receptor (PR). These effects correlated with the levels of FRs in dust and were similar to the endocrine-disrupting potencies of some individual FRs. In another study, rats were exposed to a complex brominated FR mixture mimicking the relative individual levels of the flame retardants in house dust. This affected liver and thyroid physiology in adult male rats (Ernest et al., 2012) and increased abnormalities of bone development in fetal rats, which are novel phenotypes that have not been reported in previous studies of the effects of individual brominated FR congeners (Berger et al., 2014). Altered gene expression patterns of MCF-7 cells have been reported after

exposure to an urban dust standard reference material (SRM) 1649a, which is a complex mixture containing PAHs (Mahadevan et al., 2005).

However, most studies to date have characterised the toxicity of FRs using doses that are unlikely to be achieved through human exposure. Furthermore, the majority of investigations have targeted specific molecular or cellular responses. Here, to discover the acute responses of human cells to concentrations of FRs that attempt to simulate indoor exposure scenarios, hepatoma cells were exposed to FR mixtures and molecular changes were investigated using an array of non-targeted approaches including transcriptomics, metabolomics and lipidomics.

HepG2/C3A cells were used as the *in vitro* model; they have previously been successfully employed in hepatotoxicity testing, for example by evaluating the cytotoxic and metabolic effects of a commercial oil dispersant mixture (Bandelet et al., 2012). Furthermore, a solvent extract of SRM 2585 was used as a surrogate dust sample, representing the environmental mixture, in which we characterised four FRs (TCEP, TCIPP, TDCIPP and HBCD) (Abdallah et al., 2015b). SRM 2585 is an indoor dust reference material developed recently by the National Institute of Standards and Technology (NIST) for determination of concentrations for organic contaminants including flame retardants, polychlorinated biphenyls (PCBs), polycyclic aromatic hydrocarbons (PAHs) and organochlorine pesticides in house dust and similar matrices (Poster et al., 2007; Stapleton et al., 2006; Wise et al., 2006). We also employed a mixture of four FRs, namely TCEP, TCIPP, TDCIPP and HBCD each at the same concentration as in the dust extract, and a second mixture with 100-fold greater concentrations. The 100-fold concentrated mixture provided us a worst case

scenario for our hazard assessment. Oligonucleotide microarray based transcriptomics and direct infusion mass spectrometry (DIMS) based metabolomics and lipidomics were then applied to assess the molecular responses of HepG2/C3A cells exposed to the FR mixtures and dust extract. The aims of this chapter were (1) to evaluate the cytotoxic effects of mixture of four FRs and a dust extract to HepG2/C3A cells; (2) to determine changes in the gene expression, metabolic and lipid profiles of HepG2/C3A cells after the exposures; and (3) to search for any FR mixture-specific molecular responses in HepG2/C3A cells.

5.2 Materials and Methods

5.2.1 Chemicals and reagents

All chemicals were obtained from Sigma-Aldrich Chemical Company (UK) unless otherwise stated.

5.2.2 Cell culture

HepG2/C3A cells culture were described as in Section 2.2.

5.2.3 Design of Exposure experiment

Since hepatocytes are vital to the liver's detoxification role in humans, HepG2/C3A cells were employed as an *in vitro* model to test the toxicity of FRs. Dust ingestion is one of the primary routes of exposure to chemical contaminants. Relating environmental levels to concentrations achievable intracellularly represents a significant challenge. We have taken a conservative approach (from a hazard assessment perspective) that assumes total uptake of the ingested material, all of

which is processed by the liver. Since this is an overestimate of hepatocyte exposure, we have also measured cellular uptake levels which can be compared directly to reported tissue levels. The average amount of ingested dust is ca. 100-200 mg per day (Johnson-Restrepo and Kannan, 2009) for toddlers (ca. 12 kg), who are estimated to have ca. 350 million hepatocytes (Sohlenius-Sternbeck, 2006). In this study, therefore, the concentrations of FRs in the exposure system (ca. 0.6 mg dust per million hepatocytes) were designed on the basis of an average uptake of dust in toddlers. A solvent extract of the indoor dust reference material SRM2585 (NIST, USA) was used as a surrogate dust sample to mimic human exposure to all chemicals from dust. Four FRs (TCEP, TCIPP, TDCIPP and HBCD) were measured in the dust extract allowing preparation of a mixture (Mix 1) that reflected the concentrations of the four FRs in the dust extract, and a second mixture (Mix 2) of the same FRs at 100 times higher concentrations. DMBA (7,12-dimethylbenz[*a*]anthracene) (2 μ M), a polyaromatic hydrocarbon (PAH) was used as a positive control, while 0.1 % (v/v) DMSO was used as a vehicle for all exposures and as the vehicle control. An additional group treated with 4 μ M HBCD was also included in this design to compare the effect of an individual FR (Table 5.1).

HepG2/C3A cells were seeded into 96 well or 6 well plates at 2×10^4 or 4×10^5 cells/well respectively. After overnight acclimatization, cells were exposed to SRM2585 dust extract (equivalent to ca. 0.6mg dust per million cells), Mix 1, Mix 2, DMBA (2 μ M), HBCD (4 μ M) or 0.1% (v/v) DMSO as control. For cytotoxicity tests and quantification of FRs, cells were exposed for 24 or 72 hours; for omics study, the exposure time was 72 hours.

Table 5.1 Experimental design of mixture of FRs and dust extracts exposure study.

Groups	Description	Concentration of quantified chemicals	No. of replicates for transcriptomics	No. of replicates for metabolomics
Control	0.1% DMSO as solvent control.	-	4	5
Dust Extract	One million cells were exposed to solvent extract equivalent to ca. 0.6 mg dust.	TCEP: 1.57 nM (0.45 ng/mL); TCIPP: 1.49 nM (0.49 ng/mL); TDCIPP: 2.67 nM (1.15 ng/mL); HBCD: 0.153 nM (0.099 ng/mL). (other chemicals were not characterized in this study.)	4	5
Mix 1	Mixture of four FRs at the same concentrations as quantified in the dust extract.	TCEP: 1.57 nM; TCIPP: 1.49 nM; TDCIPP: 2.67 nM; HBCD: 0.153 nM.	4	5
Mix 2	Mixture of four FRs at 100 times higher concentrations as in the Mix 1 group.	TCEP: 157 nM (45.00 ng/mL); TCIPP: 149 nM (48.75 ng/mL); TDCIPP: 267 nM (115.00 ng/mL); HBCD: 15.3 nM (9.85 ng/mL).	4	5
DMBA	Positive control	DMBA: 2 μ M (512.7 ng/mL)	4	5
HBCD	Quality control, a FR at the same concentration as in Chapter 3.	HBCD: 4 μ M (2566.8 ng/mL)	4	5

5.2.4 Cytotoxicity assays

To evaluate the cytotoxicity of dust extracts and mixture of FRs to HepG2/C3A cells, the CCK-8 assay and AK assay were employed to assess mitochondrial dehydrogenase activity and loss of cell integrity, respectively. Briefly, HepG2/C3A cells were exposed to dust extracts, mixture of FRs, DMBA and HBCD (Table 5.1) for 24 or 72 hours. The detailed procedure of CCK-8 assay and AK assays were as described in Section 2.3.2 and 2.3.3, respectively.

5.2.5 Transcriptomics analysis

After 72 hours exposure, HepG2/C3A cells were harvested after two brief PBS washes. Cell pellets were collected and flash frozen in liquid nitrogen for further RNA extraction. Each treatment group included four biological replicates. The total RNA isolation and microarray analysis were also described as in Section 2.4.1 and 2.4.2.

Microarray datasets are available in the ArrayExpress database

(www.ebi.ac.uk/arrayexpress) under accession number: E-MTAB-3324.

5.2.6 Metabolomics analysis

5.2.6.1 Extraction of Metabolites

After 72 hours exposure, HepG2/C3A cells were harvested and metabolites were extracted as previously described in Section 2.5.1.2. Briefly, cells were quickly washed with PBS twice before the 6-well plates were quenched on liquid nitrogen. Then, metabolites were extracted by liquid-liquid extraction method (methanol: chloroform: water (v/v/v) ratio was 1:1:0.9). After vortexing and centrifuge, the mixture separated into two phases (upper polar phase and lower non-polar phase). 300 μ L aliquots of the polar phase were transferred into clean 1.5mL Eppendorf tubes and then dried in a speed vac concentrator (Thermo Savant, Holbrook, NY) for 4 hr. 300 μ L aliquots of the non-polar phase were transferred into clean 1.8mL glass vial and then were dried under a stream of nitrogen to minimise oxidation. All dried samples were then stored at -80°C until analysis.

5.2.6.2 DIMS analysis and data processing

The DIMS analysis method was similar to that reported previously in Section 2.5.2. Briefly, the dried polar extracts of cells were re-suspended in 75 μ L 80:20 (v/v) methanol:water (HPLC grade) with 0.25% formic acid (for positive ion mode). For the dried non-polar extracts of cells, it was re-suspended in with 2:1 (v/v) MeOH:chloroform with 5 mM ammonium acetate. After centrifugation at 22000 rcf, 4°C for 10 min, 10 μ L supernatant of each sample was loaded into one well in a 384-well plate and then analysed (in triplicate) using direct infusion Fourier transform ion cyclotron resonance mass spectrometry in positive ion mode (for polar metabolomics) or negative ion mode (for lipidomics) (LTQ FT Ultra, Thermo Fisher Scientific, Germany, coupled with a Triversa nanoelectrospray ion source, Advion Biosciences, Ithaca, NY, USA). Mass spectra were recorded utilizing the selected ion monitoring (SIM) stitching approach from m/z 70 to 590 (for polar metabolomics) or from m/z 100 to 2000 (for lipidomics) (Southam et al., 2007) and then processed using custom-written Matlab scripts as previously reported (Kirwan et al., 2014; Southam et al., 2007). Univariate and multivariate statistical analysis of DIMS datasets are described in Section 2.5.2.

5.2.6.3 MS peaks annotation and pathway analysis

For significantly changed DIMS peaks, putative empirical formulae and metabolite names were assigned by searching against HMDB, KEGG and LIPIDMAPS database in the metabolite identification package (MI-Pack) (Weber and Viant, 2010). And the details are in Section 2.5.3. Putative annotation of significantly changed DIMS peaks from non-polar DIMS dataset was not subjected to pathway over-representation

analysis due to the less reliable annotation results.

5.2.7 Quantification of FRs in HepG2/C3A cells and cell media

(conducted by Dr. Mohamed Abou-Elwafa Abdallah, University of Birmingham)

To evaluate the cellular uptake of FRs after exposure, their concentrations were measured in treated cells and cell media after 24 or 72 hours using LC-MS/MS according to a previously reported method (Abdallah et al., 2015b). The detailed procedure is available in the Section 2.6.2.

5.3 Results

5.3.1 Cytotoxicity of dust extracts and mixture of FRs to HepG2/C3A cells

To evaluate the cytotoxicity of the dust extract and mixtures of FRs to HepG2/C3A cells, the CCK-8 assay and AK assay were employed after 24- and 72-hour treatments. As shown in Figure 5.1, there was no significant cytotoxic effect in any treatment group compared to the control group after 24 hours, although a slight decrease (not statistically significant) of cell viability was observed in the 2 μ M DMBA group. After a 72-hour exposure, there was still no obvious toxic effect in any group except the DMBA group. Specifically, in the 2 μ M DMBA group (positive control), there was a significant decrease of average cell viability (48.6%) and remarkable increase of AK release due to the loss of cellular integrity after 72 hours. The AK release of cells in the 4 μ M HBCD group declined slightly after 72 hours (81.8%) compared to the control group.

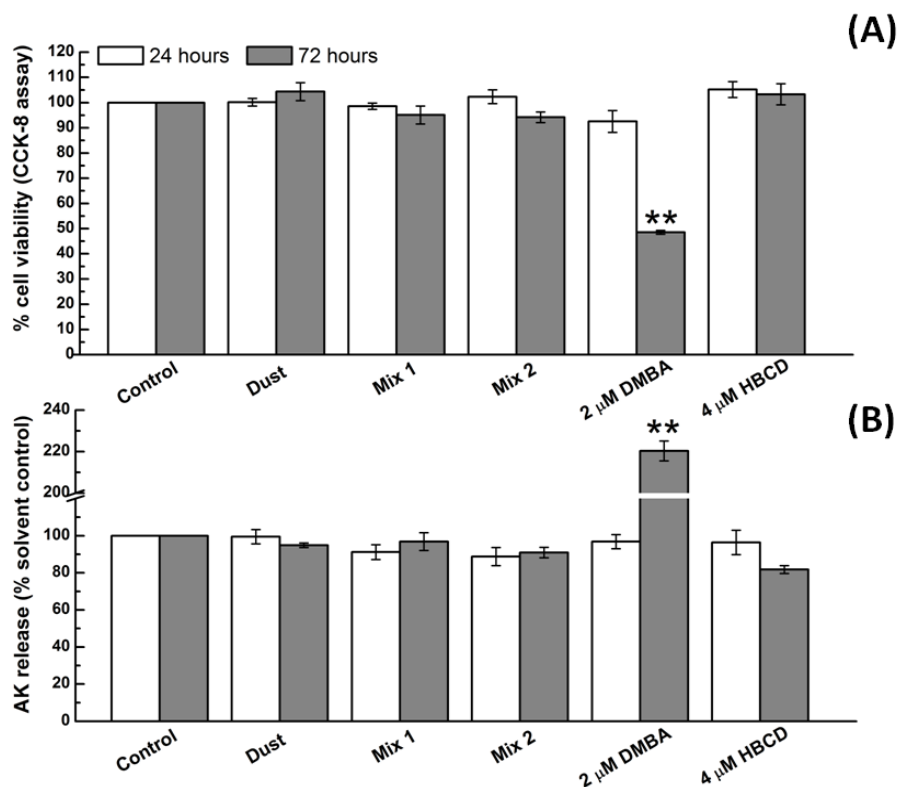


Figure 5.1 Cytotoxicity assays of HepG2/C3A cells exposed to dust extract, mixture of FRs, DMBA and HBCD. Cell viability of HepG2/C3A cells were evaluated using CCK-8 assay (A) and AK assay (B) after exposed to dust extract, Mix 1, Mix 2, 2 μ M DMBA and 4 μ M HBCD for 24 hours or 72 hours. Results are expressed as the percentage of cell viability or AK release compared to solvent controls treated with the appropriate vehicle (DMSO). Data represent mean \pm SEM from at least three independent experiments. Two asterisks indicate a p-value of less than 0.01 in t-test.

5.3.2 Transcriptomic analysis

The oligonucleotide microarrays were employed to evaluate gene expression profiles of HepG2/C3A cells after 72-hour exposures to a dust extract and mixtures of FRs, as detailed above. The PCA scores plot (Figure 5.2 A) showed that there was a clear separation of gene expression patterns between the DMBA group (positive control) and the other treatment groups, while there was no obvious separation between the Dust extract group, the FR mixture groups and the control group (Figure 5.2 B).

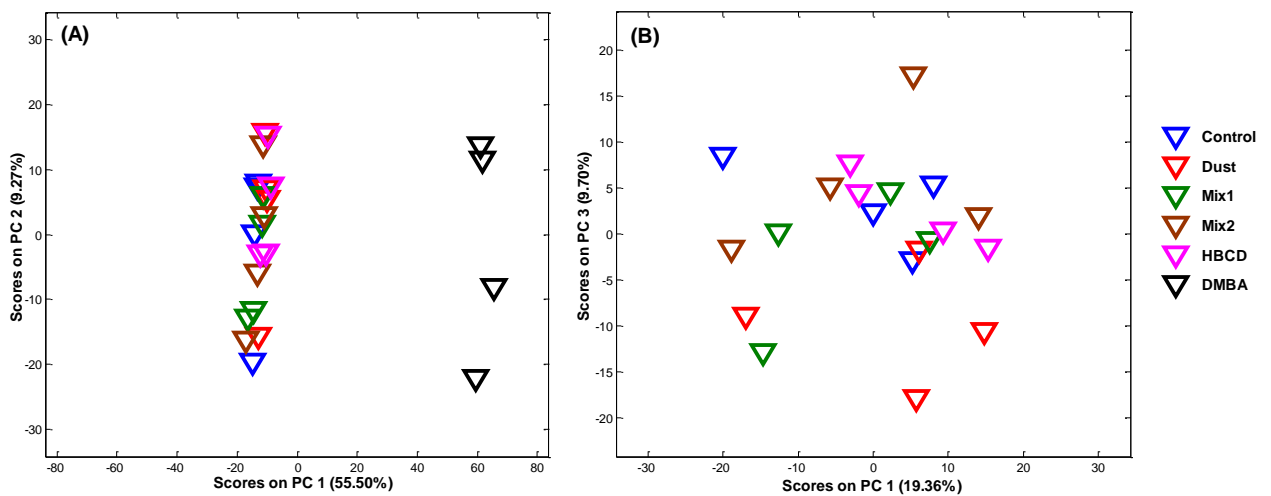


Figure 5.2 PCA scores plots of the gene expression of HepG2/C3A cells (A) and (B, which excludes DMBA group) following 72-hour treatments (n=4). Legend: Blue represents solvent control, red is dust extract, green is Mix 1 of flame retardants, brown is Mix 2 of flame retardants, pink is 4 μ M HBCD control and black is 2 μ M DMBA group control.

The statistical significance of the top six PC scores was verified by ANOVAs combined with a Tukey-Kramer's post hoc test (Table 5.2). The results showed that PC 1 (representing 55.5% of the variance in the whole microarray dataset) was significant ($p=7.20 \times 10^{-21}$). However, when the DMBA group was excluded from the dataset, only PC 3 and PC 5 were significant, which represented 9.70% ($p=0.029$) and 6.22% ($p=0.007$) variance of the modified dataset, respectively.

Table 5.2 Summary of principal component (PC) analyses of both microarray and MS datasets of HepG2/C3A cells after 72 hours treatment

Dataset		PC1	PC2	PC3	PC4	PC5	PC6
Microarray	variance	55.50%	9.27%	4.46%	3.86%	3.13%	2.59%
	p value	7.20E-21	0.935	0.763	0.084	0.494	0.110
Microarray_excluded DMBA group	variance	19.36%	11.15%	9.70%	7.62%	6.22%	5.41%
	p value	0.832	0.658	0.029	0.439	0.007	0.141
Polar_DIMS	variance	43.22%	13.68%	6.92%	6.30%	4.85%	3.59%
	p value	4.73E-06	0.040	0.765	0.563	0.499	0.654
Polar_DIMS_excluded DMBA and HBCD group	variance	35.75%	12.97%	9.46%	6.93%	6.52%	5.07%
	p value	0.464	0.667	0.232	0.049	0.460	0.166
Non-Polar_DIMS	variance	32.02%	14.23%	12.01%	8.53%	5.56%	3.66%
	p value	1.16E-08	4.63E-06	0.399	0.562	0.038	0.042
Non-Polar_DIMS_excluded DMBA and HBCD group	variance	23.87%	19.92%	13.85%	6.62%	6.16%	5.29%
	p value	0.355	0.531	0.812	0.222	0.019	0.001

(Groups in each dataset as described in section 5.2.3). The variance explained (%) by PCs 1-6 are listed together with p values from ANOVAs of these PC scores across all treatments (values in bold indicate significance at a false discovery rate (FDR) <10%).

Significance analysis of microarrays (SAM) in MeV was employed to identify the significant differentially expressed genes between the treatment groups and controls. The results (File 5.1, in Appendix) showed that 49 probe sets were up-regulated in the Dust extract group compared to the control group (Figure 5.3 A), among which several genes (e.g. *CYP1A1*, *CYP1A2*, *GSTP1* and *UGT1A6*) were related to the metabolism of xenobiotics by cytochrome 450, revealed by DAVID analysis (File 5.2, in Appendix). There was no significantly changed gene expression in either Mix 1 or Mix 2 groups compared to the control group (Figure 5.3 A).

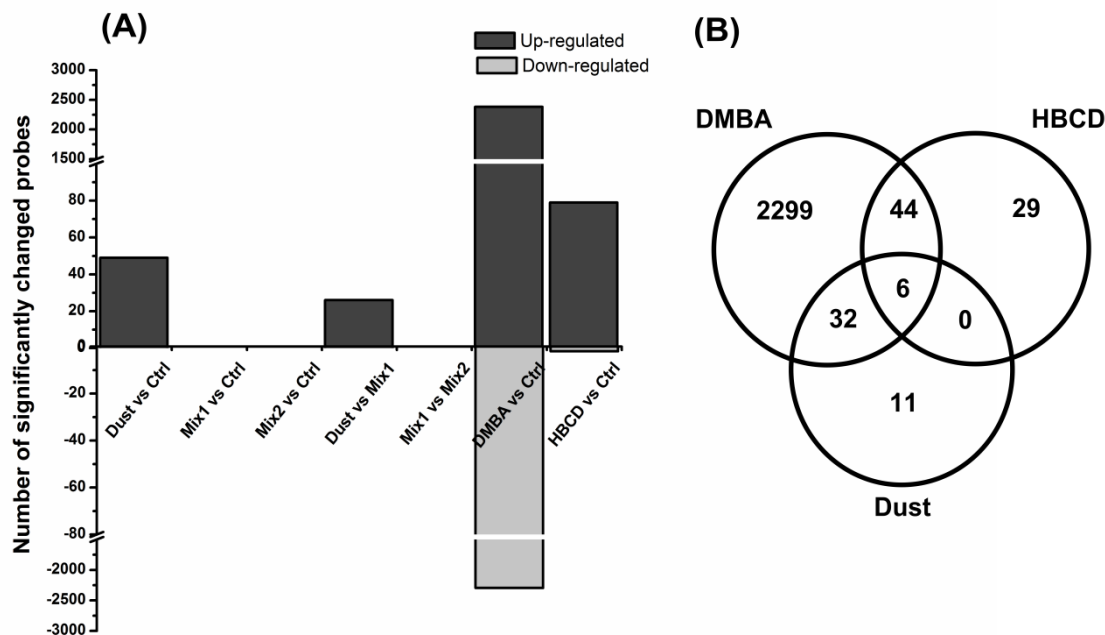


Figure 5.3 Univariate statistics analysis of significantly changed transcripts in HepG2/C3A cells following 72-hour treatments (n=4). (A) Number of significantly changed probes between various treatment groups. (B) The Venn diagram indicates the number of significantly up-regulated probes (all compared with control) in the DMBA group, dust group and HBCD group.

In the 4 μ M HBCD group, 81 probe sets were significantly changed compared to the control group (File 5.1, in Appendix). 4 μ M HBCD exposure resulted in transcriptional induction of a group of metallothionein genes (*MT1A*, *MT1B*, *MT1E*, *MT1L*, *MT1H* and *MT1X*) while the expression of glutathione S-transferase gene (*GSTP1*) was down-regulated. More than 4000 probe sets (File 5.1, in Appendix) were significantly altered in the DMBA group compared to controls. DMBA responsive transcripts were related to apoptosis/cell death pathways and suppressed cell proliferation pathways (e.g. cell cycle, cell division) as well as xenobiotic metabolism (e.g. *CYP1A1*) (File 5.2, in Appendix). Interestingly, 26 probe sets (File 5.1, in Appendix) were up-regulated in the Dust extract group compared to the Mix 1 group. These changes are likely to be in response to the many other components of this complex mixture, not the four FRs

that were investigated here. DAVID analysis also suggested that the metabolism of xenobiotics by cytochrome 450 was the most significantly enriched pathway in response to the dust extract. However, no significantly expressed genes were found in the comparison of the Mix1 and Mix 2 groups.

The results of GSEA (Table 5.3) were similar to DAVID analysis. Pathways related to metabolism of xenobiotics by cytochrome P450 were also found to be increased, while ribosomal transcripts were down-regulated in the Dust extract group. There was no significant enrichment of gene sets in either Mix1 or Mix2 groups compared to the controls. In the 4 μ M HBCD group, pathways relevant to ribosome and steroid biosynthesis were decreased, and gap junction transcripts were up-regulated. In the positive control group, 2 μ M DMBA caused extensive changes including significant elevation of apoptosis/cell death related pathways and down-regulation of cell proliferation related pathways (e.g. cell cycle, DNA replication).

Table 5.3 GSEA of gene expression of HepG2/C3A cells from different treatment groups for 72 hours.

TREATMENT GROUPS	Up-regulated pathways					Down-regulated pathways				
	NAME	SIZE	NES	NOM p-val	FDR q-val	NAME	SIZE	NES	NOM p-val	FDR q-val
	KEGG_DRUG_METABOLISM_CYTOCHROME_P450	36	2.169	0.000	0.000	KEGG_RIBOSOME	87	-2.868	0.000	0.000
	KEGG_TRYPTOPHAN_METABOLISM	31	2.073	0.000	0.001	KEGG_OLFACTORY_TRANSDUCTION	39	-2.435	0.000	0.000
	KEGG_METABOLISM_OF_XENOBIOTICS_BY_CYTOCHROME_P450	37	2.072	0.000	0.000	KEGG_MATURITY_ONSET_DIABETES_OF_THE_YOUNG	19	-1.935	0.001	0.005
	KEGG_PROTEASOME	41	2.025	0.000	0.001	KEGG_SYSTEMIC_LUPUS_ERYTHEMATOSUS	96	-1.782	0.000	0.020
	KEGG_VALINE_LEUCINE_AND_ISOLEUCINE_DEGRADATION	41	1.882	0.000	0.010					
	KEGG_TYROSINE_METABOLISM	29	1.875	0.001	0.009					
	KEGG_HISTIDINE_METABOLISM	22	1.847	0.000	0.013					
	KEGG_NICOTINATE_AND_NICOTINAMIDE_METABOLISM	17	1.824	0.002	0.015					
Dust extract	KEGG_COMPLEMENT_AND_COAGULATION_CASCADES	49	1.774	0.001	0.024					
	KEGG_PYRUVATE_METABOLISM	34	1.744	0.002	0.033					
	KEGG_FATTY_ACID_METABOLISM	35	1.735	0.002	0.034					
	KEGG_DORSO_VENTRAL_AXIS_FORMATION	15	1.720	0.011	0.037					
	KEGG_EPITHELIAL_CELL_SIGNALING_IN_HELICOBACTER_PYLORI_INFECTION	52	1.715	0.001	0.036					
	KEGG_GLYCOLYSIS_GLUONEOGENESIS	47	1.706	0.002	0.038					
	KEGG_BUTANOATE_METABOLISM	26	1.696	0.006	0.039					
	KEGG_PROPANOATE_METABOLISM	30	1.689	0.005	0.040					
	KEGG_BETA_ALANINE_METABOLISM	17	1.685	0.011	0.039					
	KEGG_GLIOMA	50	1.676	0.003	0.041					
	KEGG_SELENOAMINO_ACID_METABOLISM	23	1.658	0.016	0.048					
Mix1	NA	NA	NA	NA	NA	NA	NA	NA	NA	NA
Mix2	NA	NA	NA	NA	NA	NA	NA	NA	NA	NA
	KEGG_GAP_JUNCTION	57	1.934	0.000	0.031	KEGG_RIBOSOME	87	-1.882	0.000	0.020
HBCD						KEGG_STEROID_HORMONE_BIOSYNTHESIS	24	-1.903	0.000	0.031
						KEGG_STEROID_BIOSYNTHESIS	15	-1.762	0.012	0.038
						KEGG_OLFACTORY_TRANSDUCTION	39	-1.774	0.005	0.046

DMBA	KEGG_EPITHELIAL_CELL_SIGNALING_IN_HELICOBACTER_PYLORI_INFECTION	52	2.012	0.000	0.003	KEGG_DNA_REPLICATION	36	-2.646	0.000	0.000
	KEGG_APOPTOSIS	70	1.966	0.000	0.004	KEGG_SYSTEMIC_LUPUS_ERYTHEMATOSUS	96	-2.560	0.000	0.000
	KEGG_CYTOKINE_CYTOKINE_RECEPTOR_INTERACTION	113	2.035	0.000	0.005	KEGG_CELL_CYCLE	115	-2.513	0.000	0.000
	KEGG_ENDOCYTOSIS	150	1.920	0.000	0.007	KEGG_RIBOSOME	87	-2.362	0.000	0.000
	KEGG_TOLL_LIKE_RECEPTOR_SIGNALING_PATHWAY	62	1.835	0.000	0.015	KEGG_SPLICEOSOME	124	-2.270	0.000	0.000
	KEGG_TYPE_I_DIABETES_MELLITUS	24	1.821	0.002	0.015	KEGG_MISMATCH_REPAIR	23	-2.134	0.000	0.000
	KEGG_AMYOTROPHIC_LATERAL_SCLEROSIS_ALS	39	1.844	0.000	0.015	KEGG_AMINOACYL_TRNA_BIOSYNTHESIS	40	-1.944	0.001	0.002
	KEGG_RIG_I_LIKE_RECEPTOR_SIGNALING_PATHWAY	48	1.800	0.000	0.018	KEGG_PYRIMIDINE_METABOLISM	88	-1.915	0.000	0.002
	KEGG_CHEMOKINE_SIGNALING_PATHWAY	106	1.776	0.000	0.021	KEGG_PURINE_METABOLISM	117	-1.924	0.000	0.002
	KEGG_P53_SIGNALING_PATHWAY	60	1.717	0.001	0.037	KEGG_HOMOLOGOUS_RECOMBINATION	28	-1.947	0.000	0.002
	KEGG_HEMATOPOIETIC_CELL_LINEAGE	39	1.676	0.008	0.047	KEGG_OOCYTE_MEIOSIS	91	-1.960	0.000	0.002
	KEGG_INTESTINAL_IMMUNE_NETWORK_FOR_IGA_PRODUCTION	22	1.660	0.009	0.050	KEGG_BASE_EXCISION_REPAIR	33	-1.837	0.002	0.005
						KEGG_LYSINE_DEGRADATION	41	-1.819	0.001	0.005
						KEGG_PROGESTERONE_MEDIATED_OOCYTE_MATURATION	64	-1.823	0.001	0.005
						KEGG_RNA_DEGRADATION	55	-1.790	0.002	0.006
						KEGG_VALINE_LEUCINE_AND_ISOLEUCINE_DEGRADATION	41	-1.711	0.007	0.013
						KEGG_ONE_CARBON_POOL_BY_FOLATE	15	-1.690	0.005	0.015
						KEGG_NUCLEOTIDE_EXCISION_REPAIR	43	-1.675	0.005	0.017
						KEGG_CITRATE_CYCLE_TCA_CYCLE	29	-1.646	0.008	0.021
						KEGG_NITROGEN_METABOLISM	16	-1.628	0.022	0.023
						KEGG_PENTOSE_PHOSPHATE_PATHWAY	22	-1.601	0.017	0.027
						KEGG_RNA_POLYMERASE	28	-1.595	0.021	0.027
						KEGG_PROANOATE_METABOLISM	30	-1.537	0.032	0.042

5.3.3 Metabolomic analysis

Polar and non-polar metabolites of HepG2/C3A cells from different treatment groups were analysed by DIMS based metabolomics. The polar and non-polar DIMS datasets included 2943 and 489 mass spectral peaks after data processing, respectively. To visualise the similarities and differences of the metabolic profiles between control and treatment groups, these data were subjected to PCA.

The PCA scores plot (Figure 5.4 A) showed the polar metabolic profiles of DMBA-exposed cells separated clearly from the other treatment groups and the controls. The PCA plot of non-polar metabolic profiles, shown in Figure 5.4 B, suggested that both the HBCD group and the DMBA group are distinct from the other treatment groups. The ANOVAs (combined with a Tukey-Kramer's post hoc test) of the top six PC scores showed PC 1 and PC 2 in the polar DIMS analysis were significant (Table 5.2). In the non-polar DIMS analysis, PC 1, PC 2, PC 5 and PC 6 were significant in the top six PC scores.

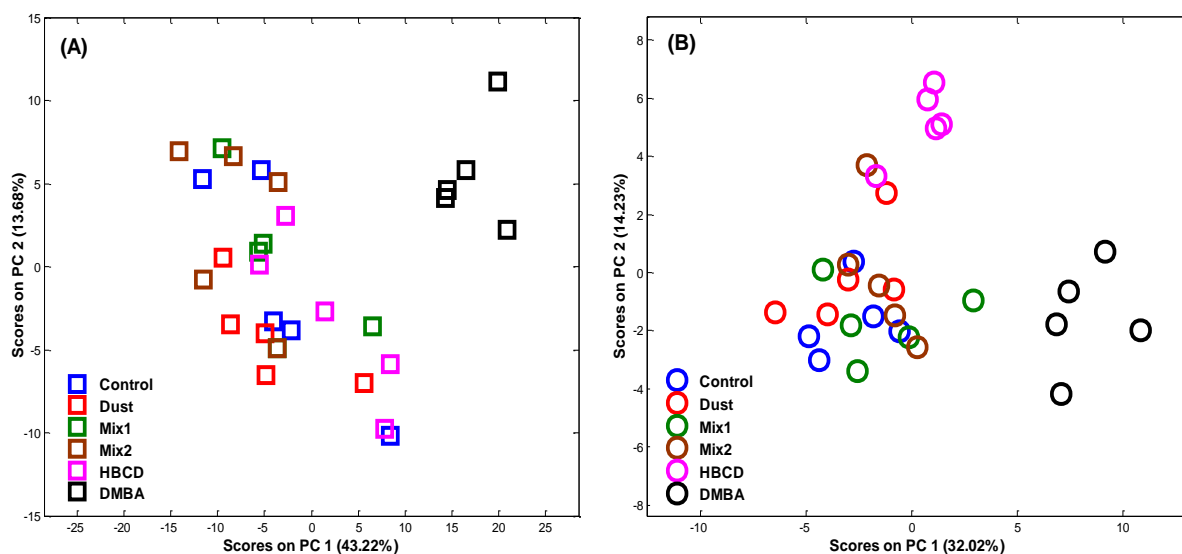


Figure 5.4 PCA scores plots of the DIMS datasets of polar (A) and non polar (B) extracts of HepG2/C3A cells following 72-hour treatments (n=5). Legend: Open squares represent polar samples, while open circles represent non-polar samples. Blue represents solvent control, red is dust extract, green is Mix 1, brown is Mix 2, pink is 4 μ M HBCD control group and black is 2 μ M DMBA control group.)

Univariate statistical analyses were conducted on the DIMS datasets (File 5.3, in Appendix and Figure 5.5). In the polar DIMS dataset, 994 peaks (of a total of 2943 peaks) in the DMBA group significantly changed intensity compared to controls, while only five peaks changed in response to HBCD treatment compared to controls. The other treatment groups had no significantly changed peaks relative to controls. However, in the non-polar DIMS dataset, 50.7% of the peaks (248 out of 489 peaks) in the DMBA group significantly changed compared to controls. There were also 186 peaks (38.0%) that significantly changed in the HBCD group. Meanwhile, only 4 peaks (of 489 in total) changed significantly between the Dust extract group and the controls.

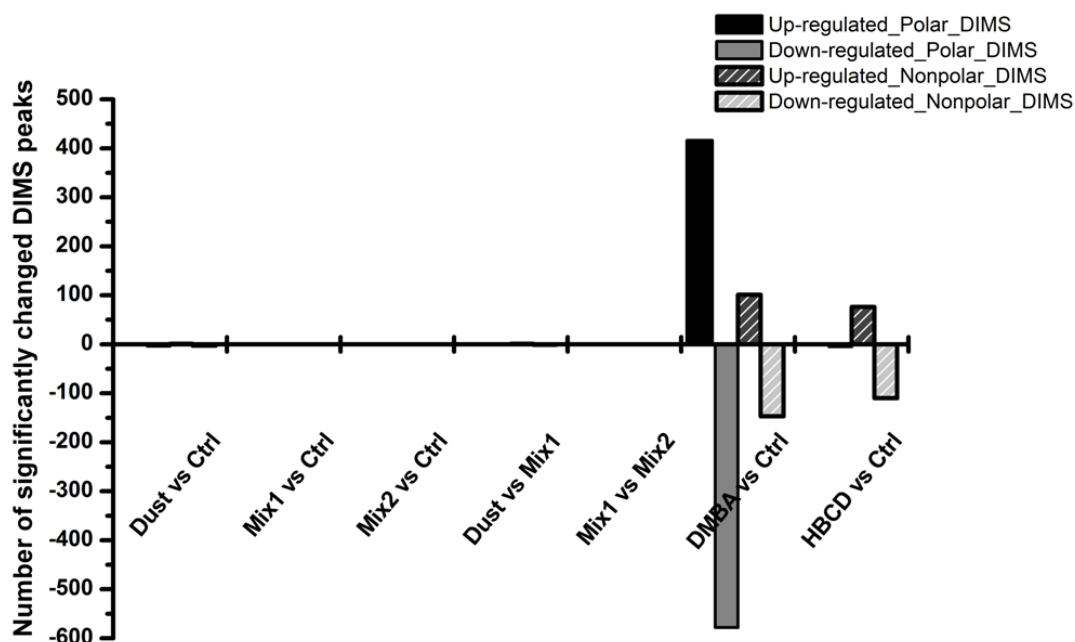


Figure 5.5 Number of significantly changed DIMS peaks between various treatment groups in the polar and non-polar DIMS datasets of HepG2/C3A cells following 72-hour treatments (n=5).

Putative annotation of these significantly changing peaks (File 5.3, in Appendix) was performed in MI-Pack by searching against HMDB, KEGG and LIPIDMAPS databases. The assigned metabolite names of these putatively annotated peaks in the polar DIMS dataset were subjected to pathway over-representation analysis in IMPaLA. Pathway analysis (Table 5.4) suggested the dysregulation of metabolic pathways related to metabolism of amino acids and derivatives (i.e. arginine and proline metabolism, glycine and serine metabolism) and glutathione conjugation in the DMBA group. Only one of the significantly changing peaks in the polar DIMS dataset of the HBCD group was putatively annotated as taurine.

Table 5.4 Pathway over-representation analysis of putative annotation of significant MS peaks from polar metabolomics dataset in the DMBA group

Pathway name	Pathway source	Number of overlapping metabolites	Number of all pathway metabolites	P value	Q value
Transport of inorganic cations-anions and amino acids-oligopeptides	Wikipathways	18	32	2.47E-16	5.88E-14
Central carbon metabolism in cancer - Homo sapiens (human)	KEGG	19	37	3.47E-16	7.28E-14
Protein digestion and absorption - Homo sapiens (human)	KEGG	19	47	8.90E-14	1.67E-11
Glycine_serine and threonine metabolism - Homo sapiens (human)	KEGG	18	50	4.35E-12	7.06E-10
Aminoacyl-tRNA biosynthesis - Homo sapiens (human)	KEGG	18	52	9.44E-12	1.47E-09
Metabolism of amino acids and derivatives	Wikipathways	33	187	2.74E-11	3.76E-09
Mineral absorption - Homo sapiens (human)	KEGG	13	29	1.76E-10	2.32E-08
tRNA Aminoacylation	Wikipathways	18	65	6.29E-10	8.02E-08
Phase II conjugation	Wikipathways	23	115	2.82E-09	3.15E-07
Lysine degradation - Homo sapiens (human)	KEGG	15	52	9.63E-09	1.01E-06
Cyanoamino acid metabolism - Homo sapiens (human)	KEGG	14	45	1.03E-08	1.05E-06
Arginine and proline metabolism - Homo sapiens (human)	KEGG	19	91	3.47E-08	3.31E-06
Valine_leucine and isoleucine biosynthesis - Homo sapiens (human)	KEGG	10	23	3.52E-08	3.31E-06
Glucose Homeostasis	Wikipathways	9	21	2.05E-07	9.50E-06
Cysteine and methionine metabolism - Homo sapiens (human)	KEGG	13	57	1.90E-06	7.22E-05
ABC transporters - Homo sapiens (human)	KEGG	19	123	4.66E-06	0.000173
Urea cycle and metabolism of amino groups	Wikipathways	9	30	6.82E-06	0.000251
Ascorbate and aldarate metabolism - Homo sapiens (human)	KEGG	11	47	9.20E-06	0.000335
Tyrosine metabolism - Homo sapiens (human)	KEGG	14	77	1.30E-05	0.00047
Alanine_aspartate and glutamate metabolism - Homo sapiens (human)	KEGG	8	28	3.36E-05	0.00103
Biogenic Amine Synthesis	Wikipathways	6	17	9.05E-05	0.00236
Phenylalanine metabolism - Homo sapiens (human)	KEGG	12	72	0.000132	0.00322
D-Glutamine and D-glutamate metabolism - Homo sapiens (human)	KEGG	5	12	0.000146	0.0035
Trans-sulfuration and one carbon metabolism	Wikipathways	6	20	0.000251	0.00598
Valine_leucine and isoleucine degradation - Homo sapiens (human)	KEGG	8	40	0.000504	0.011
Amino acid conjugation of benzoic acid	Wikipathways	4	9	0.000537	0.0116
Propanoate metabolism - Homo sapiens (human)	KEGG	8	44	0.000983	0.02
Amino acid conjugation	Wikipathways	3	5	0.00101	0.0205
Phenylalanine_tyrosine and tryptophan biosynthesis - Homo sapiens (human)	KEGG	7	35	0.00113	0.0227
Glutathione metabolism	Wikipathways	5	18	0.00125	0.0241
Glyoxylate and dicarboxylate metabolism - Homo sapiens (human)	KEGG	9	58	0.00157	0.0279
Pantothenate and CoA biosynthesis - Homo sapiens (human)	KEGG	6	28	0.00177	0.0304
Metabolism of water-soluble vitamins and cofactors	Wikipathways	12	96	0.00194	0.033
Neurotransmitter uptake and Metabolism In Glial Cells	Wikipathways	3	6	0.00196	0.033
Dopamine metabolism	Wikipathways	6	31	0.00306	0.045
Effects of Nitric Oxide	Wikipathways	3	7	0.0033	0.0476

5.3.4 Quantification of FRs in HepG2/C3A cells after exposure

To evaluate the cellular uptake of FRs following exposure, their concentrations were measured in treated cells and cell media after 24 hours and 72 hours (Table 5.5). The detection of these four FRs in cells and the decreased concentrations in cell media show that these FRs can be taken up into HepG2/C3A cells. Compared with the nominal concentrations, the concentrations of the three PFRs in cell media after exposure declined significantly for the Dust extract group and Mix 1 group but not for the Mix 2 group, in which they were even higher than the nominal concentrations before exposure. Considering that the concentrations of these three PFRs in the Mix 2 group was 100 times higher than in the Mix 1 group, this suggests that the uptake rate of these three PFRs to HepG2/C3A cells did not increase proportionally. However, the uptake rate of HBCD did increase accordingly when the nominal concentration of HBCD increased, as the concentration of HBCD in cell pellets increased and in cell media decreased proportionally after exposure. This discrepancy may be explained by the hydrophilic feature of the three PFRs (with log K_{ow} values of TCEP, TCIPP and TDCIPP equal to 1.47, 2.59 and 3.27) and the relatively high lipophilicity of HBCD (log K_{ow} of 7.92). There was minimal change between the concentrations of the four FRs in cell pellets after a 24-hour exposure compared to a 72-hour exposure.

Table 5.5 Concentration of FRs in cell pellets and cell media in HepG2/C3A cells after 72 hours exposure.

Exposure time	Treatment groups	Wet weight of cell pellets (mg)	TCEP		TCIPP		TDCIPP		HBCD	
			Concentration in cell pellets (ng/mg)	Concentration in cell media (ng/mL)	Concentration in cell pellets (ng/mg)	Concentration in cell media (ng/mL)	Concentration in cell pellets (ng/mg)	Concentration in cell media (ng/mL)	Concentration in cell pellets (ng/mg)	Concentration in cell media (ng/mL)
24 hours	Control	10.73 ± 1.17	ND	ND	ND	ND	ND	ND	ND	ND
	Dust	11.67 ± 1.07	0.045 ± 0.006	0.312 ± 0.019	0.038 ± 0.005	0.247 ± 0.023	0.061 ± 0.001	0.633 ± 0.056	0.008 ± 0.001	0.042 ± 0.003
	Mix1	15.70 ± 3.24	0.031 ± 0.006	0.320 ± 0.019	0.027 ± 0.003	0.252 ± 0.029	0.054 ± 0.012	0.762 ± 0.014	0.006 ± 0.001	0.039 ± 0.004
	Mix2	14.33 ± 3.35	2.112 ± 0.685	45.717 ± 1.982	1.639 ± 0.375	41.233 ± 2.886	1.702 ± 0.644	138.943 ± 4.773	0.671 ± 0.163	3.987 ± 0.269
	HBCD (4 µM)	17.23 ± 7.44	NA	NA	NA	NA	NA	NA	160.59 ± 86.58	1071.48 ± 111.43
72 hours	Control	13.33 ± 1.67	ND	ND	ND	ND	ND	ND	ND	ND
	Dust	13.67 ± 0.86	0.038 ± 0.004	0.302 ± 0.012	0.032 ± 0.002	0.240 ± 0.018	0.052 ± 0.003	0.642 ± 0.070	0.007 ± 0.000	0.043 ± 0.002
	Mix1	11.87 ± 0.86	0.045 ± 0.003	0.307 ± 0.017	0.036 ± 0.000	0.236 ± 0.032	0.061 ± 0.006	0.628 ± 0.056	0.008 ± 0.001	0.036 ± 0.004
	Mix2	13.37 ± 1.11	1.918 ± 0.203	48.355 ± 2.334	1.839 ± 0.204	42.597 ± 2.254	1.605 ± 0.213	145.417 ± 6.398	0.684 ± 0.044	4.154 ± 0.247
	HBCD (4 µM)	13.23 ± 1.29	NA	NA	NA	NA	NA	NA	185.98 ± 14.58	964.95 ± 27.30

ND: not detected; NA: not analyzed.

5.4 Discussion

To date, there is a paucity of studies about the effects of human exposure to mixture of flame retardants. This explorative investigation aimed to evaluate the cytotoxic effects and molecular responses of human hepatoma cells (HepG2/C3A) to mixture of FRs at concentrations relevant to environmental exposure. Since ingestion of dust is one of the primary routes of human exposure to FRs (Abdallah and Harrad, 2009), a solvent extract of an indoor dust reference SRM2585 was employed as a surrogate dust sample. SRM2585 is an indoor dust reference material developed for determination of concentrations for organic contaminants including flame retardants, PCBs, PAHs and organochlorine pesticides in house dust (Wise et al., 2006). The certified or/and reference concentrations of PCBs and PAHs have been reported previously (Poster et al., 2007; Stapleton et al., 2006; Wise et al., 2006). In our study we quantified several FRs (TCEP, TCIPP, TDCIPP and HBCD) within the solvent extract of SRM2585 (Abdallah et al., 2015b). To mimic environmental reality, we studied the effects of the FRs at concentrations estimated on the basis of average uptake of dust by toddlers (ca. 0.6 mg dust per million hepatocytes), which is comparable with a previous publication (Riechelmann et al., 2007).

The concentration of HBCD detected in HepG2/C3A cell pellets in the Dust

extract group and Mix 1 group, after exposure, was ca. 0.006 - 0.008 ng/mg cell pellet (wet weight) (Table 5.5), which is equivalent to 300 - 400 ng/g lipid (assuming 2% of cells are lipids, similar to that reported for human liver (Rawn et al., 2014a)). This is approximately ten times higher than the average concentrations of HBCD reported in human fetal liver (median of 29 ng/g lipid) and placental tissue (median of 49 ng/g lipid), but ten times lower than the highest concentrations reported in these human tissues (4,500 ng/g lipid in liver; 5,600 ng/g lipid in placenta; Rawn et al., 2014a). Although the potential to bioaccumulate organophosphate FRs such as TDCIPP and TCIPP was suggested to be low in rodents (due to rapid metabolism; European Union, 2008a, 2008b), concentrations of TDCIPP have been reported up to 252 ng/g lipid in human adipose tissue (LeBel and Williams, 1986) and up to 162 ng/g lipids in human breast milk (Kim et al., 2014). In addition, the concentration of BDCIPP (which is the primary metabolite of TDCIPP) in human urine has been reported as high as 25 ng/mL (Meeker et al., 2013). In this study, the concentrations of TDCIPP in HepG2/C3A cell pellets in the Dust extract group and Mix 1 group were estimated at ca. 2600-3050 ng/g lipid (ca. 0.052 -0.061 ng/mg cell pellets (Table 5.5)), which is approximately ten times higher than the levels in human adipose tissue. Taken together, these values suggest the exposure concentrations of FRs in the present study are relevant to those found

in humans.

Cytotoxicity tests indicated that there was no significant change of cell viability or cell integrity after 24- and 72-hour exposures of HepG2/C3A cells to the environmentally-relevant mixture of FRs or dust extract. However, comparative analyses of transcriptomic and metabolic responses suggest that the mixture of the four FRs studied here, representing environmental exposure levels, were less toxic than the dust extract containing similar concentrations of FRs. For example, the up-regulated genes in the cells exposed to the dust extract were related to the metabolism of xenobiotics by cytochrome P450. As these were not induced by Mix 1 or Mix 2 of the FRs, other compounds from the dust extract must be responsible. The well known molecular responses to PAH (e.g. benzo[*a*]pyrene (B[*a*]P)) and PCB exposures occur primarily via aryl hydrocarbon receptor (AHR) binding and subsequently induction of transcription of mRNA encoding the drug-metabolizing cytochrome P450 enzymes such as CYP1A1 and CYP1A2 (Hennig et al., 2002; Jungnickel et al., 2014). In the present study, a series of xenobiotic responsive genes (e.g. *CYP1A1*, *CYP1A2*, *CYP3A5*, *UGT1A6*, *ALDH3A1*) were induced by 2µM DMBA that was used as a positive control. Combined, the up-regulation of xenobiotic metabolism related genes (e.g. *CYP1A1*, *CYP1A2* and *CYP2B6*) in the dust extract group suggests induction by PAHs, PCBs or dioxin like compounds, not FRs.

Uncertainty factors are often employed in chemical risk assessment when there is lack of toxicity information of chemicals (Kalberlah et al., 2003). Conversely, Mix 2 was used to test the potential toxicity of the FR mixture at 100 times the concentrations estimated to be achievable from environmental exposure.

However, even this relatively higher concentration of FRs did not induce any changes in gene expression. This lack of response was also supported by the metabolomics analyses which showed no significant changes at the metabolic level after HepG2/C3A cells were exposed to Mix 1 or Mix 2.

Although there were no significantly changed molecular responses to the mixture of four FRs, multiple and univariate statistical analyses of the non-polar DIMS dataset showed statistically significant changes in the lipid profiles of HepG2/C3A cells exposed to 4 μ M HBCD. A detailed interpretation of the dysregulation of metabolism at this relatively high concentration of HBCD (4 μ M) would require robust identification of DIMS peaks in the lipidomics dataset which is not currently achievable. In Chapter 3, 4 μ M HBCD did not induce any gene expression changes after a 24-hour exposure in HepG2/C3A cells. Here, after extended exposure to 72 hours, 81 probe sets were found to change significantly, including the up-regulation of several metallothionein genes (*MT1A*, *MT1B*, *MT1E*, *MT1L*, *MT1H* and *MT1X*). Metallothionein is a family of intracellular cysteine-rich proteins with metal-binding activity, while it has also been

associated with oxidative stress (Coyle et al., 2002). MTs can be induced not only by a variety of heavy metals but also by xenobiotics (Coyle et al., 2002). For example, 100 μ M TDCIPP also induced the *MT1L* gene in HepG2/C3A cells in Chapter 4.

In a parallel study, the quantification of the potential metabolites of these four FRs in HepG2/C3A cells using LC-MS/MS method (Abdallah et al., 2015b) suggested that the FRs were metabolised. Several hydroxylated and debrominated metabolites of HBCD (i.e. di-hydroxylated and mono-hydroxylated HBCD, mono-hydroxylated pentabromocyclododecene (PBCD) and mono-hydroxylated tetrabromocyclododecadiene (TBCD)) were identified in HepG2/C3A cells after a 24-hour exposure, while glucuronic acid-conjugated HBCDs were also observed. Therefore, the metabolism of HBCDs in HepG2/C3A cells was proposed as in Figure 5.6 based on the available identification of metabolites of HBCD. Similarly, hydroxylated, oxidised and glutathione-conjugated metabolites of chlorinated PFRs have also been detected in HepG2 cells or human liver microsomes (Abdallah et al., 2015b; Van den Eede et al., 2013). For example, as shown in Figure 5.7, oxidation and glutathione conjugation are proposed as metabolic pathways of TDCIPP in human hepatocytes according to the identification of several metabolites of TDCIPP after exposure.

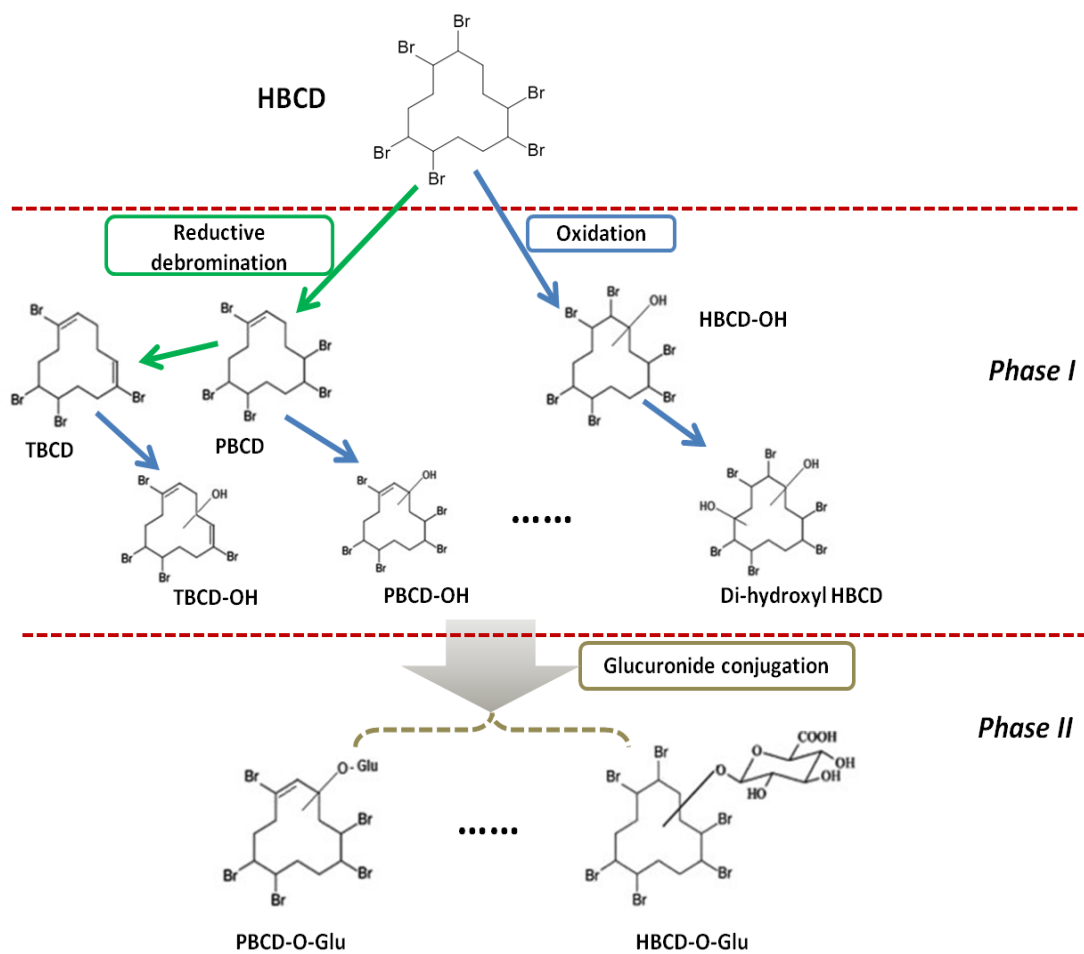


Figure 5.6 Proposed metabolic profile of biotransformation of HBCDs by human HepG2/C3A cells (Adapted from Abdallah et al., 2015b).

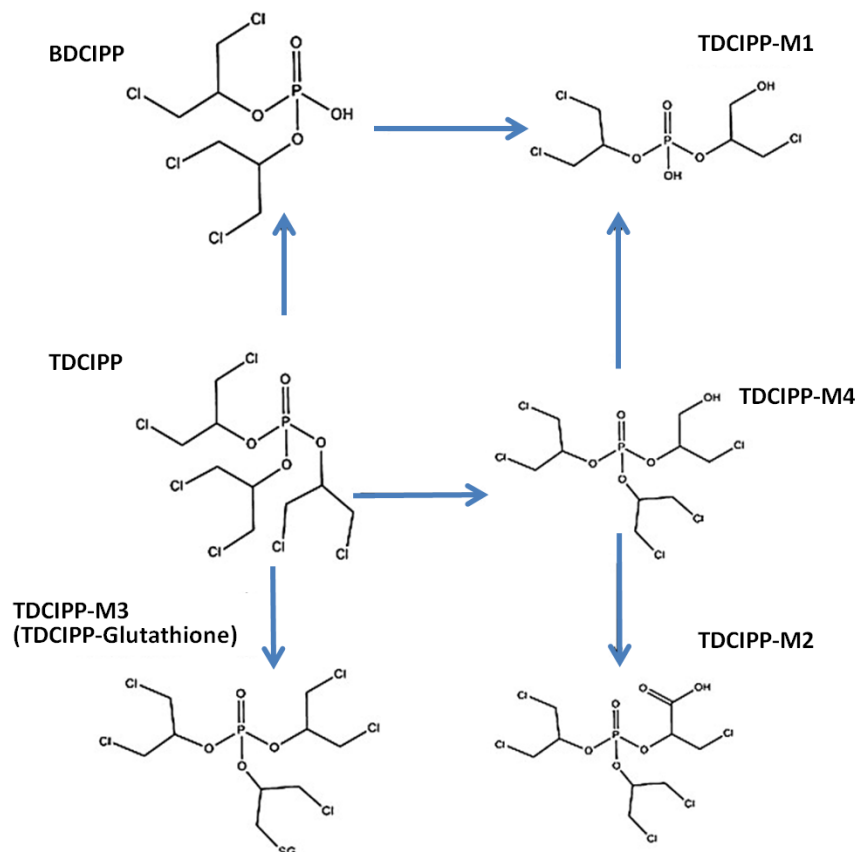


Figure 5.7 Representation of metabolic profile of TDCIPP by human hepatocytes (Adapted from Abdallah et al., 2015b; Van den Eede et al., 2013).

Although these metabolites of FRs detected in cells might contribute to the potential toxic effects of FRs in cells, the DIMS based untargeted metabolomics data showed few significantly changed peaks corresponding to such xenobiotic processes in the Dust extract group, Mix 1 and Mix 2 groups. In the 2 μ M DMBA and 4 μ M HBCD groups, untargeted metabolomics revealed dysregulation of metabolic pathways related to the metabolism of amino acids and derivatives (i.e. arginine and proline metabolism, glycine and serine metabolism) and glutathione conjugation which require further confirmation by a targeted approach (e.g.

LC-MS/MS).

5.5 Conclusions

In summary, toxicogenomic responses of human hepatoma cells exposed to a mixture of flame retardants were investigated at concentrations mimicking those maximally achievable following human exposure in real-life scenarios. Although there were no cytotoxic effects in HepG2/C3A cells following exposures to a dust extract and to mixture of FRs (at the same FR concentrations as detected in the dust), transcriptomics analysis revealed significant changes in gene expression associated with the metabolism of xenobiotics in the Dust extract group but not in the FRs mixture groups. Moreover, few significant changes were detected by untargeted metabolomics and lipidomics analyses following exposure to a dust extract and mixture of FRs, though a relatively high concentration of HBCD (4 μM) was discovered to disrupt the lipid profile of HepG2/C3A cells. Given the dust extract contained compounds that elicited a molecular response, in contrast to the lack of effect induced by the FR mixtures (Mix 1 group), we can conclude that concern for the potential toxicity of dust should focus on compounds other than the four flame retardants studied here.

CHAPTER 6 Conclusions and Future work

The potential for human exposure to FRs has given rise to increasing health concerns, yet there is relatively limited knowledge about their possible adverse effects and the underlying molecular mechanisms that may mediate any impacts on health. Therefore, at the start of this research, the overall aim (Section 1.6) was to investigate the potential toxic effects of human exposure to FRs in *in vitro* systems using non-targeted (unbiased) transcriptomic and metabolomic approaches. To address such aim, the molecular responses of A549 and HepG2/C3A cells exposed to HBCD (Chapter 3) and TDCIPP (Chapter 4) were studied using microarray based transcriptomics and DIMS based metabolomics. HBCD represents one of the widely used BFRs, while TDCIPP is one of the commonly used PFRs. Then, in Chapter 5, the potential effects of a mixture of FRs at concentrations relevant to indoor environmental exposures were also assessed using transcriptomics and metabolomics.

6.1 Molecular responses of A549 and HepG2/C3A cells exposed to HBCD

The work of Chapter 3 represented the first use of unbiased transcriptomic and metabolomic approaches to investigate the potential molecular changes in human cell lines which could lead to toxicity of HBCD under concentrations relevant to human exposure conditions. A concentration-dependent cytotoxic effect of HBCD to A549 and HepG2/C3A cells was observed with EC₅₀ values of

27.4 μM and 63.0 μM , respectively. Following a 24-hour exposure to HBCD at several sub-lethal concentrations (2, 20, 200 and 2000 nM), both microarray-based transcriptomics and DIMS-based untargeted metabolomics revealed few molecular changes occurred in A549 cells. Similarly, no significant transcriptional or metabolic changes in HepG2/C3A cells were detected after exposure for 24 hours. However, in Chapter 5, after an extended exposure time to 72 hours, 4 μM HBCD caused significant changes to the lipid profile and induced expression of some xenobiotic-related genes including several metallothionein genes (*MT1A*, *MT1B*, *MT1E*, *MT1L*, *MT1H* and *MT1X*) in HepG2/C3A cells. Quantification of the level of HBCD in the A549 and HepG2/C3A cells exposed to 2 or 4 μM HBCD respectively suggested that the HBCDs were present at several orders of magnitude higher concentration compared to those reported to occur in human tissues. Thus, it can be concluded that HBCD exhibits no detectable acute toxicity in A549 cells, representative of a major cell type of the lung, and HepG2/C3A cells, representing a cell type that shows some xenobiotic metabolic capacity, studied here at the concentrations known to be achievable following exposure in humans. Since the metabolomics analysis in Chapter 3 was focusing on the polar metabolome only, future work on lipidomic analysis (of the non polar metabolome) would be beneficial for a more comprehensive understanding of

the effects of HBCD exposure. The treatments with HBCD in this study used a technical mixture of HBCDs, which is composed of the three main diastereomers denoted as alpha (α -HBCD), beta (β -HBCD) and gamma (γ -HBCD). Thus, the effects of HBCD measured in the current study represent the overall effects of HBCDs rather than that of individual isomers. In the future study of toxicity of HBCD, the detailed specific effect of individual HBCD isomers need to be investigated to fully understand the potential mechanisms of toxicity of HBCD.

6.2 Defensive and adverse energy-related molecular responses precede TDCIPP cytotoxicity

In Chapter 4, as one of the widely used OPFRs, the effect of TDCIPP was investigated in human cell lines. Similar combined transcriptomic and metabolomic approaches were employed to investigate the molecular responses of two human cell lines (HepG2/C3A and A549) exposed to different concentrations of TDCIPP. Firstly, the concentration-dependent cytotoxicity of TDCIPP was determined by CCK-8 assays with EC_{50} values of 167.9 μ M for HepG2/C3A cells and 193.1 μ M for A549 cells after 24-hour exposures. Next, comparative analyses of transcriptional and metabolic profiles of the two cell lines were performed after exposure to 1, 10 and 100 μ M TDCIPP for 24 and 72 hours. Stress responses (e.g. xenobiotic metabolism and ABC transporter pathways) were observed at the transcriptional level following a 24-hour

exposure to a sub-cytotoxic concentration (10 μ M). Transcription of an energy metabolism-related pathway (oxidative phosphorylation) was down-regulated more severely at 100 μ M TDCIPP exposure, accompanied by the suppression of pathways relevant to cell proliferation (e.g. cell cycle, DNA replication), while no significant cytotoxic effects were observed.

Metabolomics analysis revealed that several metabolic pathways related to ABC transporters, metabolism of amino acids and derivatives (i.e. arginine and proline metabolism, cysteine and methionine metabolism, glycine and serine metabolism) and glutathione conjugation were dysregulated in both HepG2/C3A and A549 cells exposed to 100 μ M TDCIPP for 24 hours. Similar functional metabolic changes (but to a greater extent) were also observed after 72 hours in HepG2/C3A cells exposed to 100 μ M TDCIPP that corresponded to changes detected at the transcriptional level after 24 hours. Taken together, defensive responses to TDCIPP exposure and energy-related changes both precede the cytotoxic effects of TDCIPP in HepG2/C3A cells.

Since only polar metabolic profiles of the two cell lines were analysed using DIMS-based metabolomics, the understanding of the molecular responses to TDCIPP in this study just reflect part of the whole metabolic system. In addition, annotation of DIMS data remains a considerable challenge in metabolomics, and

consequently only a fraction of the significantly changing DIMS peaks have been assigned putative metabolite names. Therefore, future analyses of the non-polar part of the intracellular metabolome as well as a more advanced MS peak annotation platform might contribute novel insights into the lipidomic changes, providing a more comprehensive metabolic profile. Quantification of TDCIPP in the treatments can also provide a clue about the bioaccessibility of such chemical. A further need is to gain more information on the likely cellular concentrations of TDCIPP that can be achieved through human exposure, which will enable a more accurate risk assessment.

6.3 Mixture of FRs at environmental level are less toxic than indoor dust extract

While most studies (including those shown in Chapters 3 and 4 in this thesis) have attempted to investigate the potential adverse effects of individual FRs, the real-life scenario of human exposure to FRs comprises the exposure to mixtures of FR chemicals from multiple resources. Chapter 5 was aimed at exploring the potential effects of human exposure to a mixture of FRs from indoor dust. A solvent extract of an indoor dust standard reference material SRM2585 was employed as a surrogate dust sample, while an artificial mixture of four FRs (TCEP, TCIPP, TDCIPP and HBCD) was used to mimic the FR mixture in the dust. HepG2/C3A cells were exposed to such a mixture for 24 or 72 hours. The

quantification of four individual FRs after exposure suggested that the exposure concentrations of FRs in the present study are relevant to FR levels in humans. Cytotoxicity screening tests (CCK-8 assays and AK assays) indicated there were no significant changes of cell viability or cell integrity after 24 or 72 hours exposure of HepG2/C3A cells to the mixtures of FRs or dust extract. Microarray analysis revealed changes in gene expression associated with the metabolism of xenobiotics (e.g. *CYP1A1*, *CYP1A2*, *CYP2B6*) in the dust extract group but not in the FR mixture groups after 72 hours exposure. Few metabolic or lipidomic changes were detected in the mixture of the FRs group and the dust extract group. Given the dust extract contained components that elicited a biological response in contrast to the negative effect of the mixture of FRs group (Mix 1 group), it appears that the greatest concern around potential toxicity from dust exposure lies in components other than the FRs contained within, e.g. PAH, PCBs. Although combined omics approaches revealed the different molecular responses to a mixture of FRs or dust extract in HepG2/C3A cells which classic toxicological tests did not, further validation experiments (e.g. qPCR or targeted tandem MS analysis of significantly changed features) might be helpful to confirm such subtle changes at transcriptional and metabolic levels.

6.4 Future work

The work presented in this thesis contributes valuable knowledge to understand

the potential effects of human exposure to FRs. However, there are still gaps in knowledge which should be investigated in future work so as to overcome the current issues to achieve a more comprehensive understanding of FRs toxicity.

First, while A549 and HepG2/C3A cells used in this study have also been widely employed in various toxicological studies, they are not expected to fully recapitulate whole organism physiology. Therefore, to investigate other aspects of FRs toxicity (e.g. endocrine mediated effects or neurotoxicity), other types of cells (e.g. human adenocarcinoma cells such as H295R cells, MCF-7 cells and human neuronal cell line such as SH-SY5Y cells) could be used for assessing site specific FR toxicity. Furthermore, using primary cultured cells or *in vivo* models for the studies of FRs toxicity can also be valuable to illustrate the mechanisms of potential effects of exposure to FRs and the risk assessment of such FRs.

Second, the untargeted DIMS-based metabolomics approach employed in this study suffers from the technological limitation of limited annotation of the MS peaks. Combining new computational tools and the application of hyphenated techniques such as LC-MS or tandem MS in metabolomics could generate more reliable metabolite annotation or identification though the capabilities of these techniques still need to be improved to increase their sensitivity and sample

high-throughput. Targeted metabolomics using LC-MS/MS could be beneficial to obtain more accurate identification of the MS peaks as well as high sensitivity.

Yet such approaches do not allow unbiased analyses of the metabolic response.

Moreover, the explorative study of the effects of a FR mixture, described in Chapter 5, was focusing on a simple mixture of four FRs. To fully understand the potential effects of exposure to mixtures of FRs, further evaluation of more FRs or other groups of chemicals are necessary due to the complexity and variability of multiple chemicals which humans are exposed to in real life scenarios.

In conclusion, the work presented in this thesis has assessed the molecular responses of human cell lines to several FRs using high-throughput omics approaches. Unbiased analyses of gene expression and metabolic profiles provide more insights of human exposure to FRs investigated in this project, which would be beneficial for both understanding the potential mechanisms of effects of FRs investigated here and future risk assessment.

References

- Abdallah, M.A.-E., Covaci, A., 2014. Organophosphate Flame Retardants in Indoor Dust from Egypt: Implications for Human Exposure. *Environ. Sci. Technol.* doi:10.1021/es501078s
- Abdallah, M.A.-E., Harrad, S., 2009. Personal exposure to HBCDs and its degradation products via ingestion of indoor dust. *Environ. Int.* 35, 870–6. doi:10.1016/j.envint.2009.03.002
- Abdallah, M.A.-E., Harrad, S., Covaci, A., 2008a. Hexabromocyclododecanes and tetrabromobisphenol-A in indoor air and dust in Birmingham, U.K: implications for human exposure. *Environ. Sci. Technol.* 42, 6855–61.
- Abdallah, M.A.-E., Harrad, S., Ibarra, C., Diamond, M., Melymuk, L., Robson, M., Covaci, A., 2008b. Hexabromocyclododecanes in indoor dust from Canada, the United Kingdom, and the United States. *Environ. Sci. Technol.* 42, 459–64.
- Abdallah, M.A.-E., Pawar, G., Harrad, S., 2015a. Evaluation of in vitro vs. in vivo methods for assessment of dermal absorption of organic flame retardants: A review. *Environ. Int.* 74C, 13–22. doi:10.1016/j.envint.2014.09.012
- Abdallah, M.A.-E., Zhang, J., Pawar, G., Viant, M.R., Chipman, J.K., D'Silva, K., Bromirski, M., Harrad, S., 2015b. High-resolution mass spectrometry provides novel insights into products of human metabolism of organophosphate and brominated flame retardants. *Anal. Bioanal. Chem.* 407, 1871–1883. doi:10.1007/s00216-015-8466-z
- Ahamed, M., Akhtar, M.J., Siddiqui, M. a, Ahmad, J., Musarrat, J., Al-Khedhairi, A. a, AlSalhi, M.S., Alrokayan, S. a, 2011. Oxidative stress mediated apoptosis induced by nickel ferrite nanoparticles in cultured A549 cells. *Toxicology* 283, 101–8. doi:10.1016/j.tox.2011.02.010
- Alaee, M., Arias, P., Sjödin, A., Bergman, A., 2003. An overview of commercially used brominated flame retardants, their applications, their use patterns in different countries/regions and possible modes of release. *Environ. Int.* 29, 683–9. doi:10.1016/S0160-4120(03)00121-1
- Al-Mousa, F., Michelangeli, F., 2012. Some Commonly Used Brominated Flame Retardants Cause Ca²⁺-ATPase Inhibition, Beta-Amyloid Peptide Release

and Apoptosis in SH-SY5Y Neuronal Cells. PLoS One 7, e33059.
doi:10.1371/journal.pone.0033059

An, J., Chen, C., Wang, X., Zhong, Y., Zhang, X., Yu, Y., Yu, Z., 2014. Oligomeric proanthocyanidins alleviate hexabromocyclododecane-induced cytotoxicity in HepG2 cells through regulation on ROS formation and mitochondrial pathway. *Toxicol. Vitro.* 28, 319–326. doi:10.1016/j.tiv.2013.11.009

An, J., Zou, W., Chen, C., Zhong, F.Y., Yu, Q.Z., Wang, Q.J., 2013. The cytological effects of HBCDs on human hepatocyte L02 and the potential molecular mechanism. *J. Environ. Sci. Health. A. Tox. Hazard. Subst. Environ. Eng.* 48, 1333–42. doi:10.1080/10934529.2013.781875

ATSDR, 2012. Toxicological profile for phosphate ester flame retardants.

Bandeled, O.J., Santillo, M.F., Ferguson, M., Wiesenfeld, P.L., 2012. In vitro toxicity screening of chemical mixtures using HepG2/C3A cells. *Food Chem. Toxicol.* 50, 1653–9. doi:10.1016/j.fct.2012.02.016

Benjamini, Y., Hochberg, Y., 1995. Controlling the false discovery rate: a practical and powerful approach to multiple testing. *J. R. Stat. Soc.* doi:10.2307/2346101

Berger, R.G., Lefèvre, P.L.C., Ernest, S.R., Wade, M.G., Ma, Y.Q., Rawn, D.F.K., Gaertner, D.W., Robaire, B., Hales, B.F., 2014. Exposure to an environmentally relevant mixture of brominated flame retardants affects fetal development in Sprague-Dawley rats. *Toxicology* 320, 56–66. doi:10.1016/j.tox.2014.03.005

Besis, A., Samara, C., 2012. Polybrominated diphenyl ethers (PBDEs) in the indoor and outdoor environments - A review on occurrence and human exposure. *Environ. Pollut.* doi:10.1016/j.envpol.2012.04.009

Billet, S., Abbas, I., Le Goff, J., Verdin, A., André, V., Lafargue, P., Hachimi, A., Cazier, F., Sichel, F., Shirali, P., Garçon, G., Garc, G., 2008. Genotoxic potential of Polycyclic Aromatic Hydrocarbons-coated onto airborne Particulate Matter (PM 2.5) in human lung epithelial A549 cells. *Cancer Lett.* 270, 144–55. doi:10.1016/j.canlet.2008.04.044

Bouhifd, M., Hartung, T., Hogberg, H.T., Kleensang, A., Zhao, L., 2013. Review: toxicometabolomics. *J. Appl. Toxicol.* 33, 1365–83. doi:10.1002/jat.2874

- Brommer, S., 2014. CHARACTERISING HUMAN EXPOSURE TO ORGANOPHOSPHATE ESTER FLAME RETARDANTS. University of Birmingham.
- Brommer, S., Harrad, S., Van den Eede, N., Covaci, A., 2012. Concentrations of organophosphate esters and brominated flame retardants in German indoor dust samples. *J. Environ. Monit.* 14, 2482–7. doi:10.1039/c2em30303e
- Brown, M., Dunn, W.B., Ellis, D.I., Goodacre, R., Handl, J., Knowles, J.D., O'Hagan, S., Spasić, I., Kell, D.B., 2005. A metabolome pipeline: from concept to data to knowledge. *Metabolomics* 1, 39–51. doi:10.1007/s11306-005-1106-4
- Brusick, D., Matheson, D., Jagannath, D.R., Goode, S., Lebowitz, H., Reed, M., Roy, G., Benson, S., 1979. A comparison of the genotoxic properties of tris(2,3-dibromopropyl)phosphate and tris(1,3-dichloro-2-propyl)phosphate in a battery of short-term bioassays. *J. Environ. Pathol. Toxicol.* 3, 207–26.
- BSEF, 2012. Fast Facts on Fire Safety and Flame Retardants [WWW Document]. URL [http://www.bsef.com/uploads/MediaRoom/documents/BSEF_Fast Facts on Fire Safety and Flame Retardants.pdf](http://www.bsef.com/uploads/MediaRoom/documents/BSEF_Fast_Facts_on_Fire_Safety_and_Flame_Retardants.pdf) (accessed 3.6.15).
- Bundy, J.G., Davey, M.P., Viant, M.R., 2009. Environmental metabolomics: a critical review and future perspectives. *Metabolomics* 5, 3–21. doi:10.1007/s11306-008-0152-0
- Butt, C.M., Congleton, J., Hoffman, K., Fang, M., Stapleton, H.M., 2014. Metabolites of organophosphate flame retardants and 2-ethylhexyl tetrabromobenzoate in urine from paired mothers and toddlers. *Environ. Sci. Technol.* 48, 10432–8. doi:10.1021/es5025299
- Butte, W., Heinzow, B., 2002. Pollutants in house dust as indicators of indoor contamination. *Rev. Environ. Contam. Toxicol.* 175, 1–46.
- Cantón, R.F., Peijnenburg, A.A.C.M., Hoogenboom, R.L.A.P., Piersma, A.H., Ven, L.T.M. Van Der, Berg, M. Van Den, Heneweer, M., 2008. Subacute effects of hexabromocyclododecane (HBCD) on hepatic gene expression profiles in rats. *Toxicol. Appl. Pharmacol.* 231, 267–272. doi:10.1016/j.taap.2008.04.013
- Carignan, C.C., McClean, M.D., Cooper, E.M., Watkins, D.J., Fraser, A.J., Heiger-Bernays, W., Stapleton, H.M., Webster, T.F., 2013. Predictors of

- tris(1,3-dichloro-2-propyl) phosphate metabolite in the urine of office workers. *Environ. Int.* 55, 56–61. doi:10.1016/j.envint.2013.02.004
- Castorena-Torres, F., de León, M.B., Cisneros, B., Zapata-Pérez, O., Salinas, J.E., Albores, A., 2008. Changes in gene expression induced by polycyclic aromatic hydrocarbons in the human cell lines HepG2 and A549. *Toxicol. Vitr.* 22, 411–421. doi:10.1016/j.tiv.2007.10.009
- Cequier, E., Ionas, A.C., Covaci, A., Marcé, R.M., Becher, G., Thomsen, C., 2014. Occurrence of a broad range of legacy and emerging flame retardants in indoor environments in Norway. *Environ. Sci. Technol.* 48, 6827–35. doi:10.1021/es500516u
- Cequier, E., Sakhi, A.K., Marcé, R.M., Becher, G., Thomsen, C., 2015. Human exposure pathways to organophosphate triesters — A biomonitoring study of mother–child pairs. *Environ. Int.* 75, 159–165. doi:10.1016/j.envint.2014.11.009
- Chen, M., Zhang, M., Borlak, J., Tong, W., 2012. A decade of toxicogenomic research and its contribution to toxicological science. *Toxicol. Sci.* 130, 217–28. doi:10.1093/toxsci/kfs223
- Chu, Y., Corey, D.R., 2012. RNA sequencing: platform selection, experimental design, and data interpretation. *Nucleic Acid Ther.* 22, 271–4. doi:10.1089/nat.2012.0367
- Coen, M., Holmes, E., Lindon, J.C., Nicholson, J.K., 2008. NMR-based metabolic profiling and metabolomic approaches to problems in molecular toxicology. *Chem. Res. Toxicol.* 21, 9–27. doi:10.1021/tx700335d
- Corney, D.C., 2013. RNA-seq Using Next Generation Sequencing. *Mater. Methods* 3, 203. doi:10.13070/mm.en.3.203
- Courcot, E., Leclerc, J., Lafitte, J., Mensier, E., Jaillard, S., Gosset, P., Shirali, P., Pottier, N., Broly, F., 2012. Xenobiotic Metabolism and Disposition in Human Lung Cell Models : Comparison with In Vivo Expression Profiles. *Drug Metab Dispos.* 40, 1953–1965.
- Covaci, A., Gerecke, A.C., Law, R.J., Voorspoels, S., Kohler, M., Heeb, N. V., Leslie, H., Allchin, C.R., Boer, J. de, 2006. Hexabromocyclododecanes (HBCDs) in the environment and humans: a review. *Environ. Sci. Technol.* 40, 3679–3688.

- Coyle, P., Philcox, J.C., Carey, L.C., Rofe, A.M., 2002. Metallothionein: The multipurpose protein. *Cell. Mol. Life Sci.* 59, 627–647.
- Crump, D., Chiu, S., Egloff, C., Kennedy, S.W., 2008. Effects of hexabromocyclododecane and polybrominated diphenyl ethers on mRNA expression in chicken (*Gallus domesticus*) hepatocytes. *Toxicol. Sci.* 106, 479–87. doi:10.1093/toxsci/kfn196
- Crump, D., Chiu, S., Kennedy, S.W., 2012. Effects of tris(1,3-dichloro-2-propyl) phosphate and tris(1-chloropropyl) phosphate on cytotoxicity and mRNA expression in primary cultures of avian hepatocytes and neuronal cells. *Toxicol. Sci.* 126, 140–8. doi:10.1093/toxsci/kfs015
- Danielson, P.B., 2002. The cytochrome P450 superfamily: biochemistry, evolution and drug metabolism in humans. *Curr. Drug Metab.* 3, 561–97.
- Darnerud, P.O., 2003. Toxic effects of brominated flame retardants in man and in wildlife. *Environ. Int.* 29, 841–53. doi:10.1016/S0160-4120(03)00107-7
- Dingemans, M.M.L., de Groot, A., van Kleef, R.G.D.M., Bergman, A., van den Berg, M., Vijverberg, H.P.M., Westerink, R.H.S., 2008. Hydroxylation increases the neurotoxic potential of BDE-47 to affect exocytosis and calcium homeostasis in PC12 cells. *Environ. Health Perspect.* 116, 637–43. doi:10.1289/ehp.11059
- Dingemans, M.M.L., Heusinkveld, H.J., de Groot, A., Bergman, A., van den Berg, M., Westerink, R.H.S., 2009. Hexabromocyclododecane inhibits depolarization-induced increase in intracellular calcium levels and neurotransmitter release in PC12 cells. *Toxicol. Sci.* 107, 490–7. doi:10.1093/toxsci/kfn249
- Dishaw, L. V, J Macaulay, L., Roberts, S.C., Stapleton, H.M., 2014. Exposures, mechanisms, and impacts of endocrine-active flame retardants. *Curr. Opin. Pharmacol.* 19C, 125–133. doi:10.1016/j.coph.2014.09.018
- Dishaw, L. V, Powers, C.M., Ryde, I.T., Roberts, S.C., Seidler, F.J., Slotkin, T. a, Stapleton, H.M., 2011. Is the PentaBDE replacement, tris (1,3-dichloro-2-propyl) phosphate (TDCPP), a developmental neurotoxicant? Studies in PC12 cells. *Toxicol. Appl. Pharmacol.* 256, 281–9. doi:10.1016/j.taap.2011.01.005

- Dodson, R.E., Perovich, L.J., Covaci, A., Van den Eede, N., Ionas, A.C., Dirtu, A.C., Brody, J.G., Rudel, R. a, 2012. After the PBDE phase-out: a broad suite of flame retardants in repeat house dust samples from California. *Environ. Sci. Technol.* 46, 13056–66. doi:10.1021/es303879n
- Domingo, J.L., 2012. Polybrominated diphenyl ethers in food and human dietary exposure: a review of the recent scientific literature. *Food Chem. Toxicol.* 50, 238–49. doi:10.1016/j.fct.2011.11.004
- Dunn, W.B., Broadhurst, D.I., Atherton, H.J., Goodacre, R., Griffin, J.L., 2011. Systems level studies of mammalian metabolomes: the roles of mass spectrometry and nuclear magnetic resonance spectroscopy. *Chem. Soc. Rev.* 40, 387–426. doi:10.1039/b906712b
- EFRA, 2007. Frequently Asked Questions on Flame Retardants [WWW Document]. URL http://www.flameretardants-online.com/images/userdata/pdf/168_DE.pdf (accessed 3.6.15).
- Eisenbrand, G., Pool-Zobel, B., Baker, V., Balls, M., Blaauboer, B., Boobis, A., Carere, A., Kevekordes, S., Lhuguenot, J.-C., Pieters, R., Kleiner, J., 2002. Methods of in vitro toxicology. *Food Chem. Toxicol.* 40, 193–236. doi:10.1016/S0278-6915(01)00118-1
- Eljarrat, E., Guerra, P., Martínez, E., Farré, M., Alvarez, J.G., López-Teijón, M., Barceló, D., 2009. Hexabromocyclododecane in human breast milk: levels and enantiomeric patterns. *Environ. Sci. Technol.* 43, 1940–6.
- Ema, M., Fujii, S., Hirata-Koizumi, M., Matsumoto, M., 2008. Two-generation reproductive toxicity study of the flame retardant hexabromocyclododecane in rats. *Reprod. Toxicol.* 25, 335–51. doi:10.1016/j.reprotox.2007.12.004
- Environment Canada, 2011. Screening Assessment Report on Hexabromocyclododecane (HBCD) [WWW Document]. URL <http://ec.gc.ca/ese-ees/default.asp?lang=En&n=7882C148-1> (accessed 3.8.15).
- Eriksson, P., Fischer, C., Wallin, M., Jakobsson, E., Fredriksson, A., 2006. Impaired behaviour, learning and memory, in adult mice neonatally exposed to hexabromocyclododecane (HBCDD). *Environ. Toxicol. Pharmacol.* 21, 317–22. doi:10.1016/j.etap.2005.10.001

- Ernest, S.R., Wade, M.G., Lalancette, C., Ma, Y.-Q., Berger, R.G., Robaire, B., Hales, B.F., 2012. Effects of chronic exposure to an environmentally relevant mixture of brominated flame retardants on the reproductive and thyroid system in adult male rats. *Toxicol. Sci.* 127, 496–507. doi:10.1093/toxsci/kfs098
- EU, 2006. European Union Risk Assessment Report on TBBPA [WWW Document]. URL http://www.bsef.com/uploads/library/final_tbbpa_human_health_report.pdf
- European Chemicals Bureau, 2008a. European Union Risk Assessment Report Tris(2-chloro-1-methylethyl)phosphate (TCPP).
- European Chemicals Bureau, 2008b. SUMMARY RISK ASSESSMENT REPORT: Tris(2-chloroethyl) phosphate [WWW Document]. URL <http://echa.europa.eu/documents/10162/f42be21b-33a3-4063-ad4d-2b0f937e41b4>
- European Union, 2008. European Union Risk Assessment Report: Tris (1,3-dichloro-2-propyl) phosphate.
- Fang, Z., Martin, J., Wang, Z., 2012. Statistical methods for identifying differentially expressed genes in RNA-Seq experiments. *Cell Biosci.* 2, 26. doi:10.1186/2045-3701-2-26
- Farhat, A., Buick, J.K., Williams, A., Yauk, C.L., O'Brien, J.M., Crump, D., Williams, K.L., Chiu, S., Kennedy, S.W., 2014a. Tris(1,3-dichloro-2-propyl) phosphate perturbs the expression of genes involved in immune response and lipid and steroid metabolism in chicken embryos. *Toxicol. Appl. Pharmacol.* 275, 104–112. doi:10.1016/j.taap.2013.12.020
- Farhat, A., Crump, D., Chiu, S., Williams, K.L., Letcher, R.J., Gauthier, L.T., Kennedy, S.W., 2013. In ovo effects of two organophosphate flame Retardants-TCPP and TDCPP-on pipping success, development, mRNA expression, and thyroid hormone levels in chicken embryos. *Toxicol. Sci.* 134, 92–102. doi:10.1093/toxsci/kft100
- Farhat, A., Crump, D., Porter, E., Chiu, S., Letcher, R.J., Su, G., Kennedy, S.W., 2014b. Time-dependent effects of the flame retardant tris(1,3-dichloro-2-propyl) phosphate (TDCPP) on mRNA expression, in vitro and in ovo, reveal optimal sampling times for rapidly metabolized compounds. *Environ. Toxicol. Chem.* 33, 2842–2849. doi:10.1002/etc.2755

- Fery, Y., Buschauer, I., Salzig, C., Lang, P., Schrenk, D., 2009. Technical pentabromodiphenyl ether and hexabromocyclododecane as activators of the pregnane-X-receptor (PXR). *Toxicology* 264, 45–51. doi:10.1016/j.tox.2009.07.009
- Föllmann, W., Wober, J., 2006. Investigation of cytotoxic, genotoxic, mutagenic, and estrogenic effects of the flame retardants tris-(2-chloroethyl)-phosphate (TCEP) and tris-(2-chloropropyl)-phosphate (TCPP) in vitro. *Toxicol. Lett.* 161, 124–34. doi:10.1016/j.toxlet.2005.08.008
- Foster, W.R., Robertson, D.G., Car, B.D., 2013. CHAPTER 11 The Application of Toxicogenomics to the Interpretation of Toxicologic Pathology, Third Edit. ed, Haschek and Rousseaux's Handbook of Toxicologic Pathology. Elsevier. doi:10.1016/B978-0-12-415759-0.00011-X
- Frederiksen, M., Thomsen, C., Frøshaug, M., Vorkamp, K., Thomsen, M., Becher, G., Knudsen, L.E., 2010. Polybrominated diphenyl ethers in paired samples of maternal and umbilical cord blood plasma and associations with house dust in a Danish cohort. *Int. J. Hyg. Environ. Health* 213, 233–42. doi:10.1016/j.ijheh.2010.04.008
- Frederiksen, M., Vorkamp, K., Thomsen, M., Knudsen, L.E., 2009. Human internal and external exposure to PBDEs--a review of levels and sources. *Int. J. Hyg. Environ. Health* 212, 109–34. doi:10.1016/j.ijheh.2008.04.005
- Freudenthal, R.I., Henrich, R.T., 2000. Chronic Toxicity and Carcinogenic Potential of Tris-(1,3-Dichloro-2-propyl) Phosphate in Sprague-Dawley Rat. *Int. J. Toxicol.* 19, 119–125. doi:10.1080/109158100224926
- Gabig, M., Węgrzyn, G., 2001. An introduction to DNA chips: Principles, technology, applications and analysis. *Acta Biochim. Pol.* 48, 615–622.
- Genies, C., Maître, A., Lefèbvre, E., Jullien, A., Chopard-Lallier, M., Douki, T., 2013. The Extreme Variety of Genotoxic Response to Benzo[a]pyrene in Three Different Human Cell Lines from Three Different Organs. *PLoS One* 8, e78356. doi:10.1371/journal.pone.0078356
- Gerets, H.H.J., Tilmant, K., Gerin, B., Chanteux, H., Depelchin, B.O., Dhalluin, S., Atienzar, F. a, 2012. Characterization of primary human hepatocytes, HepG2 cells, and HepaRG cells at the mRNA level and CYP activity in response to inducers and their predictivity for the detection of human hepatotoxins. *Cell Biol. Toxicol.* 28, 69–87. doi:10.1007/s10565-011-9208-4

- Germer, S., Piersma, A.H., van der Ven, L., Kamyschnikow, A., Fery, Y., Schmitz, H.-J., Schrenk, D., 2006. Subacute effects of the brominated flame retardants hexabromocyclododecane and tetrabromobisphenol A on hepatic cytochrome P450 levels in rats. *Toxicology* 218, 229–36. doi:10.1016/j.tox.2005.10.019
- Gold, M., Blum, A., Ames, B., 1978. Another flame retardant, tris-(1,3-dichloro-2-propyl)-phosphate, and its expected metabolites are mutagens. *Science* (80-). 200, 785–787. doi:10.1126/science.347576
- Gosavi, R. a., Knudsen, G. a., Birnbaum, L.S., Pedersen, L.C., 2013. Mimicking of estradiol binding by flame retardants and their metabolites: A crystallographic analysis. *Environ. Health Perspect.* 121, 1194–1199. doi:10.1289/ehp.1306902
- Griffin, J.L., Kauppinen, R.A., 2007. A metabolomics perspective of human brain tumours. *FEBS J.* 274, 1132–9. doi:10.1111/j.1742-4658.2007.05676.x
- Gualtieri, M., Longhin, E., Mattioli, M., Mantecca, P., Tinaglia, V., Mangano, E., Proverbio, M.C., Bestetti, G., Camatini, M., Battaglia, C., 2012. Gene expression profiling of A549 cells exposed to Milan PM2.5. *Toxicol. Lett.* 209, 136–45. doi:10.1016/j.toxlet.2011.11.015
- Gülden, M., Schreiner, J., Seibert, H., 2013. In vitro toxicity testing with microplate cell cultures: Impact of cell binding. *Toxicology* In press. doi:10.1016/j.tox.2013.11.006
- Hakk, H., Szabo, D.T., Huwe, J., Diliberto, J., Birnbaum, L.S., 2012. Novel and Distinct Metabolites Identified Following a Single Oral Dose of α - or γ - Hexabromocyclododecane in Mice. *Environ. Sci. Technol.* 46, 13494–13503.
- Hamadeh, H.K., Amin, R.P., Paules, R.S., Afshari, C. a., 2002. An overview of toxicogenomics. *Curr. Issues Mol. Biol.* 4, 45–56.
- Hamers, T., Kamstra, J.H., Sonneveld, E., Murk, A.J., Kester, M.H.A., Andersson, P.L., Legler, J., Brouwer, A., 2006. In vitro profiling of the endocrine-disrupting potency of brominated flame retardants. *Toxicol. Sci.* 92, 157–73. doi:10.1093/toxsci/kfj187
- Harrad, S., de Wit, C., Abdallah, M.A.-E., Bergh, C., Björklund, J.A., Covaci, A., Darnerud, P.O., de Boer, J., Diamond, M., Huber, S., Leonards, P.,

- Mandalakis, M., Ostman, C., Haug, L.S., Thomsen, C., Webster, T.F., 2010. Indoor contamination with hexabromocyclododecanes, polybrominated diphenyl ethers, and perfluoroalkyl compounds: an important exposure pathway for people? *Environ. Sci. Technol.* 44, 3221–31. doi:10.1021/es903476t
- Harrad, S., Hazrati, S., Ibarra, C., 2006. Concentrations of Polychlorinated Biphenyls in Indoor Air and Polybrominated Diphenyl Ethers in Indoor Air and Dust in Birmingham, United Kingdom: Implications for Human Exposure. *Environ. Sci. Technol.* 40, 4633–4638. doi:10.1021/es0609147
- Harrad, S., Ibarra, C., Diamond, M., Melymuk, L., Robson, M., Douwes, J., Roosens, L., Dirtu, A.C., Covaci, A., 2008. Polybrominated diphenyl ethers in domestic indoor dust from Canada, New Zealand, United Kingdom and United States. *Environ. Int.* 34, 232–8. doi:10.1016/j.envint.2007.08.008
- Harrad, S., Wijesekera, R., Hunter, S., Halliwell, C., Baker, R., 2004. Preliminary Assessment of U.K. Human Dietary and Inhalation Exposure to Polybrominated Diphenyl Ethers. *Environ. Sci. Technol.* 38, 2345–2350. doi:10.1021/es0301121
- Hart, S.N., Li, Y., Nakamoto, K., Subileau, E., Steen, D., Zhong, X., 2010. A comparison of whole genome gene expression profiles of HepaRG cells and HepG2 cells to primary human hepatocytes and human liver tissues. *Drug Metab. Dispos.* 38, 988–94. doi:10.1124/dmd.109.031831
- Heijne, W.H.M., Kienhuis, A.S., van Ommen, B., Stierum, R.H., Groten, J.P., 2005. Systems toxicology: applications of toxicogenomics, transcriptomics, proteomics and metabolomics in toxicology. *Expert Rev. Proteomics* 2, 767–80. doi:10.1586/14789450.2.5.767
- Hennig, B., Hammock, B.D., Slim, R., Toborek, M., Saraswathi, V., Robertson, L.W., 2002. PCB-induced oxidative stress in endothelial cells: modulation by nutrients. *Int. J. Hyg. Environ. Health* 205, 95–102. doi:10.1078/1438-4639-00134
- Hoffman, K., Garantziotis, S., Birnbaum, L.S., Stapleton, H.M., 2015. Monitoring Indoor Exposure to Organophosphate Flame Retardants: Hand Wipes and House Dust. *Environ. Health Perspect.* 123, 160–165. doi:10.1289/ehp.1408669

- Hu, X., Hu, D., Xu, Y., 2009. Effects of tetrabrominated diphenyl ether and hexabromocyclododecanes in single and complex exposure to hepatoma HepG2 cells. *Environ. Toxicol. Pharmacol.* 27, 327–37. doi:10.1016/j.etap.2008.11.014
- Huang, D.W., Sherman, B.T., Lempicki, R. a, 2009. Systematic and integrative analysis of large gene lists using DAVID bioinformatics resources. *Nat. Protoc.* 4, 44–57. doi:10.1038/nprot.2008.211
- Hukkanen, J., Lassila, a, Päivärinta, K., Valanne, S., Sarpo, S., Hakkola, J., Pelkonen, O., Raunio, H., 2000. Induction and regulation of xenobiotic-metabolizing cytochrome P450s in the human A549 lung adenocarcinoma cell line. *Am. J. Respir. Cell Mol. Biol.* 22, 360–6. doi:10.1165/ajrcmb.22.3.3845
- ISO/TC92, 2014. Fire safety in ISOInformation about ISO/TC92 [WWW Document]. *Fire Saf. Secur.* URL http://www.sp.se/sv/units/fire/Documents/BR/ISO_TC_92_Information_Sheet.pdf (accessed 3.6.15).
- Jairaj, M., Watson, D.G., Grant, M.H., Skellern, G.G., 2003. The toxicity of opiates and their metabolites in HepG2 cells. *Chem. Biol. Interact.* 146, 121–129. doi:10.1016/S0009-2797(03)00091-7
- Johnson, P.I., Stapleton, H.M., Sjodin, A., Meeker, J.D., 2010. Relationships between polybrominated diphenyl ether concentrations in house dust and serum. *Environ. Sci. Technol.* 44, 5627–32. doi:10.1021/es100697q
- Johnson, W.E., Li, C., Rabinovic, A., 2007. Adjusting batch effects in microarray expression data using empirical Bayes methods. *Biostatistics* 8, 118–27. doi:10.1093/biostatistics/kxj037
- Johnson-Restrepo, B., Kannan, K., 2009. An assessment of sources and pathways of human exposure to polybrominated diphenyl ethers in the United States. *Chemosphere* 76, 542–8. doi:10.1016/j.chemosphere.2009.02.068
- Jungnickel, H., Potratz, S., Baumann, S., Tarnow, P., von Bergen, M., Luch, A., 2014. Identification of lipidomic biomarkers for coexposure to subtoxic doses of benzo[a]pyrene and cadmium: the toxicological cascade biomarker approach. *Environ. Sci. Technol.* 48, 10423–31. doi:10.1021/es502419w

- Kalberlah, F., Schneider, K., Schuhmacher-Wolz, U., 2003. Uncertainty in toxicological risk assessment for non-carcinogenic health effects. *Regul. Toxicol. Pharmacol.* 37, 92–104. doi:10.1016/S0273-2300(02)00032-6
- Kamburov, A., Cavill, R., Ebbels, T.M.D., Herwig, R., Keun, H.C., 2011. Integrated pathway-level analysis of transcriptomics and metabolomics data with IMPaLA. *Bioinformatics* 27, 2917–8. doi:10.1093/bioinformatics/btr499
- Kankainen, M., Gopalacharyulu, P., Holm, L., Oresic, M., 2011. MPEA--metabolite pathway enrichment analysis. *Bioinformatics* 27, 1878–9. doi:10.1093/bioinformatics/btr278
- Kawata, K., Osawa, M., Okabe, S., 2009. In Vitro Toxicity of Silver Nanoparticles at Noncytotoxic Doses to HepG2 Human Hepatoma Cells. *Environ. Sci. Technol.* 43, 6046–6051. doi:10.1021/es900754q
- Khalaf, H., Larsson, A., Berg, H., McCrindle, R., Arsenault, G., Olsson, P.-E., 2009. Diastereomers of the brominated flame retardant 1,2-dibromo-4-(1,2-dibromoethyl)cyclohexane induce androgen receptor activation in the hepg2 hepatocellular carcinoma cell line and the Incap prostate cancer cell line. *Environ. Health Perspect.* 117, 1853–9. doi:10.1289/ehp.0901065
- Kiciński, M., Viaene, M.K., Den Hond, E., Schoeters, G., Covaci, A., Dirtu, A.C., Nelen, V., Bruckers, L., Croes, K., Sioen, I., Baeyens, W., Van Larebeke, N., Nawrot, T.S., 2012. Neurobehavioral function and low-level exposure to brominated flame retardants in adolescents: a cross-sectional study. *Environ. Health* 11, 86. doi:10.1186/1476-069X-11-86
- Kim, J.W., Isobe, T., Muto, M., Tue, N.M., Katsura, K., Malarvannan, G., Sudaryanto, A., Chang, K.H., Prudente, M., Viet, P.H., Takahashi, S., Tanabe, S., 2014. Organophosphorus flame retardants (PFRs) in human breast milk from several Asian countries. *Chemosphere.* doi:10.1016/j.chemosphere.2014.02.033
- Kirwan, J.A., Weber, R.J.M., Broadhurst, D.I., Viant, M.R., 2014. Direct infusion mass spectrometry metabolomics dataset: a benchmark for data processing and quality control. *Sci. Data* 1, 1–13. doi:10.1038/sdata.2014.12
- Kling, P., Förlin, L., 2009. Proteomic studies in zebrafish liver cells exposed to the brominated flame retardants HBCD and TBBPA. *Ecotoxicol. Environ. Saf.* 72, 1985–93. doi:10.1016/j.ecoenv.2009.04.018

- Kojima, H., Takeuchi, S., Itoh, T., Iida, M., Kobayashi, S., Yoshida, T., 2013. In vitro endocrine disruption potential of organophosphate flame retardants via human nuclear receptors. *Toxicology* 314, 76–83. doi:10.1016/j.tox.2013.09.004
- Komori, K., Murai, K., Miyajima, S., Fujii, T., Mohri, S., Ono, Y., Sakai, Y., 2008. Development of an in vitro batch-type closed gas exposure device with an alveolar epithelial cell line, A549, for toxicity evaluations of gaseous compounds. *Anal. Sci.* 24, 957–62.
- Kramer, N.I., Krismartina, M., Rico-Rico, A., Blaauboer, B.J., Hermens, J.L.M., 2012. Quantifying processes determining the free concentration of phenanthrene in Basal cytotoxicity assays. *Chem. Res. Toxicol.* 25, 436–45. doi:10.1021/tx200479k
- Kroeger, M., 2006. How omics technologies can contribute to the “3R” principles by introducing new strategies in animal testing. *Trends Biotechnol.* 24, 343–6. doi:10.1016/j.tibtech.2006.06.003
- Kuehnbaum, N.L., Britz-McKibbin, P., 2013. New advances in separation science for metabolomics: resolving chemical diversity in a post-genomic era. *Chem. Rev.* 113, 2437–68. doi:10.1021/cr300484s
- Law, R.J., Covaci, A., Harrad, S., Herzke, D., Abdallah, M.A.-E., Fernie, K., Toms, L.-M.L., Takigami, H., 2014. Levels and trends of PBDEs and HBCDs in the global environment: Status at the end of 2012. *Environ. Int.* 65C, 147–158. doi:10.1016/j.envint.2014.01.006
- LeBel, G.L., Williams, D.T., 1986. Levels of triaryl/alkyl phosphates in human adipose tissue from Eastern Ontario. *Bull. Environ. Contam. Toxicol.* 37, 41–46. doi:10.1007/BF01607726
- Lei, Z., Huhman, D. V., Sumner, L.W., 2011. Mass spectrometry strategies in metabolomics. *J. Biol. Chem.* 286, 25435–42. doi:10.1074/jbc.R111.238691
- Li, Z., Srivastava, S., Yang, X., Mittal, S., Norton, P., Resau, J., Haab, B., Chan, C., 2007. A hierarchical approach employing metabolic and gene expression profiles to identify the pathways that confer cytotoxicity in HepG2 cells. *BMC Syst. Biol.* 1, 21. doi:10.1186/1752-0509-1-21
- Lilienblum, W., Dekant, W., Foth, H., Gebel, T., Hengstler, J.G., Kahl, R., Kramer, P.J., Schweinfurth, H., Wollin, K.M., 2008. Alternative methods to safety

- studies in experimental animals: Role in the risk assessment of chemicals under the new European Chemicals Legislation (REACH). *Arch. Toxicol.* 82, 211–236. doi:10.1007/s00204-008-0279-9
- Liu, C., Wang, Q., Liang, K., Liu, J., Zhou, B., Zhang, X., Liu, H., Giesy, J.P., Yu, H., 2013. Effects of tris(1,3-dichloro-2-propyl) phosphate and triphenyl phosphate on receptor-associated mRNA expression in zebrafish embryos/larvae. *Aquat. Toxicol.* 128-129, 147–57. doi:10.1016/j.aquatox.2012.12.010
- Liu, X., Ji, K., Choi, K., 2012. Endocrine disruption potentials of organophosphate flame retardants and related mechanisms in H295R and MVLN cell lines and in zebrafish. *Aquat. Toxicol.* 114-115, 173–81. doi:10.1016/j.aquatox.2012.02.019
- Livak, K.J., Schmittgen, T.D., 2001. Analysis of relative gene expression data using real-time quantitative PCR and the 2^{(-Delta Delta C(T))} Method. *Methods* 25, 402–8. doi:10.1006/meth.2001.1262
- Lorber, M., 2008. Exposure of Americans to polybrominated diphenyl ethers. *J. Expo. Sci. Environ. Epidemiol.* 18, 2–19. doi:10.1038/sj.jes.7500572
- Lu, Y., Morimoto, K., Takeshita, T., Takeuchi, T., Saito, T., 2000. Genotoxic effects of alpha-endosulfan and beta-endosulfan on human HepG2 cells. *Environ. Health Perspect.* 108, 559–61.
- Ma, Q., Lu, A.Y.H., 2007. CYP1A induction and human risk assessment: an evolving tale of in vitro and in vivo studies. *Drug Metab. Dispos.* 35, 1009–16. doi:10.1124/dmd.107.015826
- Mahadevan, B., Keshava, C., Musafia-jeknic, T., Pecaj, A., Weston, A., Baird, W.M., 2005. Altered Gene Expression Patterns in MCF-7 Cells Induced by the Urban Dust Particulate Complex Mixture Standard Reference Material 1649a. *Cancer Res.* 65, 1251–1258.
- Marvin, C.H., Tomy, G.T., Armitage, J.M., Arnot, J.A., McCarty, L., Covaci, A., Palace, V., 2011. Hexabromocyclododecane: current understanding of chemistry, environmental fate and toxicology and implications for global management. *Environ. Sci. Technol.* 45, 8613–23. doi:10.1021/es201548c
- Meeker, J.D., Cooper, E.M., Stapleton, H.M., Hauser, R., 2013. Urinary metabolites of organophosphate flame retardants: temporal variability and

correlations with house dust concentrations. *Environ. Health Perspect.* 121, 580–5. doi:10.1289/ehp.1205907

Meeker, J.D., Stapleton, H.M., 2010. House dust concentrations of organophosphate flame retardants in relation to hormone levels and semen quality parameters. *Environ. Health Perspect.* 118, 318–23. doi:10.1289/ehp.0901332

Mitsopoulos, P., Suntres, Z.E., 2010. Cytotoxicity and gene array analysis of alveolar epithelial A549 cells exposed to paraquat. *Chem. Biol. Interact.* 188, 427–36. doi:10.1016/j.cbi.2010.09.022

Murphy, D., 2002. Gene expression studies using microarrays: principles, problems, and prospects. *Adv. Physiol. Educ.* 26, 256–270. doi:10.1152/advan.00043.2002

Nakagawa, Y., Suzuki, T., Ishii, H., Ogata, A., 2007. Biotransformation and cytotoxicity of a brominated flame retardant, tetrabromobisphenol A, and its analogues in rat hepatocytes. *Xenobiotica* 37, 693–708.

National Research Council (US), C. on A. of T.T. to P.T., 2007. Applications of Toxicogenomic Technologies to Predictive Toxicology and Risk Assessment.

Nicholson, J.K., Connelly, J., Lindon, J.C., Holmes, E., 2002. Metabonomics: a platform for studying drug toxicity and gene function. *Nat. Rev. Drug Discov.* 1, 153–61. doi:10.1038/nrd728

Nobels, I., Vanparys, C., Van den Heuvel, R., Vercauteren, J., Blust, R., 2012. Added value of stress related gene inductions in HepG2 cells as effect measurement in monitoring of air pollution. *Atmos. Environ.* 55, 154–163. doi:10.1016/j.atmosenv.2012.02.073

OEHHA, 2011. Evidence on the carcinogenicity of tris(1,3-dichloro-2-propyl) phosphate.

OEHHA, 2013. Chemicals known to the state to cause cancer or reproductive toxicity November 8, 2013.

Palace, V., Park, B., Pleskach, K., Gemmill, B., Tomy, G., 2010. Altered thyroxine metabolism in rainbow trout (*Oncorhynchus mykiss*) exposed to

hexabromocyclododecane (HBCD). *Chemosphere* 80, 165–9.
doi:10.1016/j.chemosphere.2010.03.016

- Palace, V.P., Pleskach, K., Halldorson, T., Danell, R., Wautier, K., Evans, B., Alae, M., Marvin, C., Tomy, G.T., 2008. Biotransformation enzymes and thyroid axis disruption in juvenile rainbow trout (*Oncorhynchus mykiss*) exposed to hexabromocyclododecane diastereoisomers. *Environ. Sci. Technol.* 42, 1967–72.
- Payne, T.G., Southam, A.D., Arvanitis, T.N., Viant, M.R., 2009. A signal filtering method for improved quantification and noise discrimination in fourier transform ion cyclotron resonance mass spectrometry-based metabolomics data. *J. Am. Soc. Mass Spectrom.* 20, 1087–95.
doi:10.1016/j.jasms.2009.02.001
- Persicke, M., Rückert, C., Plassmeier, J., Stutz, L., Kessler, N., Kalinowski, J., Goesmann, A., Neuweger, H., 2012. MSEA: metabolite set enrichment analysis in the MeltDB metabolomics software platform: metabolic profiling of *Corynebacterium glutamicum* as an example. *Metabolomics* 8, 322.
- PINFA, 2015. Nitrogen based flame retardants [WWW Document]. URL <http://pinfa.eu/non-halogenated-pin-frs/nitrogen-based-flame-retardants.html> (accessed 3.7.15).
- Poster, D.L., Kucklick, J.R., Schantz, M.M., Vander Pol, S.S., Leigh, S.D., Wise, S. a, 2007. Development of a house dust standard reference material for the determination of organic contaminants. *Environ. Sci. Technol.* 41, 2861–7.
- Pulkrabová, J., Hrádková, P., Hajslová, J., Poustka, J., Nápravníková, M., Poláček, V., 2009. Brominated flame retardants and other organochlorine pollutants in human adipose tissue samples from the Czech Republic. *Environ. Int.* 35, 63–8. doi:10.1016/j.envint.2008.08.001
- Ramirez, T., Daneshian, M., Kamp, H., Bois, F.Y., Clench, M.R., Coen, M., Donley, B., Fischer, S.M., Ekman, D.R., Fabian, E., 2013. Metabolomics in Toxicology and Preclinical Research. *ALTEX* 30, 209–25.
- Rauert, C., Lazarov, B., Harrad, S., Covaci, A., Stranger, M., 2014. A review of chamber experiments for determining specific emission rates and investigating migration pathways of flame retardants. *Atmos. Environ.* 82, 44–55. doi:10.1016/j.atmosenv.2013.10.003

- Rauert, C.B., 2014. ELUCIDATING PATHWAYS OF BROMINATED FLAME RETARDANT. University of Birmingham.
- Rawn, D.F.K., Gaertner, D.W., Weber, D., Curran, I.H.A., Cooke, G.M., Goodyer, C.G., 2014a. Hexabromocyclododecane concentrations in Canadian human fetal liver and placental tissues. *Sci. Total Environ.* 468-469, 622–629. doi:10.1016/j.scitotenv.2013.08.014
- Rawn, D.F.K., Ryan, J.J., Sadler, A.R., Sun, W.-F., Weber, D., Laffey, P., Haines, D., Macey, K., Van Oostdam, J., 2014b. Brominated flame retardant concentrations in sera from the Canadian Health Measures Survey (CHMS) from 2007 to 2009. *Environ. Int.* 63, 26–34. doi:10.1016/j.envint.2013.10.012
- Reistad, T.T., Fonnum, F., Mariussen, E., 2006. Neurotoxicity of the pentabrominated diphenyl ether mixture , DE-71 , and hexabromocyclododecane (HBCD) in rat cerebellar granule cells in vitro 785–796. doi:10.1007/s00204-006-0099-8
- Riechelmann, H., Deutsche, T., Grabow, A., Heinzow, B., Butte, W., Reiter, R., 2007. Differential response of Mono Mac 6, BEAS-2B, and Jurkat cells to indoor dust. *Environ. Health Perspect.* 115, 1325–32. doi:10.1289/ehp.9874
- Robertson, D.G., 2005. Metabonomics in toxicology: a review. *Toxicol. Sci.* 85, 809–22. doi:10.1093/toxsci/kfi102
- Robertson, D.G., Reily, M.D., Baker, J.D., 2007. Metabonomics in pharmaceutical discovery and development. *J. Proteome Res.* 6, 526–39. doi:10.1021/pr060535c
- Ronisz, D., Finne, E.F., Karlsson, H., Förlin, L., 2004. Effects of the brominated flame retardants hexabromocyclododecane (HBCDD), and tetrabromobisphenol A (TBBPA), on hepatic enzymes and other biomarkers in juvenile rainbow trout and feral eelpout. *Aquat. Toxicol.* 69, 229–45. doi:10.1016/j.aquatox.2004.05.007
- Roosens, L., Abdallah, M.A.-E., Harrad, S., Neels, H., Covaci, A., 2009. Exposure to hexabromocyclododecanes (HBCDs) via dust ingestion, but not diet, correlates with concentrations in human serum: preliminary results. *Environ. Health Perspect.* 117, 1707–12. doi:10.1289/ehp.0900869
- Ruiz-Aracama, A., Peijnenburg, A., Kleinjans, J., Jennen, D., van Delft, J., Hellfrisch, C., Lommen, A., 2011. An untargeted multi-technique

- metabolomics approach to studying intracellular metabolites of HepG2 cells exposed to 2,3,7,8-tetrachlorodibenzo-p-dioxin. *BMC Genomics* 12, 251. doi:10.1186/1471-2164-12-251
- Saeed, A.I., Sharov, V., White, J., Li, J., Liang, W., Bhagabati, N., Braisted, J., Klapa, M., Currier, T., Thiagarajan, M., Sturn, A., Snuffin, M., Rezantsev, A., Popov, D., Ryltsov, A., Kostukovich, E., Borisovsky, I., Liu, Z., Vinsavich, A., Trush, V., Quackenbush, J., 2003. TM4: a free, open-source system for microarray data management and analysis. *Biotechniques* 34, 374–377.
- Saegusa, Y., Fujimoto, H., Woo, G.-H., Inoue, K., Takahashi, M., Mitsumori, K., Hirose, M., Nishikawa, A., Shibutani, M., 2009. Developmental toxicity of brominated flame retardants, tetrabromobisphenol A and 1,2,5,6,9,10-hexabromocyclododecane, in rat offspring after maternal exposure from mid-gestation through lactation. *Reprod. Toxicol.* 28, 456–67. doi:10.1016/j.reprotox.2009.06.011
- Schechter, A., Szabo, D.T., Miller, J., Gent, T.L., Malik-Bass, N., Petersen, M., Paepke, O., Colacino, J. a, Hynan, L.S., Harris, T.R., Malla, S., Birnbaum, L.S., 2012. Hexabromocyclododecane (HBCD) stereoisomers in U.S. food from Dallas, Texas. *Environ. Health Perspect.* 120, 1260–4. doi:10.1289/ehp.1204993
- Schirmer, K., Fischer, B.B., Madureira, D.J., Pillai, S., 2010. Transcriptomics in ecotoxicology. *Anal. Bioanal. Chem.* 397, 917–923. doi:10.1007/s00216-010-3662-3
- Schriks, M., Roessig, J.M., Murk, A.J., Furlow, J.D., 2007. Thyroid hormone receptor isoform selectivity of thyroid hormone disrupting compounds quantified with an in vitro reporter gene assay. *Environ. Toxicol. Pharmacol.* 23, 302–7. doi:10.1016/j.etap.2006.11.007
- Sederlund, E.J., Dybing, E., Holme, J.A., Hongslo, J.K., Rivedal, E., Sanner, T., Nelson, S.D., 1985. Comparative Genotoxicity and Nephrotoxicity Studies of the Two Halogenated Flame Retardants Tris(1,3-Dichloro-2-propyl)phosphate and Tris(2,3-Dibromopropyl)phosphate. *Acta Pharmacol. Toxicol. (Copenh).* 56, 20–29. doi:10.1111/j.1600-0773.1985.tb01248.x
- Seo, D.-C., Sung, J.-M., Cho, H.-J., Yi, H., Seo, K.-H., Choi, I.-S., Kim, D.-K., Kim, J.-S., El-Aty AM, A., Shin, H.-C., 2007. Gene expression profiling of cancer

- stem cell in human lung adenocarcinoma A549 cells. *Mol. Cancer* 6, 75. doi:10.1186/1476-4598-6-75
- Shintu, L., Baudoin, R., Navratil, V., Prot, J.-M., Pontoizeau, C., Defernez, M., Blaise, B.J., Domange, C., Péry, A.R., Toulhoat, P., Legallais, C., Brochot, C., Leclerc, E., Dumas, M.-E., 2012. Metabolomics-on-a-chip and predictive systems toxicology in microfluidic bioartificial organs. *Anal. Chem.* 84, 1840–8. doi:10.1021/ac2011075
- Sohlenius-Sternbeck, A.-K., 2006. Determination of the hepatocellularity number for human, dog, rabbit, rat and mouse livers from protein concentration measurements. *Toxicol. In Vitro* 20, 1582–6. doi:10.1016/j.tiv.2006.06.003
- Southam, A.D., Lange, A., Hines, A., Hill, E.M., Katsu, Y., Iguchi, T., Tyler, C.R., Viant, M.R., 2011. Metabolomics reveals target and off-target toxicities of a model organophosphate pesticide to roach (*Rutilus rutilus*): implications for biomonitoring. *Environ. Sci. Technol.* 45, 3759–67. doi:10.1021/es103814d
- Southam, A.D., Payne, T.G., Cooper, H.J., Arvanitis, T.N., Viant, M.R., 2007. Dynamic Range and Mass Accuracy of Wide-Scan Direct Infusion Nanoelectrospray Fourier Transform Ion Cyclotron Resonance Mass Spectrometry-Based Metabolomics Increased by the Spectral Stitching Method Direct infusion nanoelectrospray Fourier transform ion. *Anal. Chem.* 79, 4595–4602.
- Stapleton, H., Klosterhaus, S., 2009. Detection of organophosphate flame retardants in furniture foam and US house dust. *Env. Sci Technol* 43, 7490–7495.
- Stapleton, H.M., Allen, J.G., Kelly, S.M., Konstantinov, A., Klosterhaus, S., Watkins, D., McClean, M.D., Webster, T.F., 2008. Alternate and new brominated flame retardants detected in U.S. house dust. *Environ. Sci. Technol.* 42, 6910–6.
- Stapleton, H.M., Eagle, S., Anthopolos, R., Wolkin, A., Miranda, M.L., 2011. Associations between Polybrominated Diphenyl Ether (PBDE) Flame Retardants, Phenolic Metabolites, and Thyroid Hormones during Pregnancy. *Env. Heal. Perspect* 119, 1454–1460.
- Stapleton, H.M., Harner, T., Shoeib, M., Keller, J.M., Schantz, M.M., Leigh, S.D., Wise, S. a, 2006. Determination of polybrominated diphenyl ethers in indoor

dust standard reference materials. *Anal. Bioanal. Chem.* 384, 791–800.
doi:10.1007/s00216-005-0227-y

Stapleton, H.M., Sharma, S., Getzinger, G., Ferguson, P.L., Gabriel, M., Webster, T.F., Blum, A., 2012. Novel and high volume use flame retardants in US couches reflective of the 2005 PentaBDE phase out. *Environ. Sci. Technol.* 46, 13432–9. doi:10.1021/es303471d

Subramanian, A., Tamayo, P., Mootha, V.K., Mukherjee, S., Ebert, B.L., Gillette, M.A., Paulovich, A., Pomeroy, S.L., Golub, T.R., Lander, E.S., Mesirov, J.P., 2005. Gene set enrichment analysis: a knowledge-based approach for interpreting genome-wide expression profiles. *Proc. Natl. Acad. Sci. U. S. A.* 102, 15545–50. doi:10.1073/pnas.0506580102

Suzuki, G., Tue, N.M., Malarvannan, G., Sudaryanto, A., Takahashi, S., Tanabe, S., Sakai, S., Brouwer, A., Uramaru, N., Kitamura, S., Takigami, H., 2013. Similarities in the endocrine-disrupting potencies of indoor dust and flame retardants by using human osteosarcoma (U2OS) cell-based reporter gene assays. *Environ. Sci. Technol.* 47, 2898–908. doi:10.1021/es304691a

Szakács, G., Váradi, A., Ozvegy-Laczka, C., Sarkadi, B., 2008. The role of ABC transporters in drug absorption, distribution, metabolism, excretion and toxicity (ADME-Tox). *Drug Discov. Today* 13, 379–93.
doi:10.1016/j.drudis.2007.12.010

Ta, N., Li, C., Fang, Y., Liu, H., Lin, B., Jin, H., Tian, L., Zhang, H., Zhang, W., Xi, Z., 2014. Toxicity of TDCPP and TCEP on PC12 cell: changes in CAMKII, GAP43, tubulin and NF-H gene and protein levels. *Toxicol. Lett.* 227, 164–71.
doi:10.1016/j.toxlet.2014.03.023

Taylor, N.S., 2010. NOVEL APPROACHES TO TOXICITY TESTING IN DAPHNIA MAGNA by. University of Birmingham.

Taylor, N.S., Weber, R.J.M., Southam, A.D., Payne, T.G., Hrydziuszko, O., Arvanitis, T.N., Viant, M.R., 2008. A new approach to toxicity testing in *Daphnia magna*: application of high throughput FT-ICR mass spectrometry metabolomics. *Metabolomics* 5, 44–58. doi:10.1007/s11306-008-0133-3

The Geneva Association, 2014. World Fire Statistics Bulletin 2014, The Geneva Association.

- Thomsen, C., Molander, P., Daae, H.L., Janák, K., Froshaug, M., Liane, V.H., Thorud, S., Becher, G., Dybing, E., 2007. Occupational exposure to hexabromocyclododecane at an industrial plant. *Environ. Sci. Technol.* 41, 5210–6.
- Tian, C., Gao, P., Zheng, Y., Yue, W., Wang, X., Jin, H., Chen, Q., 2008. Redox status of thioredoxin-1 (TRX1) determines the sensitivity of human liver carcinoma cells (HepG2) to arsenic trioxide-induced cell death. *Cell Res.* 18, 458–71. doi:10.1038/cr.2007.112
- Tusher, V.G., Tibshirani, R., Chu, G., 2001. Significance analysis of microarrays applied to the ionizing radiation response. *Proc. Natl. Acad. Sci. U. S. A.* 98, 5116–21. doi:10.1073/pnas.091062498
- UK Department for Communities and Local Government, 2015. Fire Statistics: Great Britain April 2013 to March 2014, UK Department for Communities and Local Government.
- UN, 2013. AMENDMENT TO ANNEX of STOCKHOLM CONVENTION ON PERSISTENT ORGANIC POLLUTANTS STOCKHOLM, 22 MAY 2001 [WWW Document]. URL <https://treaties.un.org/doc/Publication/CN/2013/CN.934.2013-Eng.pdf> (accessed 12.1.13).
- Van den Eede, N., Dirtu, A.C., Ali, N., Neels, H., Covaci, A., 2012. Multi-residue method for the determination of brominated and organophosphate flame retardants in indoor dust. *Talanta* 89, 292–300. doi:10.1016/j.talanta.2011.12.031
- Van den Eede, N., Maho, W., Erratico, C., Neels, H., Covaci, A., 2013. First insights in the metabolism of phosphate flame retardants and plasticizers using human liver fractions. *Toxicol. Lett.* 223, 9–15. doi:10.1016/j.toxlet.2013.08.012
- Van der Veen, I., de Boer, J., 2012. Phosphorus flame retardants: properties, production, environmental occurrence, toxicity and analysis. *Chemosphere* 88, 1119–53. doi:10.1016/j.chemosphere.2012.03.067
- Van der Ven, L.T.M., van de Kuil, T., Leonards, P.E.G., Slob, W., Lilienthal, H., Litens, S., Herlin, M., Håkansson, H., Cantón, R.F., van den Berg, M., Visser, T.J., van Loveren, H., Vos, J.G., Piersma, A.H., 2009. Endocrine effects of

- hexabromocyclododecane (HBCD) in a one-generation reproduction study in Wistar rats. *Toxicol. Lett.* 185, 51–62. doi:10.1016/j.toxlet.2008.12.003
- Van der Ven, L.T.M., Verhoef, A., van de Kuil, T., Slob, W., Leonards, P.E.G., Visser, T.J., Hamers, T., Herlin, M., Håkansson, H., Olausson, H., Piersma, A.H., Vos, J.G., 2006. A 28-day oral dose toxicity study enhanced to detect endocrine effects of hexabromocyclododecane in Wistar rats. *Toxicol. Sci.* 94, 281–92. doi:10.1093/toxsci/kfl113
- Viant, M.R., Sommer, U., 2012. Mass spectrometry based environmental metabolomics: a primer and review. *Metabolomics* 9, 144–158. doi:10.1007/s11306-012-0412-x
- Vulimiri, S. V, Misra, M., Hamm, J.T., Mitchell, M., Berger, A., 2009. Effects of mainstream cigarette smoke on the global metabolome of human lung epithelial cells. *Chem. Res. Toxicol.* 22, 492–503. doi:10.1021/tx8003246
- Wang, Q., Liang, K., Liu, J., Yang, L., Guo, Y., Liu, C., Zhou, B., 2013. Exposure of zebrafish embryos/larvae to TDCPP alters concentrations of thyroid hormones and transcriptions of genes involved in the hypothalamic-pituitary-thyroid axis. *Aquat. Toxicol.* 126, 207–13. doi:10.1016/j.aquatox.2012.11.009
- Wang, Z., Gerstein, M., Snyder, M., 2009. RNA-Seq: a revolutionary tool for transcriptomics. *Nat. Rev. Genet.* 10, 57–63.
- Weber, R.J.M., Southam, A.D., Sommer, U., Viant, M.R., 2011. Characterization of isotopic abundance measurements in high resolution FT-ICR and Orbitrap mass spectra for improved confidence of metabolite identification. *Anal. Chem.* 83, 3737–43. doi:10.1021/ac2001803
- Weber, R.J.M., Viant, M.R., 2010. MI-Pack: Increased confidence of metabolite identification in mass spectra by integrating accurate masses and metabolic pathways. *Chemom. Intell. Lab. Syst.* 104, 75–82. doi:10.1016/j.chemolab.2010.04.010
- Weiss, J., Meijer, L., Sauer, P., Linderholm, L., Athanassiadis, I., 2004. PBDE and HBCDD levels in blood from Dutch mothers and infants - Analysis of a Dutch Groningen Infant Cohort. *Organohalogen Compd.* 66, 2647–2652.

- Wikoff, D.S., Birnbaum, L., 2011. Human Health Effects of Brominated Flame Retardants, *The Handbook of Environmental Chemistry: Brominated Flame Retardants*. Springer. doi:10.1007/698_2010_97
- Wise, S.A., Poster, D.L., Kucklick, J.R., Keller, J.M., Vanderpol, S.S., Sander, L.C., Schantz, M.M., 2006. Standard reference materials (SRMs) for determination of organic contaminants in environmental samples. *Anal. Bioanal. Chem.* 386, 1153–90. doi:10.1007/s00216-006-0719-4
- Wu, M., Zuo, Z., Li, B., Huang, L., Chen, M., Wang, C., 2013. Effects of low-level hexabromocyclododecane (HBCD) exposure on cardiac development in zebrafish embryos. *Ecotoxicology* 22, 1200–7. doi:10.1007/s10646-013-1107-4
- Wu, N., Herrmann, T., Paepke, O., Tickner, J., Hale, R., Harvey, E., La Guardia, M., McClean, M.D., Webster, T.F., 2007. Human exposure to PBDEs: Associations of PBDE body burdens with food consumption and house dust concentrations. *Environ. Sci. Technol.* 41, 1584–1589. doi:10.1021/es0620282
- www.flameretardants-online.com, 2015. flameretardant-online - Mode of action [WWW Document]. URL <http://flameretardants-online.com/web/en/106/84575cb4764b9030e1338c8cfd52c9a2.htm> (accessed 3.7.15).
- Xia, J., Mandal, R., Sinelnikov, I. V., Broadhurst, D., Wishart, D.S., 2012. MetaboAnalyst 2.0--a comprehensive server for metabolomic data analysis. *Nucleic Acids Res.* 40, W127–33. doi:10.1093/nar/gks374
- Xia, J., Wishart, D.S., 2011. Web-based inference of biological patterns, functions and pathways from metabolomic data using MetaboAnalyst. *Nat. Protoc.* 6, 743–60. doi:10.1038/nprot.2011.319
- Yamada-Okabe, T., Sakai, H., Kashima, Y., Yamada-Okabe, H., 2005. Modulation at a cellular level of the thyroid hormone receptor-mediated gene expression by 1,2,5,6,9,10-hexabromocyclododecane (HBCD), 4,4'-diiodobiphenyl (DIB), and nitrofen (NIP). *Toxicol. Lett.* 155, 127–33. doi:10.1016/j.toxlet.2004.09.005
- Yanagisawa, R., Koike, E., Win-Shwe, T.-T., Yamamoto, M., Takano, H., 2014. Impaired lipid and glucose homeostasis in

hexabromocyclododecane-exposed mice fed a high-fat diet. *Environ. Health Perspect.* 122, 277–83. doi:10.1289/ehp.1307421

Zhang, Q., Lu, M., Dong, X., Wang, C., Zhang, C., Liu, W., Zhao, M., 2014. Potential estrogenic effects of phosphorus-containing flame retardants. *Environ. Sci. Technol.* 48, 6995–7001. doi:10.1021/es5007862

Zhang, X., Yang, F., Zhang, X., Xu, Y., Liao, T., Song, S., Wang, J., 2008. Induction of hepatic enzymes and oxidative stress in Chinese rare minnow (*Gobiocypris rarus*) exposed to waterborne hexabromocyclododecane (HBCDD). *Aquat. Toxicol.* 86, 4–11. doi:10.1016/j.aquatox.2007.07.002

Zota, A.R., Park, J.-S., Wang, Y., Petreas, M., Zoeller, R.T., Woodruff, T.J., 2011. Polybrominated diphenyl ethers, hydroxylated polybrominated diphenyl ethers, and measures of thyroid function in second trimester pregnant women in California. *Environ. Sci. Technol.* 45, 7896–905. doi:10.1021/es200422b

Zou, W., Chen, C., Zhong, Y., An, J., Zhang, X., Yu, Y., Yu, Z., Fu, J., 2013. PI3K/Akt Pathway Mediates Nrf2/ARE Activation in Human L02 Hepatocytes Exposed to Low-Concentration HBCDs. *Environ. Sci. Technol.* 2, 12434–12440. doi:10.1021/es401791s

Appendix

1. List of publications

1. Abdallah, M.A.-E., **Zhang, J.**, Pawar, G., Viant, M.R., Chipman, J.K., D'Silva, K., Bromirski, M., Harrad, S., 2015. High-resolution mass spectrometry provides novel insights into products of human metabolism of organophosphate and brominated flame retardants. *Anal. Bioanal. Chem.* 407, 1871–1883. doi:10.1007/s00216-015-8466-z
2. **Zhang, J.**, Williams, T.D., Abdallah Abou-Elwafa, M., Harrad, S., Chipman, J.K., Viant, M.R., 2015. Transcriptomic and metabolomic approaches to investigate the molecular responses of human cell lines exposed to the flame retardant hexabromocyclododecane (HBCD). submitted to *Toxicology in vitro*.
3. **Zhang, J.**, Williams, T.D., Chipman, J.K., Viant, M.R., 2015. Defensive and adverse energy-related molecular responses precede Tris (1, 3-dichloro-2-propyl) phosphate (TDCIPP) cytotoxicity. *Journal of Applied Toxicology*. DOI 10.1002/jat.3194 (In press)
4. **Zhang, J.**, Abdallah Abou-Elwafa, M., Williams, T.D., Harrad, S., Chipman, J.K., Viant, M.R., 2015. Gene expression and metabolic responses of HepG2/C3A cells exposed to flame retardants and dust extracts at concentrations relevant to indoor environmental exposures. submitted to *Chemosphere*.

2. List of conference presentations

1. **Zhang, J.**, Kirwan, J., Williams, T.D., Chipman, J.K., Viant, M.R., Transcriptomic and metabolomic approaches to investigate molecular responses of A549 and HepG2/C3A cells to HBCD. *The 7th Annual Conference of the Persistent Organic Pollutants network (POPs 2013)*, Birmingham, UK, (2013) [Poster]
2. **Zhang, J.**, Williams, T.D., Kirwan, J., Nele Van den Eede, Chipman, J.K., Viant, M.R., Transcriptomic and Metabolomic Analyses of Molecular Responses of Human Cell Lines to a Commonly Used Brominated Flame Retardant:

Hexabromocyclododecane. *The 9th Annual Conference of the Metabolomics Society 2013*, Glasgow, UK, (2013) [Poster]

3. **Zhang, J.**, Nele Van den Eede, Chipman, J.K., Viant, M.R., Metabolomic analysis of molecular responses of HepG2/C3A and A549 cell lines exposed to Tris (1, 3-dichloro-2-propyl) phosphate (TDCIPP). *International Symposium on Halogenated Persistent Organic Pollutants (Dioxins 2013)*, Daegu, South Korea (2013) [Oral presentation]

3. List of additional files saved on the enclosed CD

File 3.1 List of significant genes modulated by DMBA in HepG2 C3A cells (HBCD study)

File 4.1 List of significant genes in High concentration groups (TDCIPP study)

File 4.2 DAVID analysis of significant genes in HepG2C3A and A549 cells (TDCIPP study)

File 4.3 GSEA of HepG2C3A cells and A549 cells exposed to TDCIPP for 24 hours (TDCIPP study)

File 4.4 Putative annotation of significantly changed DIMS peaks (TDCIPP study)

File 4.5 Pathway overrepresentation analysis of putative annotated DIMS peaks (TDCIPP study)

File 5.1 List of significant genes by SAM analysis (FR mixture study)

File 5.2 DAVID analysis of significant genes in HepG2C3A cells (FR mixture study)

File 5.3 Putative annotation of DIMS peaks in polar metabolomics and lipidomics (FR mixture study)